



THE EFFECT OF PRESSURE INTENSITY AND DURATION ON THE
RESIDUAL STRESSES INDUCED BY BACKWARD-FORWARD
EXTRUSION OF POLYGONAL RODS AND TUBES

A THESIS SUBMITTED TO
THE GRADUATE SCHOOL OF NATURAL AND APPLIED SCIENCES
OF
UNIVERSITY OF THE TURKISH AERONAUTICAL ASSOCIATION

BY

BAN BAKIR AL-AMER

IN PARTIAL FULFILLMENT OF THE REQUIREMENTS
FOR
THE DEGREE OF DOCTOR OF PHILOSOPHY
IN
MECHANICAL AND AERONAUTICAL ENGINEERING

DECEMBER 2020

Approval of the thesis:

**THE EFFECT OF PRESSURE INTENSITY AND DURATION ON
THE RESIDUAL STRESSES INDUCED BY BACKWARD-FORWARD
EXTRUSION OF POLYGONAL RODS AND TUBES**

submitted by **BAN AL-AMER** in partial fulfillment of the requirements for the degree of **Doctor of Philosophy in Mechanical and Aeronautical Engineering, University of Turkish Aeronautical Association** by,

Assoc. Prof. Dr. Suat Dengiz
Dean, Graduate School of **Natural and Applied Sciences** _____

Prof. Dr. İbrahim Halil Güzelbey
Head of the Department, **Mechanical and Aeronautical Eng** _____

Prof. Dr. Çetin Karataş
Supervisor, **Manufacturing Eng, Gazi University** _____

Assist. Prof. Dr. Faruk Mert
Co-Supervisor, **Multi-Dimensional Modelling and Animation, Ankara Yıldırım Beyazıt University** _____

Examining Committee Members:

Prof. Dr. Cihan Karataş
Mechatronics Eng, UTAA _____

Prof. Dr. Çetin Karataş
Manufacturing Eng, Gazi University _____

Assoc. Prof. Dr. Hakan Gürün
Manufacturing Eng, Gazi University _____

Assoc. Prof. Dr. Mustafa Kaya
Aerospace Eng, Ankara Yıldırım Beyazıt University _____

Assist. Prof. Dr. Reza Aghazadeh
Mechatronics Eng, UTAA _____

Date: 25.12.2020



I hereby declare that all information in this document has been obtained and presented in accordance with academic rules and ethical conduct. I also declare that, as required by these rules and conduct, I have fully cited and referenced all material and results that are not original to this work.

Ban Al-Amer

Signature:

ABSTRACT

THE EFFECT OF PRESSURE INTENSITY AND DURATION ON THE RESIDUAL STRESSES INDUCED BY BACKWARD-FORWARD EXTRUSION OF POLYGONAL RODS AND TUBES

Al-Amer, Ban

Doctor of Philosophy, Mechanical and Aeronautical Engineering

Supervisor: Prof. Dr. Çetin KARATAŞ

Co supervisor: Assist Prof. Dr. Faruk MERT

December 2020, 167 pages

In cold forming, a useful process has been found in manufacturing and metal working by using a backward-forward combined extrusion process. In this process, a billet is extruded in forward and backward directions according to punch and die movements. This offers the ability to produce a variety of complex rod and tube components, improved product quality and an increase in economical production. Researchers work with this type of extrusion because most of the tools that are used in connecting an engine with a transmission system must be polygonal rods with hollow tubes. According to the literature review, there have no been many previous studies dealing with combined extrusion and the effects of process parameters because of the complicated die design and process condition control while there are many parameters influencing the process. Friction, use of lubricants, die geometry, temperature of the process, extrusion ratio, stress generation, product shape, forces and pressures, defects during the process and the use of software application are the most important points that have great effects on this process. In this study, the influence of the pressure and punch velocity of the metal flow on the residual stresses, forces, temperatures and microstructure are

investigated. The total power required for the deformation during a metal forming process to overcome shear and friction losses will be discussed for backward-forward combined extrusion to produce polygonal rods and tube components. A numerical solution was achieved using the QForm software to predict the influence of the velocity and pressure on the residual stresses generated on the products due the complexity of the parameters induced in the metal forming as the effect of opposite directions of the frictional forces and thermal stress rates on the residual stress of the product. Experimental work was conducted with die manufacturing to produce the required shape by combined extrusion and the backward direction producing the hollow hexagonal side with hexagonal punches and the forward direction to produce hollow square sides using square punches. The material used in this process was aluminum alloy AA 6061 because of its properties of good formability, medium to high strength, good toughness and surface finish, excellent corrosion resistance to atmospheric conditions, good workability and its wide availability.

The input parameters depended on three cases of increasing the pressure with a rate of reduction in the punch area of 10%, which gave three pressures of $P1 = 1.4$, $P2 = 1.6$ and $P3 = 1.8 \text{ kN/mm}^2$ and three punch velocities of $V1 = 0.25$, $V2 = 0.5$ and $V3 = 1 \text{ mm/s}$ by duplicating the velocity in each case. An XRD 3003 X-ray diffraction system was used to measure the residual stress. The increasing velocity to a maximum of $V3 = 1 \text{ mm/s}$ leads to an increase in the residual stresses, forces and work piece temperatures. On the other hand, increasing the velocity increased the laminar and homogenous flow and improved the sample finishing and accuracy of the dimensions and shape, so the velocity of $V2 = 0.5 \text{ mm/s}$ was the best choice. A maximum pressure of $P3 = 1.8 \text{ kN/mm}^2$ led to the best results on the shape of the product as well as to a homogenous deformation and uniform surface and reduction in the residual stresses generated on the sample with a reduction on the load required to achieve the process and deform the billet. A comparison of the results between experiments and simulations were in good agreement.

Keywords: Combined Extrusion, Residual Stresses, QForm, Polygonal Shape.

ÖZ

BASINÇ YOĞUNLUĞU VE SÜRESİNİN POLİGONAL ÇUBUKLAR VE TÜPLERİN GERİ-İLERİ EKSTRÜZYONUyla ŞEKİLLENDİRMESİNDE ARTIK GERİLİMLER ÜZERİNDEKİ ETKİSİ

Al-Amer, Ban
Doktora, Makine ve Uçak Mühendisliği
Tez Yöneticisi: Prof. Dr. Çetin KARATAŞ
Ortak Tez Yöneticisi: Dr. Öğr. Üyesi Faruk MERT

Aralık 2020, 167 sayfa

Soğuk şekillendirmede, geri ve ileri birleşik ekstrüzyon işlemi kullanılarak metal imalat ve işlemede faydalı bir işlem bulunmuştur. Bu işlemde, zımba ve kalıp hareketine göre bir kütük ileri ve geri yönde ekstrüde edilir. Bu, çeşitli karmaşık çubuk ve boru bileşenleri üretme, ürün kalitesini iyileştirme ve ekonomik üretimi artırma yeteneği sunar. Araştırmacılar, motoru şanzıman sistemine bağlamak için kullanılan aletlerin çoğunun içi bir tüple poligon çubuk türünde olması gerektiği için bu tip ekstrüzyon üzerinde çalışmaktadırlar. Literatür taramasına göre, işlemi etkileyen birçok parametre bulunmakla beraber, karmaşık kalıp tasarımı ve işlem koşul kontrolü nedeniyle birleşik ekstrüzyon ve işlem parametrelerinin etkileri ile ilgili daha önce yapılan çok fazla araştırma bulunmamaktadır. Sürtünme, yağlayıcı kullanımı, kalıp geometrisi, işlemin sıcaklığı, ekstrüzyon oranı, gerilme oluşumu, ürün şekli, kuvvetler ve basınçlar, işlem sırasında ortaya çıkan kusurlar ve yazılım uygulamasının kullanılması bu işlemde büyük etkiye sahip olan en önemli noktalardır. Bu çalışmada basıncın, zımba ve metal akış hızının artık gerilmeler, kuvvetler, sıcaklıklar ve mikro-yapı üzerindeki etkisi incelenmiştir. Bir metal şekillendirme işlemi sırasında kesme ve sürtünme kayıplarının üstesinden gelmek

için ve deformasyon için gereken toplam güç, poligonal çubuklar ve tüp bileşenleri üretmek için geri-ileri birleşik ekstrüzyon için tartışılacaktır. Ürünün artık gerilmesi üzerindeki ısı gerilme oranı ve sürtünme kuvvetlerinin ters yönünün etkisi olarak metal şekillendirmede indüklenen parametrelerin karmaşıklığı nedeniyle ürünler üzerinde oluşan artık gerilmeler üzerindeki hız ve basıncın etkisini tahmin etmek için QForm yazılımı kullanılarak sayısal bir çözüm elde edilmiştir. Kare zımbalar kullanılarak kare boşluklar üretmek için ileri yönde, altıgen zımbalar ile altıgen boşluklar üretmek için geri yönde olmak üzere birleşik ekstrüzyonla gerekli olan şekli üretmek için kalıp imalatı ile deneysel bir çalışma yürütülmüştür. Bu işlemde kullanılan malzeme, iyi şekillendirilebilirlik, orta ila yüksek mukavemet, iyi sertlik ve yüzey kaplama, atmosferik koşullara mükemmel korozyon direnci, iyi işlenebilirlik ve yaygın olarak bulunma özellikleri nedeniyle alüminyum alaşımı 6061'dir. Girdi parametreleri, ($P1 = 1, 4$, $P2 = 1, 6$, $P3 = 1, 8$) kN/mm^2 olmak üzere üç basınç değeri veren zımba alanının%10 oranında azaltılması ile basıncın artırılmasına ilişkin üç durum ve durumların her birindeki hızın iki katına çıkarılmasıyla elde edilen üç zımba hızına bağlıdır ($V1 = 0.25$, $V2 = 0.5$, $V3 = 1$) mm/s . Artık gerilimi ölçmek için bir X-Işını Kırınım sistemi olan XRD 3003 kullanılmıştır. Maksimum orana arttırılan hız ($V3 = 1\text{mm/s}$) işlenecek parça sıcaklıklarını, gereksinim duyulan kuvveti ve artık gerilmeleri arttırmaktadır ancak diğer yandan, hızı arttırmak akışın laminar ve homojenliğini arttırmakta ve numune kaplaması ile boyutların ve şeklin doğruluğunu iyileştirmektedir, bu nedenle $V2 = 0.5$ mm/s hızı en iyi seçimdir. Maksimum basınç $P3 = 1.8$ kN/mm^2 , ürünün şekli, homojen deformasyon ve muntazam yüzey üzerinde en iyi sonuçlara vermekte ve işlemi gerçekleştirmek ve kütüğü deforme etmek için gereken yükte azalma ile numune üzerinde oluşan artık gerilmeleri azaltmaktadır. Deneysel ve simülasyon çalışmaları arasındaki sonuç karşılaştırması, iyi bir uyum göstermektedir.

Anahtar Kelimeler: Birleşik Ekstrüzyon, Artık Gerilmeler, QForm, Poligonal Şekil.

With all my love I dedicate my efforts to my parents, my family and all people who prayed for me and supported me



ACKNOWLEDGMENTS

First of all, I want to praise and thank Allah Almighty for providing and inspiring me the willingness, opportunity and strength throughout the period of my research to complete this research successfully.

Special thanks go to my beloved homeland Iraq for having given me this opportunity to study, for which I pledge to be loyal citizen.

Thank you also to Turkey and the Turkish people and Turkish universities such as the Turkish Aeronautical Association University, Gazi University and Atılım University for their assistance.

I would like to express my deepest gratitude and appreciation to my supervisor, Prof. Dr. Çetin KARATAŞ and Co-Advisor Assist. Prof. Dr. Faruk MERT for their valuable advice, support, encouragement, competent guidance and great efforts throughout the period of this research.

My further deep gratitude, appreciation and thanks go to my father for his advice, support, encouragement, sacrifice and inspiration throughout the period of this research.

My loyalty, gratitude and appreciation of course go to my dear mother for her prayers, patience, advice and strong support for me since my childhood, all of which have sustained me thus far.

I wish to convey my appreciation to my dear brothers, who have always pushed me ahead with their encouragement and support.

Finally, all love, gratitude and loyalty to my husband and lovely son for their support and love when sharing my all difficulties and helping me to still stay strong and continue until reaching this time.

I would like to express my gratitude and appreciation to my colleagues and friends for their encouragement. I will always remember them and be grateful to them.

Thank you to Quantor Form Ltd and Stanislav Kanevskiy, Manager of the Business Development Department, for his support for the free license in the simulation program.

I am especially grateful to Assoc. Prof. Dr. Suat Dengiz and Assist. Prof. Dr. Masoud LATIFI-NAVID from UTAA for their advice and support and for their assistance in eliminating all the difficulties.

Ultimately, even though, I might have attempted to make the acknowledgment list as complete as possible, and I will undoubtedly regret any involuntary omissions of those who feel that their names are missing. For everyone who contributed, in one way or another, I will be forever grateful, thankful and humble.

TABLE OF CONTENTS

ABSTRACT	v
ÖZ.....	vii
ACKNOWLEDGMENTS	x
TABLE OF CONTENTS	xii
LIST OF TABLES	xviii
LIST OF FIGURES	xix
LIST OF ABBREVIATIONS	xxvii
LIST OF SYMBOLS.....	xxviii
CHAPTER 1	1
1 INTRODUCTION	1
1.1 Motivation.....	1
1.2 Background	2
1.3 The Problem Statement.....	3
1.4 Objective of the Study.....	4
1.5 Thesis Outline.....	5
1.6 Thesis Structure.....	7
CHAPTER 2.....	9
2 LITERATURE REVIEW	9
2.1 Introduction.....	9
2.2 Classification of Studies.....	9
2.2.1 Types of Simulation Used in Extrusion.....	9
2.2.2 Defects and Residual Stresses in Combined Extrusion	15
2.2.3 Methods and Process Parameter Effects	17
CHAPTER 3.....	25
3 PRINCIPLES OF THE EXTRUSION PROCESS	25
3.1 Extrusion Process.....	25
3.2 Advantages of Extrusion.....	26

3.3 Applications of Extrusion	27
3.4 Classification of the Extrusion Process	28
3.4.1 Extrusion Direction	29
3.4.1.1 Forward Extrusion	29
3.4.1.2 Backward Extrusion	29
3.4.1.3 Radial Extrusion	32
3.4.2 Extrusion Temperature	32
3.4.2.1 Cold Extrusion	32
3.4.2.2 Hot Extrusion.....	33
3.4.3 Extrusion Equipment.....	33
3.4.3.1 Horizontal Press Extrusion	33
3.4.3.2 Vertical Press Extrusion	34
3.4.4 Extrusion Operations	35
3.4.4.1 Continuous Extrusion	35
3.4.4.2 Discrete Extrusion	35
3.5 Special Forms of Extrusion	36
3.5.1 Impact Extrusion	36
3.5.2 Hydrostatic Extrusion.....	37
3.6 Extrusion Products Defects	38
3.7 Combined Extrusion	39
3.7.1 Combined Forward-Backward Extrusion.....	39
3.7.2 Combined Radial Forward-Backward Extrusion	40
3.7.3 Combined Backward Radial Extrusion	41
3.8 Combined Extrusion Characteristics	41
3.8.1 Advantages of Combined Extrusion.....	41
3.8.2 Combined Extrusion Products.....	42
3.8.3 Parameters Affecting the Combined Extrusion Process.....	43
3.9 Severe Plastic Deformation (SPD)	43
3.10 Residual Stresses	45
3.10.1 Effects of Residual Stresses.....	46

3.10.2	Causes of Residual Stresses	47
3.10.3	Types of Residual Stresses.....	48
3.10.4	Classification of Residual Stresses	49
3.10.5	Methods of Removing Residual Stresses.....	50
3.10.6	Methods of Measuring Residual Stresses	51
3.10.6.1	Non-Destructive Methods	52
3.10.6.2	Semi-Destructive Methods.....	54
3.10.6.3	Destructive Methods	54
3.11	Extrusion Analysis	55
3.11.1	Theoretical Analysis.....	57
3.11.2	Constitutive Equations	58
3.11.3	Experimental Work	58
CHAPTER 4	61
4	NUMERICAL ANALYSIS PROCESS.....	61
4.1	Introduction	61
4.2	Q Form Software.....	62
4.3	Numerical Analysis	63
4.4	Method	63
4.4.1	Cases of the Study.....	63
4.4.2	Types of Punch	64
4.4.3	Punch and Billet Dimensions.....	64
4.4.4	Boundary Condition.....	65
4.4.5	Material Chemical Compositions	66
4.4.5.1	Billet Material	66
4.4.5.2	Die Material	66
4.5	Die and Product Design.....	67
4.6	Simulation Analysis	71
CHAPTER 5	75
5	EXPERIMENTAL WORK.....	75
5.1	Introduction	75

5.2	The Experimental Procedure	75
5.3	(Methodology) Experimental Work	76
5.3.1	Material	77
5.3.1.1	Selection of the Work Piece Material	77
5.3.1.2	General Al 6061 Characteristics	77
5.3.1.3	Billet Preparation	77
5.3.1.4	Billet Dimensions	78
5.3.1.5	Billet Heat Treatment	79
5.4	Press Machine	79
5.5	Die Manufacturing	80
5.5.1	Die Parts	80
5.5.2	Punch Types	81
5.6	Experimental Work	82
5.6.1	Product Shape	83
5.7	Process Defects	84
5.7.1	Product Defects	84
5.7.2	Punch Defects	86
5.7.3	Defect Causes	86
5.8	Samples Preparing for Tests	87
5.8.1	Samples Cutting	87
5.8.2	Samples Molding	89
5.8.3	Samples Grinding	90
5.8.4	Samples Polishing	91
5.8.5	Sample Etching	92
5.8.5.1	Macrostructure Etching	92
5.8.5.2	Microstructure Etching	92
5.9	Tests	93
5.9.1	Macrostructure Test (Optical Micro Scope)	93
5.9.2	Microstructure Test (Stereo Macro Scope)	94
5.9.3	Residual Stress Test	95

5.9.4	Hardness Test.....	96
CHAPTER 6.....		97
6	RESULTS AND DISCUSSION.....	97
6.1	Simulation Results.....	97
6.1.1	Stress Distribution.....	97
6.1.1.1	Stress Relations at Constant Pressures.....	100
6.1.1.2	Stress Relations at Constant Velocity.....	101
6.1.2	Temperature Distribution.....	102
6.1.2.1	Temperatures Relations at Constant Pressure.....	104
6.1.2.2	Temperatures Relations at Constant Velocity.....	105
6.1.3	Process Time.....	106
6.1.4	Load.....	107
6.1.4.1	At Constant Pressure.....	107
6.1.4.2	At Constant Velocity.....	108
6.2	Experimental Results.....	109
6.2.1	Macrostructure Test (Optical Micro Scope).....	109
6.2.2	Microstructure (Stereo Macro Scope).....	116
6.2.3	Residual Stress Test.....	118
6.2.3.1	Backward Points Results.....	118
6.2.3.2	Forward Points Results.....	119
6.2.3.3	Stresses at Constant Pressure.....	120
6.2.3.4	Stresses at Constant Velocity.....	122
6.2.4	Load and Displacement.....	124
6.2.4.1	At Constant Pressure.....	124
6.2.4.2	At Constant Velocity.....	126
6.2.5	Hardness.....	127
6.2.5.1	At Constant Pressure.....	127
6.2.5.2	At Constant Velocity.....	128
6.3	Comparisons Between Simulations and Experiments.....	130
6.3.1	Loads and Displacements.....	130

6.3.2	Stress	132
6.3.2.1	At Constant Pressure	132
6.3.2.2	At Constant Velocity	133
6.4	Discussion.....	134
CHAPTER 7		139
7 CONCLUSIONS AND RECOMMENDATIONS.....		139
7.1	Conclusion	139
7.2	Recommendations	142
REFERENCES.....		143
APPENDICES		153
A.	Stresses Reports	153
B.	Aluminum Alloy 6061 Chemical Composition.....	157
C.	Engineering Drawings	158
CURRICULUM VITAE.....		165
PUBLICATIONS.....		166

LIST OF TABLES

TABLES

Table 4.1: Square Punch Dimensions.....	64
Table 4.2: Hexagonal Punch Dimensions	64
Table 4.3: Billet Dimensions.....	65
Table 4.4: Boundary condition of the process.....	65
Table 4.5: Velocity and pressure values for the three cases of the process.....	65
Table 4.6: Chemical composition of billet material of commercial Al 6061	66
Table 4.7: Chemical composition of billet material of Al 6061 from test	66
Table 4.8: Chemical composition of die and punch materials (tool steel)	66
Table 6.1: Results of stress for P1 and different velocities in three regions	120
Table 6.2: Results of stress for P2 and different velocities in three regions	120
Table 6.3: Results of stress for P3 and different velocities in three regions	120
Table 6.4: Results of stresses for V1 and different pressures in three regions	122
Table 6.5: Results of stresses for V2 and different pressures in three regions	122
Table 6.6: Results of stresses for V3 and different pressures in three regions	122
Table 6.7: Hardness values at P1 for three regions with different velocities	127
Table 6.8: Hardness values at P2 for three regions with different velocities	127
Table 6.9: Hardness values at P3 for three regions with different velocities	127
Table 6.10: Hardness values at P3 for three regions with different velocities	128
Table 6.11: Hardness values at P3 for three regions with different velocities	128
Table 6.12: Hardness values at P3 for three regions with different velocities	128

LIST OF FIGURES

FIGURES

Figure 3.1: Extrusion process	25
Figure 3.2: Billets and rods used for extrusion	26
Figure 3.3: Some applications of the extrusion process: (a) steel, (b) aluminum, and (c) plastic	27
Figure 3.4: Classification of extrusions	28
Figure 3.5: Forward extrusion process (direct extrusion)	29
Figure 3.6: Backward Extrusion process (indirect extrusion)	30
Figure 3.7: Some hollow and semi-hollow cross sections of extrusion	30
Figure 3.8: Effect of friction in (a) direct extrusion, and (b) indirect extrusion.....	31
Figure 3.9: Relationship between direct and indirect extrusion pressure	31
Figure 3.10: Radial extrusion	32
Figure 3.11: Horizontal extrusion	34
Figure 3.12: Vertical Extrusion	34
Figure 3.13: Continuous extrusion products	35
Figure 3.14: Discrete Extrusion products	36
Figure 3.15: Impact extrusion process: (a) Forward, (b) Backward, and (c) Combined	36
Figure 3.16: Impact extrusion products	37
Figure 3.17: Hydrostatic extrusion	37
Figure 3.18: Extrusion product defects	38
Figure 3.19: Combined extrusion	39
Figure 3.20: Combined forward-backward extrusion.....	40
Figure 3.21: Combined radial forward-backward extrusion	40
Figure 3.22: Combined backward radial extrusion: (1) punch, (2) die, (3) radial flow, (4) lower die, and (5) ejector	41

Figure 3.23: Applications of the combined extrusion process	42
Figure 3.24: Types of severe plastic deformation processes: (a) High- pressure torsion, (b) equal channel angular extrusion, (c) cyclic closed-die forging, and (d) accumulated roll bonding.	44
Figure 3.25: Effect of severe plastic deformation (SPD) on grain size	45
Figure 3.26: Effect of residual stresses on stress range	46
Figure 3.27: Effect of residual stresses on mechanical behavior	47
Figure 3.28: Tensile and compressive of stresses	48
Figure 3.29: Classification of residual stresses	49
Figure 3.30: Types of residual stress through different processes	50
Figure 3.31: Methods of measuring residual stresses	51
Figure 3.32: X-ray diffraction at the residual stresses	59
Figure 3.33: Residual stress measurement method	60
Figure 4.1: General steps to solve problems with the FEM simulation	62
Figure 4.2: Final product shape: (a) Hexagonal side shape produce by backward extrusion; (b) Square side shape produced by forward extrusion.....	67
Figure 4.3: Work piece shape.....	67
Figure 4.4: Punches: (a) Lower square punch for forward extrusion; (b) Upper hexagonal punch for backward extrusion	68
Figure 4.5: Shape of the die assembly of combined backward-forward extrusion	69
Figure 4.6: Parts of the die: (a) Upper punch holder; (b) Top and bottom plate; (c) Lower holder; (d) Lower billet holder; (e) Ejector; (f) Bottom plate	70
Figure 4.7: Home page of the QForm software	72
Figure 4.8: Work page of the QForm software	72
Figure 4.9: The QForm simulation for the quarter view of die and sample: (a) Billet before deformation; (b) The billet after deformation	73

Figure 4.10: QForm simulation for the half view of the die and sample:	
(a) Billet before deformation; (b) Billet after deformation	74
Figure 5.1: Billet preparation.....	78
Figure 5.2: Final aluminum billets (a) Case 1 h = 15.62 mm D = 24 mm	
(b) Case 2 h = 17.24 mm D = 24 mm (c) Case 3 h = 18.87 mm	
D = 24 mm	78
Figure 5.3: Annealing heat treatment for billets.....	79
Figure 5.4: Tensile test machine.....	79
Figure 5.5: Die parts	80
Figure 5.6: Final die.....	81
Figure 5.7: Punches: (a) Hexagonal, (b) Square, and (c) all sets	81
Figure 5.8: Combined extrusion process press, die and work piece setting.....	82
Figure 5.9: Combined extrusion process: lubrication for the die and billets.....	83
Figure 5.10: Product inside die: (a) hexagonal side, (b) square side.....	83
Figure 5.11: Final product shape	84
Figure 5.12: Samples for all cases: (a) Square side shape by forward	
extrusion; (b) Hexagonal side shape by backward extrusion.....	84
Figure 5.13: Product defects	85
Figure 5.14: Punch defects	86
Figure 5.15: (a) EDM machine for samples cutting; (b) Sample fixing in	
EDM machine.	88
Figure 5.16: Two halves of samples	89
Figure 5.17: Molded samples	89
Figure 5.18: Sample Grinding with (a) P 600; (b) P 800; (c) P 1200; and	
(d) Final grinding samples	90
Figure 5.19: Sample polishing steps: (a) 6 μm , (b) 3 μm , (c) 1 μm , and	
(d) 0.25 μm	91
Figure 5.20: Sample etching.....	92
Figure 5.21: Sample regions	93
Figure 5.22: Macro structure test (optical test).....	93

Figure 5.23: Samples micro structure test (stereo test)	94
Figure 5.24: Residual stress test machine	95
Figure 5.25: Hardness Vickers tester	96
Figure 5.26: Hardness impact and score	96
Figure 6.1: Mean stress distribution steps for Case 1 ($P_1 = 1.4 \text{ kN/mm}^2$) at V1 = 0.25 mm/s	98
Figure 6.2: Mean stress distribution steps for Case 1 ($P_1 = 1.4 \text{ kN/mm}^2$) at V2 = 0.5 mm/s	98
Figure 6.3: Mean stress distribution steps for case 1 ($P_1 = 1.4 \text{ kN/mm}^2$) for V3 = 1 mm/s	99
Figure 6.4: Mean stresses for V1 = 0.25 mm/s, V2 = 0.5 mm/s and V3 = 1 mm/s with constant pressure $P_1 = 1.4 \text{ kN/mm}^2$	100
Figure 6.5: Mean stresses for V1 = 0.25 mm/s, V2 = 0.5 mm/s and V3 = 1 mm/s with constant pressure $P_2 = 1.6 \text{ kN/mm}^2$	100
Figure 6.6: Mean stresses for V1 = 0.25 mm/s, V2 = 0.5 mm/s and V3 = 1 mm/s with constant pressure $P_3 = 1.8 \text{ kN/mm}^2$	100
Figure 6.7: Mean stresses for $P_1 = 1.4 \text{ kN/mm}^2$, $P_2 = 1.6 \text{ kN/mm}^2$ and $P_3 = 1.8 \text{ kN/mm}^2$ with constant velocity V1 = 0.25 mm/s.....	101
Figure 6.8: Mean stresses for $P_1 = 1.4 \text{ kN/mm}^2$, $P_2 = 1.6 \text{ kN/mm}^2$ and $P_3 = 1.8 \text{ kN/mm}^2$ with constant velocity V2 = 0.5 mm/s.....	101
Figure 6.9: Mean stresses for $P_1 = 1.4 \text{ kN/mm}^2$, $P_2 = 1.6 \text{ kN/mm}^2$ and $P_3 = 1.8 \text{ kN/mm}^2$ with constant velocity V3 = 1 mm/s.....	101
Figure 6.10: Temperature distribution along the work piece for $P_1 = 1.4 \text{ kN}$ and V1 = 0.25 mm/s	102
Figure 6.11: Temperature distribution along the work piece for $P_1 = 1.4 \text{ kN}$ and V2 = 0.5 mm/s	103
Figure 6.12: Temperature distribution along the work piece for $P_1 = 1.4 \text{ kN}$ and V3 = 1 mm/s	103
Figure 6.13: Temperature for V1 = 0.25 mm/s, V2 = 0.5 mm/s and V3 = 1 mm/s with constant pressure $P_1 = 1.4 \text{ kN/mm}^2$	104

Figure 6.14: Temperature for $V_1 = 0.25$ mm/s, $V_2 = 0.5$ mm/s and $V_3 = 1$ mm/s with constant pressure $P_2 = 1.6$ kN/mm ²	104
Figure 6.15: Temperature for $V_1 = 0.25$ mm/s, $V_2 = 0.5$ mm/s, $V_3 = 1$ mm/s with constant pressure $P_3 = 1.8$ kN/mm ²	104
Figure 6.16: Temperatures for $P_1 = 1.4$ kN/mm ² , $P_2 = 1.6$ kN/mm ² and $P_3 = 1.8$ kN/mm ² with constant velocity $V_1 = 0.25$ mm/s	105
Figure 6.17: Temperatures for $P_1 = 1.4$ kN/mm ² , $P_2 = 1.6$ kN/mm ² and $P_3 = 1.8$ kN/mm ² with constant velocity $V_2 = 0.5$ mm/s	105
Figure 6.18: Temperatures for $P_1 = 1.4$ kN/mm ² , $P_2 = 1.6$ kN/mm ² and $P_3 = 1.8$ kN/mm ² with constant velocity $V_3 = 1$ mm/s	105
Figure 6.19: (a) Time for $V_1 = 0.25$ mm/s, $V_2 = 0.5$ mm/s and $V_3 = 1$ mm/s with constant pressure $P_1 = 1.4$ kN/mm ² ; (b) Time for $P_1 = 1.4$ kN/mm ² , $P_2 = 1.6$ kN/mm ² and $P_3 = 1.8$ kN/mm ² with constant velocity $V_1 = 0.25$ mm/s	106
Figure 6.20: (a) Time for $V_1 = 0.25$ mm/s, $V_2 = 0.5$ mm/s and $V_3 = 1$ mm/s with constant pressure $P_2 = 1.6$ kN/mm ² ; (b) Time for $P_1 = 1.4$ kN/mm ² , $P_2 = 1.6$ kN/mm ² and $P_3 = 1.8$ kN/mm ² with constant velocity $V_2 = 0.5$ mm/s	106
Figure 6.21: (a) Time for $V_1 = 0.25$ mm/s, $V_2 = 0.5$ mm/s and $V_3 = 1$ mm/s with constant pressure $P_3 = 1.8$ kN/mm ² ; (b) Time for $P_1 = 1.4$ kN/mm ² , $P_2 = 1.6$ kN/mm ² and $P_3 = 1.8$ kN/mm ² with constant velocity $V_3 = 1$ mm/s	106
Figure 6.22: Loads for $V_1 = 0.25$ mm/s, $V_2 = 0.5$ mm/s and $V_3 = 1$ mm/s with constant pressure $P_1 = 1.4$ kN/mm ²	107
Figure 6.23: Loads for $V_1 = 0.25$ mm/s, $V_2 = 0.5$ mm/s and $V_3 = 1$ mm/s with constant pressure $P_2 = 1.6$ kN/mm ²	107
Figure 6.24: Loads for $V_1 = 0.25$ mm/s, $V_2 = 0.5$ mm/s and $V_3 = 1$ mm/s with constant pressure $P_3 = 1.8$ kN/mm ²	107
Figure 6.25: Loads for $P_1 = 1.4$ kN/mm ² , $P_2 = 1.6$ kN/mm ² and $P_3 = 1.8$ kN/mm ² with constant velocity $V_1 = 0.25$ mm/s	108

Figure 6.26: Loads for $P1 = 1.4 \text{ kN/mm}^2$, $P2 = 1.6 \text{ kN/mm}^2$ and $P3 = 1.8 \text{ kN/mm}^2$ with constant velocity $V2 = 0.5 \text{ mm/s}$	108
Figure 6.27: Loads for $P1 = 1.4 \text{ kN/mm}^2$, $P2 = 1.6 \text{ kN/mm}^2$ and $P3 = 1.8 \text{ kN/mm}^2$ with constant velocity $V3 = 1 \text{ mm/s}$	108
Figure 6.28: Backward view points of the sample for different velocities	109
Figure 6.29: Forward viewpoints of the sample for different velocities.....	110
Figure 6.30: Corner towards the backward viewpoints of the sample for different velocities	111
Figure 6.31: Corner towards the forward viewpoints of the sample for different velocities	112
Figure 6.32: Surface center between backward and forward extrusion for different velocities	113
Figure 6.33: Optical scope macrostructure for Case 2 with X50 on all sample regions at $V1 = 0.25 \text{ mm/s}$	114
Figure 6.34: Optical scope microstructure for Case 3 with X200 on all sample regions at $V1 = 0.25 \text{ mm/s}$	115
Figure 6.35: Microstructure for backward and forward views at different velocities.....	116
Figure 6.36: Microstructure for backward view points for different velocities.....	116
Figure 6.37: Forward view points for different velocities	117
Figure 6.38: Horizontal surfaces between the backward and forward view points for different velocities.....	117
Figure 6.39: Residual stress report for the backward region	118
Figure 6.40: Residual stress report for the forward region	119
Figure 6.41: Stresses at many regions with constant pressure $P1 = 1.4 \text{ kN/mm}^2$ and different velocities	121
Figure 6.42: Stresses at many regions with constant pressure $P2 = 1.6 \text{ kN/mm}^2$ and different velocities	121

Figure 6.43: Stresses at many regions with constant pressure P3 = 1.8 kN/mm ² and different velocities.....	121
Figure 6.44: Stresses in many regions with constant velocity V1 = 0.25 mm/s and different pressures	123
Figure 6.45: Stresses in many regions with constant velocity V2 = 0.5 mm/s and different pressures	123
Figure 6.46: Stresses in many regions with constant velocity V3 = 1 mm/s and different pressures	123
Figure 6.47: loads and displacements for velocities at P1 = 1.4 kN/mm ²	124
Figure 6.48: loads and displacements for velocities at P2 = 1.6 kN/mm ²	124
Figure 6.49: loads and displacements for velocities at P3 = 1.8 kN/mm ²	124
Figure 6.50: loads and displacements for velocities at P1 = 1.4 kN/mm ²	125
Figure 6.51: loads and displacements for velocities at P2 = 1.6 kN/mm ²	125
Figure 6.52: loads and displacements for velocities at P3 = 1.8 kN/mm ²	125
Figure 6.53: Loads for different pressures at V1 = 0.25mm/s.....	126
Figure 6.54: Loads for different pressures at V2 = 0.5mm/s.....	126
Figure 6.55: Loads for different pressures at V3 = 1 mm/s.....	126
Figure 6.56: Hardness in three regions for constant velocity V1 = 0.25 mm/s with different pressures	129
Figure 6.57: Hardness at three regions for constant pressure P1 = 1.4 kN/mm ² with different velocities.....	129
Figure 6.58: Comparison of loads between the simulation and experiment at V1 = 0.25 mm/s.....	130
Figure 6.59: Comparison of loads between the simulation and the experiment at V2 = 0.5 mm/s.....	130
Figure 6.60: Comparison of loads between the simulation and experiment at V3 = 1 mm/s.....	130
Figure 6.61: Comparison of loads for simulations and experiments at V1 = 0.25 mm/s.....	131

Figure 6.62: Comparison of loads for simulations and experiments at
 $V_2 = 0.5 \text{ mm/s}$ 131

Figure 6.63: Comparison of loads for simulations and experiments at
 $V_3 = 1 \text{ mm/s}$ 131

Figure 6.64: Comparison of stresses between simulations and experiments
for different velocities at constant pressure:
(a) $P_1 = 1.4 \text{ kN/mm}^2$, (b) $P_2 = 1.6 \text{ kN/mm}^2$ and
(c) $P_3 = 1.8 \text{ kN/mm}^2$ 132

Figure 6.65: Comparison of stresses between simulations and experiments
for different pressures at constant velocity:
(a) $V_1 = 0.25 \text{ mm/s}$, (b) $V_2 = 0.5 \text{ mm/s}$ and (c) $V_3 = 1 \text{ mm/s}$ 133

LIST OF ABBREVIATIONS

CFBE	:	Cyclic forward-backward extrusion
CEC	:	Cyclic extrusion compression
ECAE	:	Equal channel angular extrusion
SPD	:	Severe plastic deformation
UFG	:	Ultrafine grain
NG	:	Nano grained
QF	:	Q Form method
FE	:	Forward extrusion
BE	:	Backward extrusion
CE	:	Combined extrusion
CBFE	:	Combined backward forward extrusion
CBRE	:	Combined backward radial extrusion
FEM	:	Finite Element Method
UBT	:	Upper bound theorem
UBET	:	Upper bound element technique
KAVFS	:	Kinematically admissible velocity fields
CAPP	:	Computer aided process planning.
CAE	:	Computer aided engineering
SEM	:	Scanning electron microscopy
TEM	:	Transmission electron microscopy
RCT	:	Ring compression test
SCFBE	:	steady combined forward-backward extrusion test

LIST OF SYMBOLS

r_x	:	Extrusion ratio
A_0	:	First cross section area of work piece
A_f	:	Cross section area after extrusion
ϵ	:	True strain
P	:	Punch pressure
\bar{Y}_f	:	Flow stress average when deformation occurs
ϵ_x	:	Strain of extrusion
P	:	Pressure of indirect extrusion
p_f	:	Pressure used to pass the friction
μ	:	Friction coefficient
p_c	:	Pressure required to push work piece against die wall
Y_s	:	Shear yield strength
L	:	Length of work piece prepared for extrusion
D	:	Work piece diameter
F	:	Punch force
P^0	:	Power
v	:	Punch velocity
$\bar{\sigma}$:	Effective stress
$\bar{\epsilon}$:	Effective deformation rate
$\dot{\epsilon}_{ij}$:	Strain tensor rate
$\dot{\sigma}_{ij}$:	Stress deviator
λ	:	X-ray wavelength
d_{hkl}	:	Inter planar spacing
h	:	Billet height
D	:	Hexagonal punch diameter
S	:	Side length of hexagonal shape
L	:	Square punch length

- d : Billet diameter
A : Cross sectional area of punches



CHAPTER 1

INTRODUCTION

1.1 Motivation

In recent years, different metal forming processes have become important in industry because of the increasing cost of raw materials. Some manufacturing processes, such as machining, include the waste of material by removing material during production. Therefore, researchers have been focusing their efforts on finding more economical methods to produce a final form.

To increase competitive fields for companies and institutes and to provide for user requirements, significant changes to production methods and technologies have been achieved to decrease the time of product manufacturing, reduce production costs and increase quality of products. These are significant points that encourage competitors for more fulfillments and investigation [1].

In comparison between cold forging and extrusion against the rest manufacturing processes used in industry and production, many characteristics can be recognized such as: low rate of waste of materials, high surface finish, more proper dimensional accuracy, improvements in the mechanical properties of products when compared with main materials, and decrease the needs to further processes such as machining.

Metal forming is a process of metal working to manufacture metal parts and products by deforming pieces plastically and reshaping them into a required design with no addition or removal of material in terms of quantity and mass during the process [2].

Extrusion processes are significant because of production cost reductions with increasing product quality and production rates. In extrusion compression, stress increases as a result of the response between the billet and container and the punch, which has a great influence on decreasing fatigue and cracking in the material during the process.

The necessity to reduce production time, defects and probability of failure lead to great influences on manufacturing processes and require the invention modern methodologies and techniques of the production process [3].

The metal forming process in general and the extrusion process in particular are of special importance due to their ability to produce parts with high material properties in comparison to those produced by machining, casting or assembling many parts of various manufacturing technologies.

The extrusion process can be classified according to punch direction into three main categories: (1) forward extrusion (direct); (2) backward extrusion (indirect); and (3) radial extrusion. Moreover, two of the these can occur simultaneously in order to perform many combinations of extrusion processes. In the combined forward-backward extrusion process, the punches force the work piece on two sides into the die to produce parts with different polygonal hollow shapes and a constant cross section, such as hexagonal, square, triangle, gear and pentagonal cross sections [4].

1.2 Background

Among bulk metal forming groups, extrusion is one of the most important processes which have a wide application in different fields. It is a manufacturing process that uses high punch speeds with special dies. Some types of extrusion, such as cyclic forward-backward extrusion (CFBE), cyclic extrusion compression (CEC) and equal channel angular extrusion (ECAE), are considered to be severe plastic deformation (SPD) methods, which are followed to improve the mechanical

properties of a material by producing ultrafine grained (UFG) and nano-grained (NG) properties. In comparison with other manufacturing processes, extrusion is an economical process. A number of studies have determined flow characteristics, die geometries, temperatures, loads, lubrication and strain statuses [5]. The products of extrusion are many in number and include complex parts of collar flanges, spur gear and splines with shafts. There are three main types of extrusion process that are classified according the direction of material movement, namely forward (direct) extrusion (FE), backward (indirect) extrusion (BE) and radial (lateral) extrusion. New methods can combine two or three of these types, such as CBF or CBRE, to determine which billet is simultaneously extruded in the forward, backward and radial directions through plural orifices in the special die. Tubular parts with multiple diameters, hollow parts with polygonal shapes, nuts and bolts, adapters and flanged shapes are some of the combined extrusion applications. In recent years, studies that deal with die design and process conditions in combined backward-forward extrusion processes are limited and there are many neglected points still not highlighted which need more study, such as the effect of residual stresses, velocity and pressure during the process and lubrication [6].

1.3 The Problem Statement

In cold forming, a process of forward-backward extrusion is used for production. It has many advantages, such as economical production and an improvement of product quality as well as energy savings with mass production.

Recent studies have been performed on this type of extrusion since most tools used in connecting engines with transmission systems must be polygonal rods with hollow tubes.

It is important to know the behavior of the material, the shape of products and the alternative effects between these parts and the tools.

A number of geometrical parameters influence the flow of the material in backward-forward extrusion, such as gap height, die corner radius, and the process conditions of pressure intensity, velocity, friction and residual stresses. Moreover, the thermal stresses are introduced from the high friction with the die walls and the speed of metal flow [6].

During non-uniform inelastic loading, the result is a desirable surface with residual compressive stresses when the load is removed. Surface regions that yield in compression during non-uniform inelastic loading also result in undesirable surface residual tensile stresses when the load is removed [7].

These undesirable residual stresses are a problem and pressure with velocity durations have a major effect on them. It is necessary to know how to maintain the compression of the desirable stress and reduce any undesirable stress of the residual stresses by controlling the pressure and velocity.

1.4 Objective of the Study

Many parameters affect the combined extrusion process, and different previous studies have investigated the behavior of deformation for this process.

Previous studies discussing this process have been small in number and mention the effects of the geometries of the die and punch, the influence of the process condition and the effect of friction, the extrusion ratio effects, the temperature effects, lubrication and defects during the process.

This study focuses on manufacturing products with polygonal shapes from two sides, such as wrench sockets and valves. These shaped products have symmetric planes when divided into two parts, which helps during numerical and experimental investigations. The aims of this study are to:

- Clarify the combined backward-forward extrusion process and its characteristics.

- Produce parts with hollow cross sections from two sides, namely square and hexagonal shapes in one stage.
- Determine the residual stresses generated in this process.
- Investigate the influence of pressure and velocity on residual stresses.
- Investigate the power and forces required to produce this type of tool by combined extrusion.
- Design and manufacture a die for the experimental work of the combined forward-backward extrusion process.
- Highlight the importance of replacing many traditional processes in design and manufacturing with new development processes.
- Draw back the traditional method of manufacturing and demonstrate the alternative suitable new methods and their requirements.
- Utilize previous research in combined extrusion to develop and improve this process in manufacturing; and
- Confirm the significance of the numerical analysis and simulations in the simplification and acceleration of the process and tool design with improvements in the product quality using Q Form (QF) software.

1.5 Thesis Outline

Chapter 1

In this chapter, an introduction, background, problem statement, aims of this study of extrusion process are presented with a clarification of the thesis outline and work structure.

Chapter 2

A review of all studies related to the subject are discussed by dividing the research into three types according to the work of the respective researchers in these studies.

Chapter 3

The general conceptions, types, classification, equations of theoretical analysis, applications and basic rules of the extrusion process and residual stresses are presented.

Chapter 4

A discussion is presented of the numerical solution using the QForm method in addition to the general definitions, procedures of using the QForm program with its concepts, boundary conditions and die design.

Chapter 5

The experimental work, methodology, die manufacturing and billet prepering are explained in this chapter. Different tests being made on hardness, microstructure and the residual stresses.

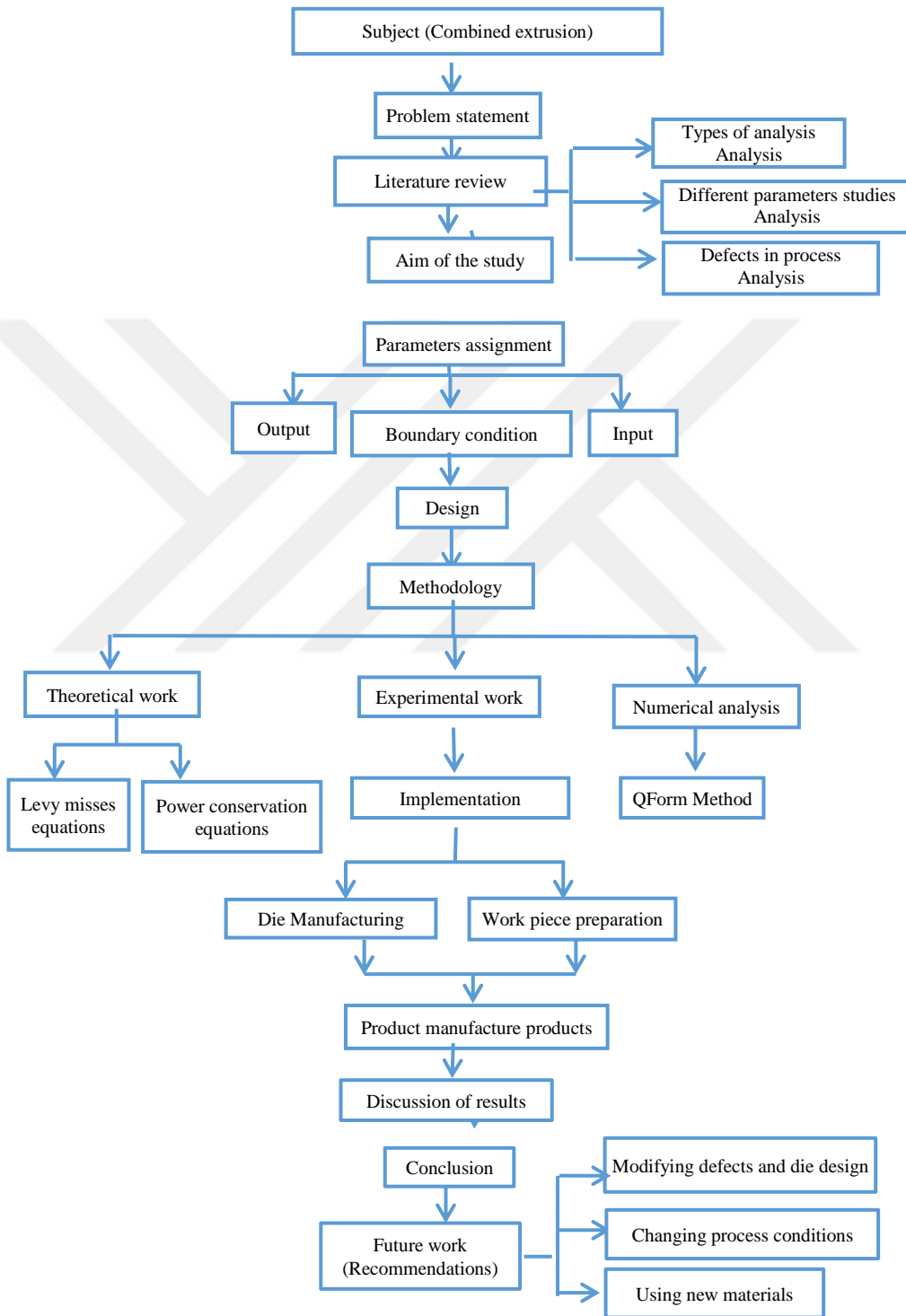
Chapter 6

This chapter presents the results with figures of the simulation analysis and experimental work with a discussion of the results and analysis.

Chapter 7

Finally, the conclusion of the study and work are revealed followed by future works and recommendations.

1.6 Thesis Structure



CHAPTER 2

LITERATURE REVIEW

2.1 Introduction

Researchers are continuing to meet the challenges in manufacturing and industry to produce parts of high strength, resistance to fatigue and corrosion, better surface finish and no further processing, all with low time and low cost production. Forming, which has the additional advantage of greater utilization of raw materials and high productivity, has the ability to produce parts with the abovementioned advantages. Among the forming processes, combined extrusion is a process which can produce many complex shaped products with high mechanical properties and near net shape production.

Research dealing with combined backward-forward extrusion and its properties is rarely found; therefore, this subject is being investigated.

2.2 Classification of Studies

The studies are classified into three fields according to the parameters and subjects with process defects that were discussed in various papers and studies.

2.2.1 Types of Simulation Used in Extrusion

M. Math and B. Grizelij discussed a numerical simulation for combined forward-backward extrusion for the body of automatic valves. The production during metal forming should be mass production with high dimensional accuracy. It is important to assign and know the material flow properties, alternative influences for the tool

and product shape. For this reason, numerical analysis was used to predict the parameters and their distribution during the work piece deformation and process. It was shown to have many advantages to reduce the cost of production and increase product quality by predicting the results before any experimental work. The study explained how to perform modelling with numerical analyses for the combined extrusion process and an investigation of the amount of stress and its distribution using Finite Element Method (FEM) method. During simulation, many problems appeared, such as thermal effects and mechanical troubles. The plastic deformation process caused an increase in the inside temperature of the part which enhanced heat transfer. These numerical analyses help engineers in design and development by avoiding being dependent on experience and trial and error methods. The residual stress calculation showed equilibrium. To achieve a successful simulation, important points should be considered, such as the size of the elements of the mesh, numbers, shapes and precise boundary conditions [1].

A. Farhoumand et al. showed the benefits of using numerical analysis (NA) of FEM to analyze the process of combined forward, backward and radial extrusions by studying the effects of die shape parameters and input method factors. A comparison of load results was made between the numerical analysis and the experimental work with the aluminum work piece and shaving foam as lubrication at many parts of the die. The strain rate and hardness were calculated in various cross sectional areas. It was shown that for different die shapes and factors, there was a great effect on the load. An important influence of the direction of the material flow was the height of the gap with a great influence of the radius of the die corner to control the friction factor and the direction of material flow towards radial or backward extrusion and to reduce the friction factor for a balance in the material flow to occur. For the hardness tests, the results were used to draw the curve [2].

Wu Shi-Chun et al. explained the upper bound theorem (UBT) using rigid triangle velocity to perform a numerical analysis of the combined extrusion process. A derivation of pressure was done and compared with the results of the slip line

theory. Lead (Pb) was used as work piece material with rape oil lubrication. A dead zone was noticed and controlled to reduce the region that was not deformed. The goal was to achieve minimum friction between the billet and die parts during the process by using effective lubrication. The curves of the forces for both the experimental work and theoretical analysis were parallel. An equation, which was used with high accuracy, to calculate the punch pressure was derived with the Upper Bound Method [8].

J.C. Choi et al. used a semi solid material as their work piece in a combined extrusion to analyze the different factors using the Finite Element Method because of the wide use of products that are produced by semisolid forming, such as airplane and automobile products. The study investigated the microstructure of the parts and the temperature distributions using Aluminum alloy A 365. The benefit of using semisolid working is to produce the final shape near net shape. Many factors affect semisolid forming, such as the heating temperature, the time of compression and velocity of pressing. Four steps were taken for their procedure: (1) Preparation of the material; (2) Heating the material (3) Product compression holding; and (4) Product ejection. For this type of forming, there were two phases: (1) solid with visco-plasticity behavior, and (2) the liquid obeying the Darcy equation [9].

B.C. Hwang et al. investigated the load and velocity for combined extrusion processes in non-axisymmetric conditions using the upper bound element technique (UBET). An analysis of kinematic admissible velocity fields (KAVKS) was made with a solid cylinder-shaped lead workpiece being used. Experimental work was performed to produce a wrench socket part and then the results of the loads and velocities were compared with the numerical analysis. The equation of the stress-strain relation was derived while the results showed increases in load with the stroke increase [10].

P. Petro et al. discussed the use of Q-Form 2D as an FEM technique to investigate the modern forging method for a circle product with edges. The best boundary condition was decided by using finite element simulation, which led to optimum production for the required part which was free of defects along with a reduction in

production cost and time. The mechanical properties were also found for the new product. As a result, the researchers found that the development method reduced the force required for the forging process and it improved the ability of filling the die. Depending on numerical method results, the die design was easier and the new method proved that it was able to produce round parts with edges by using isothermal and surrounded dies for the forging process to produce items with a final shape without subsequent processes. The simulation results showed a broad consistency with the experimental values [11].

M. Milutinovic et al. showed that in other work of combined extrusion, a backward and radial extrusion can occur together to produce flanged parts. A simulation was made to investigate the stresses generated in the product during the process. The ABAQUS application, which is a type of finite element program, was used to study the forming process in the shape of solids and frames when an external load is applied with linear and nonlinear conditions. There were many advantages of using these computer programs, such as easier and faster processing with suitable and correct die designs. They also helped to improve and develop the steps of the process, as well as produce less material waste, improve product quality, and decrease production costs. Steel was used as the work piece material to find the important regions and points in material flow during the process. It was found that the highest stress value would occur at the sharp edges of the die, implying that die geometry had a great effect on stress distribution [12].

H. Haghghat et al. showed that there were many studies taking into account the use of the Upper Bound Method as a method of simulation, especially in extrusion processes. The study calculated the power required for the process and found the effect of velocity changing and friction effects when increasing the power. A conical die was improved to use in the process for bimetallic rods and the best angles of die were found with other input parameters [13].

A. Milenin, et al. worked with a simulation method related to the QForm 8 method to predict the nature of fractures that may occur while producing tubes of high thickness walls using steel with low ductility in metal forming. In low ability of

working for steel alloy, fractures are likely to occur due to brittleness for such steel. By depending on stress and strain in the Finite Element Method, occurrences of fractures were studied. In addition, during production of thick wall tubes, the process was repeated many times as a cyclic deformation. This led to residual stresses being formed. The general residual stresses were divided into compression and tension residual stresses with the latter always enhancing the occurrences of cracking and fracturing. The paper discussed the problem by dividing the work into two types. The first used a model depending on elastic plastic deformation and elastic unloading, while the second used the rigid plastic flow rule. It was found that for the first type, the residual stresses occurred in the region of deformation as well as on the entire tube, while for the second model, the residual stresses formed only in the region of deformation [14].

T. Milek et al. used a modeling method by applying the QForm-2D numerical method to evaluate the ability to manufacture axisymmetric walls with thin thickness and square sections by indirect extrusion. The billet they used was Aluminum 1050 and the boundary conditions were specified for use in a simulation to find the mechanical properties of the aluminum alloy. As a result, it was found that they could manufacture thin square sections of thin walls made of aluminum die stampings with $h_1/b = 3.6$ and a ratio of $h_1/b = 8.5$ for lead dies. The load increment belonged to the displacement of the punch increment when disregarding the effect of friction in the simulation work. The same results occurred in their experimental work; however, a lubricant had been used. The researchers found that they could check the same process with other h_1 to b ratios. This process could be taken as a reference to improve the manufacturing methods to achieve die stampings in indirect extrusions [15].

R.K. Sahu, et al. analyzed a combined extrusion process for multi-hole extrusion. The effects of the extrusion load and the length of the extrusion stroke were studied with the help of the Finite Element Method by using punch velocity and die length as input parameters. It is shown that the ironing influence had a great effect on the load. When comparing two different dies, one with five holes and the other

with nine holes, a variety of effects on material flow was observed. Multi-hole extrusions are performed to improve the production in which a work piece can move through many holes so different extruded parts can be produced in the same process. Many parameters affect this process and the features of the products from this process, such as the number and region of the holes, extrusion ratio, velocity, and process lubrication [16].

P. Abhari et al. worked with radial extrusion to produce parts without flashes or flanges. The study discussed the effects of load for the upper die and punch, the disposal of the material during the process, and the amount of stress and strain. It used both theoretical calculations and numerical simulations for the two shapes of the radial extrusion without flash. The investigation was made of the die shape factors, work piece size, and power. The paper showed the relation between stress and strain, load and stroke of the punch, the shape of deformation by using gridlines, and the load of the upper die with the space not filled at one end or two ends without the flash extrusion process. The results showed that the maximum values of stress and strain would occur at a ratio of $R_i/R_o = 2$ and the load amount at one end would be greater than those of the two ends [17].

B. Moroz et al. studied the FEM model using the QForm program to predict extrusion process parameters. The paper shows the direct and indirect extrusion process and calculations of the friction force during the process. The pattern of the product could be predicted according to the boundary condition. The relation between the flow and the friction force value was found between the work piece and die wall. The properties of material flow, the distribution of the pressure in the contact area, and normal stresses were found. During the QForm simulation, the extrusion force was calculated in addition to the thermal properties of the work piece and the effect when using air for cooling when touching the tool. The numerical solution was found as well as the stresses and strains through the process. The features and extrusion properties were found through a simulation when disregarding the friction force in the first steps of the process. The results showed good agreement with the basic rules related to metal forming and stress

states. The numerical results proved the validity of using the QForm applicaiton to predict the parameters as an arrangement step to the experimental work [18].

K.C. Nayak and S.K. Sahoo discussed a method that would produce parts with complicated shapes and many details. Their method passed through various manufacturing procedures and subsequent processes such that while using a combined forward-backward extrusion process, it would be easy to produce different parts with many details. In this study, a closed die was used to produce four various geometries of socket adapters by using combined extrusion with aluminum work piece material. A simulation was performed and a solution was found and compare with experimental work by preparing a suitable die to produce four shapes of socket adapters. It was considered most important that the load and material flow was calculated in this process [19].

2.2.2 Defects and Residual Stresses in Combined Extrusion

E.H. Lee and R.L. Mallett showed the residual stresses in parts produced by extrusion, which is one of the important problems that should receive great attention from researchers. In fact, studies that have been dealing with stress generated in combined extrusion are still limited. In one direction extrusion, there are many studies investigating the stress distribution along the part. The stresses inside the product lead to many defects, such as internal or external cracks while such parts are being used. To understand the stress and strain behavior, it is necessary to analyze elastic and plastic deformation [20].

R.M. McMeeking et al. investigated the existence of residual stresses in parts after metal forming processes had led to many problems. Such problems occurred because of non-uniform deformation and different distributions of strains in billets during pressing. In order to gain useful residual stresses, it was shown that controlling the die geometry had great effects. In this study, a numerical analysis depended on very accurate boundary conditions and exact equations were used for perfect results of the analysis. The reduction of the area in the die during

deformation had a great influence on residual stresses and the amount of friction occurring during the deformation [21].

D.J. Lee et al. showed that during combined extrusion, many defects can occur that reduced product quality and decreased service times, which in turn would lead to high production costs. There found a significant zone called the dead metal zone in which material cannot flow uniformly inside it, thereby causing metal flow defects or deformation defects, also known as a folding defect. This would usually appear in parts of low thickness, which reduced the accuracy of the dimensions and decreased the strength of the product and increased the probability of fatigue. The study was conducted to investigate how to avoid this defect by reducing this dead zone and maintaining uniform metal flow. FEM was used for this analysis to predict a suitable die design followed by comparing the results of the experimental work. Alloy steel was used as the work piece material to produce piston pins in two extrusion modes, namely forward and backward. The study demonstrated that controlling the die design can reduce or remove this type of defect by filling all die parts during the flow and avoiding dead zones [22].

X. Ma et al. showed that for metal forming in general and aluminum extrusion in practice, the amount of friction between the billet and die wall has a great influence. In addition, the use of lubrication would also affect the process. Occasional sticking would occur because of the high friction factor, which resulted in a reduction in metal sliding. Die design with a friction effect can control these metal flow defects. If friction increases, the dimension of metal sliding decreases and the metal sticking dimension increases. Sticking also increases when pressure is high while the sliding length decreases with a decrease in die angle [23].

N.S. Rossini, et al. investigated how residual stresses always had an important effect on product quality and product properties, such as strength fatigue resistance. The study explained the types of residual stress and the measurement methods, which would provide a good reference to any researcher to select a suitable technique according to their subject states. The research classified the types of residual stress measurement methods into three types according to how the

materials were treated, namely destructive; half destructive; and non-destructive. Generally, the destructive method was used more than the other types of method because of its easy technique and requirement for less accurate measurement that depends on essential magnitudes and constants. Every technique has its beneficial and non-beneficial aspects. A suitable method and most economical technique was demonstrated in this study and there are new points as recommendations to investigate and develop these techniques [24].

P. Abhari discussed the defects in the combined radial-forward extrusion process for rounded dies. The study showed how to produce accurate products without any defects with this method of metal forming. The numerical method used in this paper was the QForm-2D program to demonstrate the properties of the flow, the main stresses and the strains during various steps of the process with many parameters changes. The pressure changes with punch movement were also calculated in the study. By using the gridlines method, the forming features were found. The researcher discussed how to obviate the folding defect during the process. As a result, it was observed that a higher pressure on the punch would occur with a ratio of $h/R_1 = 1$, while for $h/R_1 = 1.4$, it was 1.8 or less. There were two general steps to reduce or cancel the folding defect [25].

2.2.3 Methods and Process Parameter Effects

S. Abd Alkadam discussed the effect of metal forming speed on the stress distribution on combined backward-forward extrusion with high surface finishes for dies and punches with high viscosity lubrication. Three punch speeds were selected. Two types of punch were used: a circular head punch and a hexagonal punch. Two reductions in cross-sectional area for backward extrusion were used and two different reductions in cross-sectional area for forward extrusion were selected. The experimental results showed that there were significant effects from the backward geometrical factors when they combined with the forward factors. The results showed that the profiles of die surfaces have an important effect on the homogeneity of the material flow in the forward direction [3].

K.C. Nayak and S.K. Sahoo studied the estimation of the forming force for the combined extrusion-forging process of regular shapes. The micro hardness of components and grain structure were studied. Experimental studies were performed by comparing some of the simulation results using Finite Element Analysis. The experimental work included a male-female socket spanner or adapter with a round billet and a flat die. Finite Element Analysis was performed for loads with stress, strains, total velocity punch displacements, and metal flow patterns. The results showed good agreement between the experiments and simulations [4].

K. Kuzman et al. worked with a combined extrusion process and showed that there were many parameters affecting the process and having direct influences on product quality and production costs. To understand die geometry and friction effects, a numerical analysis was made to demonstrate the effects of these parameters during the process and to determine the optimal values that would reduce production cost and time and increase product quality. This was done when the DEFORM method was applied and the results were compared with the experimental work of the backward-forward extrusion work. Computer Aided Process Planning (CAPP) and Computer Aided Engineering (CAE) helped to organize the die and tool dimensions and their accuracy, and these aids would be used in all fields of severe plastic deformation both in mass production and in private forming processes [7].

D.J. Yoon et al. used many materials to investigate the effect of forming properties during extrusion processes. A magnesium alloy was one of these materials used as a work piece material to be deformed in two extrusion directions: (1) forward, and (2) backward to demonstrate the influence of the extrusion ratio and process temperature. It was shown that good and accurate results could be achieved for magnesium at temperatures near 225°C with an increase in the strain, which increased the fatigue and crack range. However, reducing the pressure was shown to avoid the start of fast cracking. The experimental work of combined extrusion was performed by using a proper die of tungsten carbide and high tool steel punch material. The results were compared with the numerical analysis for the cup

product shape. Heat treatment was applied to the billets prior to deformation to increase the uniform grain distribution followed by uniform deformation [26].

J.H. Muhamed et al. studied the effect of die geometry on combined extrusion, which is still under investigation as it is an important process that even attracts other researchers. However, there is still much that has not been studied but should be studied and demonstrated. The punch shape and reduction area was studied as the input parameters for the experimental work to produce samples with different polygonal shapes with forward and backward extrusion. The output parameter was the load required to deform the aluminum billets with two different punch shapes. It was shown that the load changed with area reduction changing [27].

R.A. Hussien showed that there was another effect of die geometry during combined backward-forward extrusion processes, especially an effect on stress and temperature during deformation. When the temperature distribution changed, the load and power also changed, so a numerical analysis was performed to determine the influence of flat and curved punch shapes on temperature rises and stress generation. An aluminum alloy work piece was used in the simulation to predict the temperature and pressure distribution. The results showed that the process would be more complicated when the backward and forward extrusions were combined, and generally there would be a small influence of the die shape on temperature distribution but great influence of the die shape on stress distribution. A rounded punch had better effects and results than a flat punch and generally sharp edges would always increase the temperatures and stresses in those regions, while curved surfaces would decrease the temperatures and stresses [28].

H. Alihosseini et al. studied many processes that depended on high plastic deformation in order to increase mechanical properties of a number of soft materials, such as magnesium and aluminum, by reducing the grain size with high strains. These processes were called severe plastic deformations and repeating combined extrusion was one of the processes in which the pressing was repeated many times in different directions in order to decrease the grain size and reach

ultrafine grains, thereby increasing the strength of the materials. In this manner, the ductility decreased against the increase in the yield strength of the metals. For three repeating cycles, it was shown that three cycles increased the strength four times more than one cycle with hardness also being improved in each cycle of combined forward-backward extrusion [29].

H. Alihossieni et al. worked on the severe plastic deformation of many pressing processes for aluminum Alloy 1050 with a combined extrusion process to increase the strength of materials by decreasing the grain size. Hardness was doubled after one pressing process and the grain size decreased to approximately 1 μm . Two types of punch were used in this process, namely a hollow punch for backward extrusion and a solid flat punch for forward extrusion [30].

R. Matsumoto et al. studied many methods to find the optimal method for lubrication during combined extrusion processes. The new method of lubrication depended on an existing small channel inside the punch to maintain continuous lubrication during pressing by using a servo press; the lubricants would flow during recovery of the press and pushing it. It was found that a high aspect ratio gave good results and the friction force would decrease between the work piece and die. Numerical analyses with the experimental work were performed for comparison and a suitable die was designed to achieve combined extrusion for an aluminum billet. The new method with self-lubrication was more efficient than the normal punch, especially for the friction factor and load. The material flow and deformation depended on the punch movement speed and the wearing of the punch was affected by the amount of lubrication as well as the friction factor that could reduce the forces, increase punch life and improve product quality of good surface finishing [31].

H. Jafazadeh et al. demonstrated how the combined extrusion process depended on merging two or three extrusion processes at the same time of pressing. They showed that this could be either forward with backward extrusion or forward with radial or forward-backward-radial extrusion. This process showed many advantages, such as decreased cost, increased product quality and safe times. To

perform this process efficiently, it was important to understand the parameters affecting the deformation process and how to control these parameters to obtain good results. The researchers showed that die design and die shape had a great effect on combined extrusion and the study used an aluminum alloy to demonstrate the influence of die geometry on the metal flow with finite element analysis. A number of defects and problems had occurred, such as a separation of material parts from the height or length as well as non-symmetric material flow. Different wall thicknesses of the product produced many defects in the shape, which can be avoided by controlling the die design. The high friction factor led to an improvement in the material flow; however, it increased the load and power required and reduced die life [32].

J. Piwnik et al. showed that in the same procedure of extrusion, microextrusion would take the researchers' concentration to investigate the effect of lubrication and the friction factor on the load required and on product quality. To produce micro products, the process had to be micro forming and it was considered to be mass production with good product surface finish. The study used the Finite Element Method to explain the effect of friction on tool roughness and forces during deformation. The effects of roughness on tool life appeared more clearly in the fine grain material than in the coarse material [33].

P. Koprowski et al. investigated combined extrusion with KoBo extrusion, a process that is performed with the help of the cyclic rotation of the die. The mechanical properties, such as ductility and strength, were studied at different changes of die frequency for the aluminum alloy work piece which was heat treated before the process. Hardness and microstructure tests were performed on the products to demonstrate the influence of frequencies with transmission electron microscopy (SEM) and transmission electron microscopy (TEM). These tests would also show how precipitation processes were affected by changes in frequency. The results revealed that decreasing the frequency would increase grain boundary numbers, which means a decrease in grain size. For high frequencies, new arrangements in the grains and recrystallization of the grains would occur [34].

C. Hu et al. studied complicated geometries and parts with many details and found that combined extrusion was the optimal choice to achieve the process. In such forging processes, it was found that friction was a great problem that should be controlled; otherwise, costs would increase and product quality would decrease. Their first step was to avoid or reduce dead zones. A new method was followed to determine the friction and control it during backward and forward extrusion. A numerical analysis utilized many parameters, such as die shape and different friction factors to demonstrate the optimal process condition with various types of lubricants in the process in addition a process without lubrication. When comparing the two types of tests to determine the friction factor, 1) a ring compression test (RCT) and 2) a steady combined forward-backward extrusion test (SCFBE) were conducted and observed. The results showed that the SCFBE test needed less load than the RCT and the values of the friction factors determined by SCFBE were larger than those of the RCT test. Moreover, they found that in the steady combined forward-backward extrusion tests, there were no dead zones [35].

C.Y. Sun et al. investigated combined extrusion processes that included lateral and axial directions used to produce parts with many branches. Stainless steel was used to investigate the advantages of the combined process for the type of part consisting of many junctions. The results showed that this extrusion would produce parts with fine grain and no defects at the junctions as well as high loads and forging would reduce the friction factors. It was found that product life would increase because of grain refinement in the corner areas [36].

C.C. Chang et al. discussed how the friction factor during pressing in combined extrusion of forward-backward extrusion processes was a serious problem which had drawn the attention of many researchers. The contact area between the billet and die surface showed friction, which increased the load and power. Brass was used as a micro scale to produce hollow shapes and to demonstrate the influence of lubrication and grain size on reducing the friction during the process. Both a numerical analysis and experimental work were applied to reveal the results and to compare them. Lubrication reduced the friction factor and the influence of friction,

while they decrease when in a non-lubricated condition. For grain size, it was shown that friction rose with and increase in grain size [37].

S.S. Jamali et al. worked on a combined extrusion process using small magnesium alloy billets to produce parts of seamless tubes with large diameters. Two directions of material flow were achieved simultaneously: 1) the radial direction, and 2) the forward direction, which was able to apply high strains during deformation, thereby increasing the mechanical properties of the products. Generally, it was most suitable for magnesium alloys to be deformed with hot working to allow recrystallization to occur. In such deformation, severe plastic changes would occur and grain sizes were refined with increases in strength and hardness. The results of the section tests showed that there was good homogeneity in the product due to the high strains. the load required is halved if it is compared with traditional extrusion processes [38].

M.H. Paydar et al. investigated another application for combined extrusion in powder metallurgy to find the optimal method to merge particles of aluminum. Two modes of material deformation would occur, first in the forward deformation direction and second as equal channel angular pressing on the same die. Another process for normal extrusion processing was done to another billet in order to compare the effect of these two processes in terms of strength and hardness by achieving optimal merging to increase grain cohesion. The results showed that their new method of forward extrusion with equal channel angular pressing was more efficient than traditional extrusion processes to increase powder density and strength, They also showed that it could decrease costs by apply two processes in the same die. In addition, the grain was size also finer than that of conventional extrusion [39].

A.K. Rout et al. used a round work piece to produce parts with sections using the Upper Bound Method with three dimensions. The study was performed to determine KAVF with the use of a special technique of spatial elementary rigid regions that can produce parts with hexagonal cross sections. Different parameters,

such as punch pressure and die geometry and process condition, were used to investigate their effects on the process [40].

M. Plancak et al. showed the influence of the shape of a punch cross section, which is one of the important factors that affects the extrusion process especially in backward extrusion. Non-circular punch cross sections were taken into account while studying the cold extrusion of aluminum alloy to find the pressures and loads required for the process. Two modes, experimental and numerical, were utilized to compare the results [41].

In this field, it can be observed that not many papers or studies discuss the different parameters affecting combined backward-forward extrusion and few studies deal with numerical analysis with this process. This study is presents unique work in this field for a number of reasons. (1) It is the first work that demonstrates the combined extrusion process that can produce hollow polygonal parts with two sides. (2) New and developed methods of simulation were used with QForm software for numerical analysis. (3) No research has discussed the residual stresses on products after using combined extrusion processes. (4) This study is the first work dealing with the influence of punch pressure and velocity on stresses and temperatures generated during the process. (5) A special X-ray device is used to measure the residual stresses on products that can give good indications on each region. (6) Aluminum Alloy 6061 has not previously been used on combined extrusion.

CHAPTER 3

PRINCIPLES OF THE EXTRUSION PROCESS

3.1 Extrusion Process

Extrusion is a plastic deformation process used to create objects of a fixed cross sectional profile. A material is pushed through a die of the desired cross-section. It is used to produce long parts of constant cross-section (Figure 3.1).

Extrusion can be cold or hot, depending on the alloy and the method used. In hot extrusion, the billet is heated to make plastic deformation easier. In extrusion processes, the effect of the billet with a container and die leads to high compression stress which results in a decrease of fatigue during break down from an ingot. This is a significant cause to raise the extrusion application on the metal form in order to form nickel alloy, stainless steel and other high temperature materials [5].

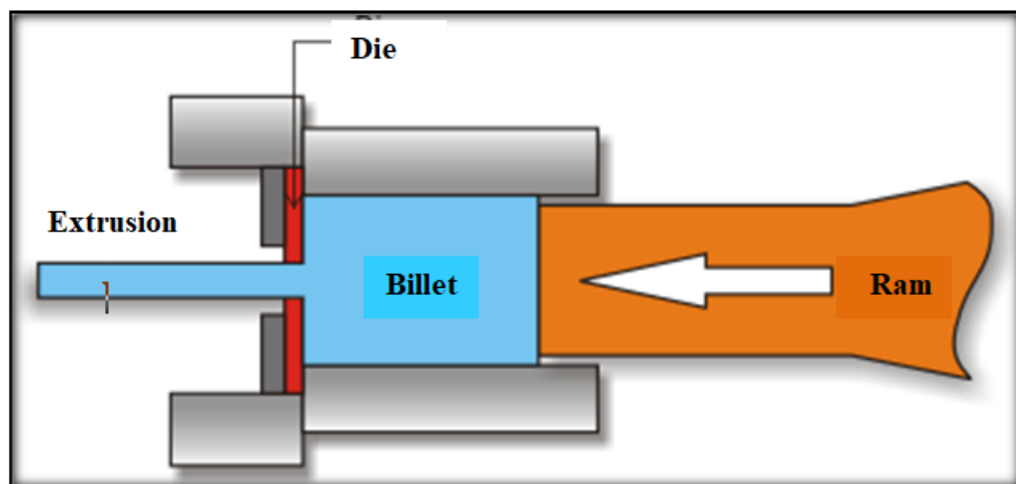


Figure 3.1: Extrusion process [42]

Extruded materials include metals, polymers, ceramics, concrete, play dough and foodstuffs. The products of extrusion are generally called “extrudes” (Figure 3.2).

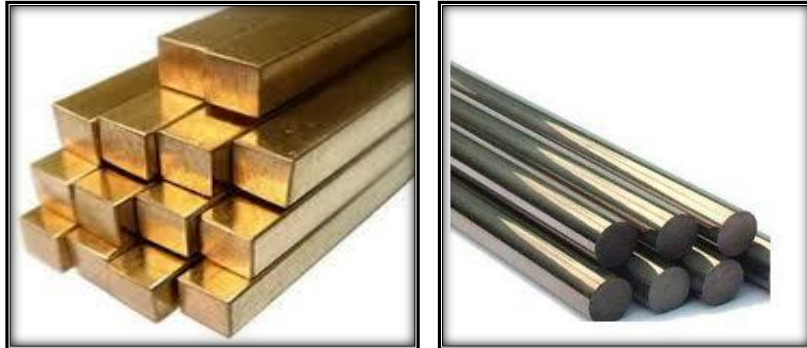


Figure 3.2: Billets and rods used for extrusion [43, 44]

During extrusion process, a compressive stress occurs in the work piece, which allow for large deformations to occur with lower probability of cracking.

The ratio of the work piece cross-sectional area to the final extruded part cross-sectional area is called the extrusion ratio [45].

3.2 Advantages of Extrusion

The main advantages of this process over other manufacturing processes are:

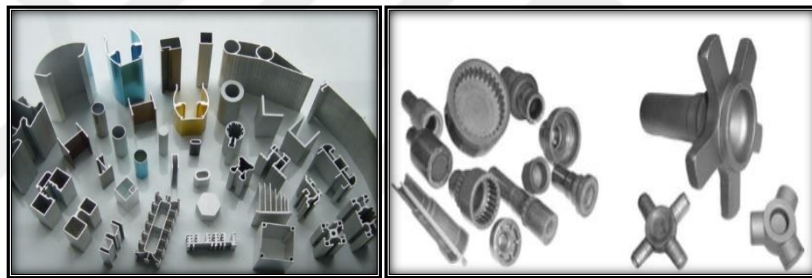
- 1- Its ability to create very complex cross-sections and different shapes.
- 2- Brittle materials can be extruded because the material only encounters compressive and shear stresses.
- 3- Its ability to form parts with an excellent surface finish and close tolerances.
- 4- Its ability to produce long or semi-continuous materials.
- 5- Extrusion molding at low cost relative to other molding processes.
- 6- Good grain structure and strength especially in cold and warm extrusion.
- 7- Little or no waste material. [46]

3.3 Applications of Extrusion

The extrusion process is one of the significant methods of metal forming. Many products of high industrial applications with good quality can be produced as shown below (Figure 3.3) [4].



(a)



(b)



(c)

Figure 3.3: Some applications of the extrusion process: (a) steel, (b) aluminum, and (c) plastic [47-49]

3.4 Classification of the Extrusion Process

The extrusion process can be classified according to the direction of movement of the work piece, billet temperature, types of operation and equipment orientation, as shown in Figure 3.4.

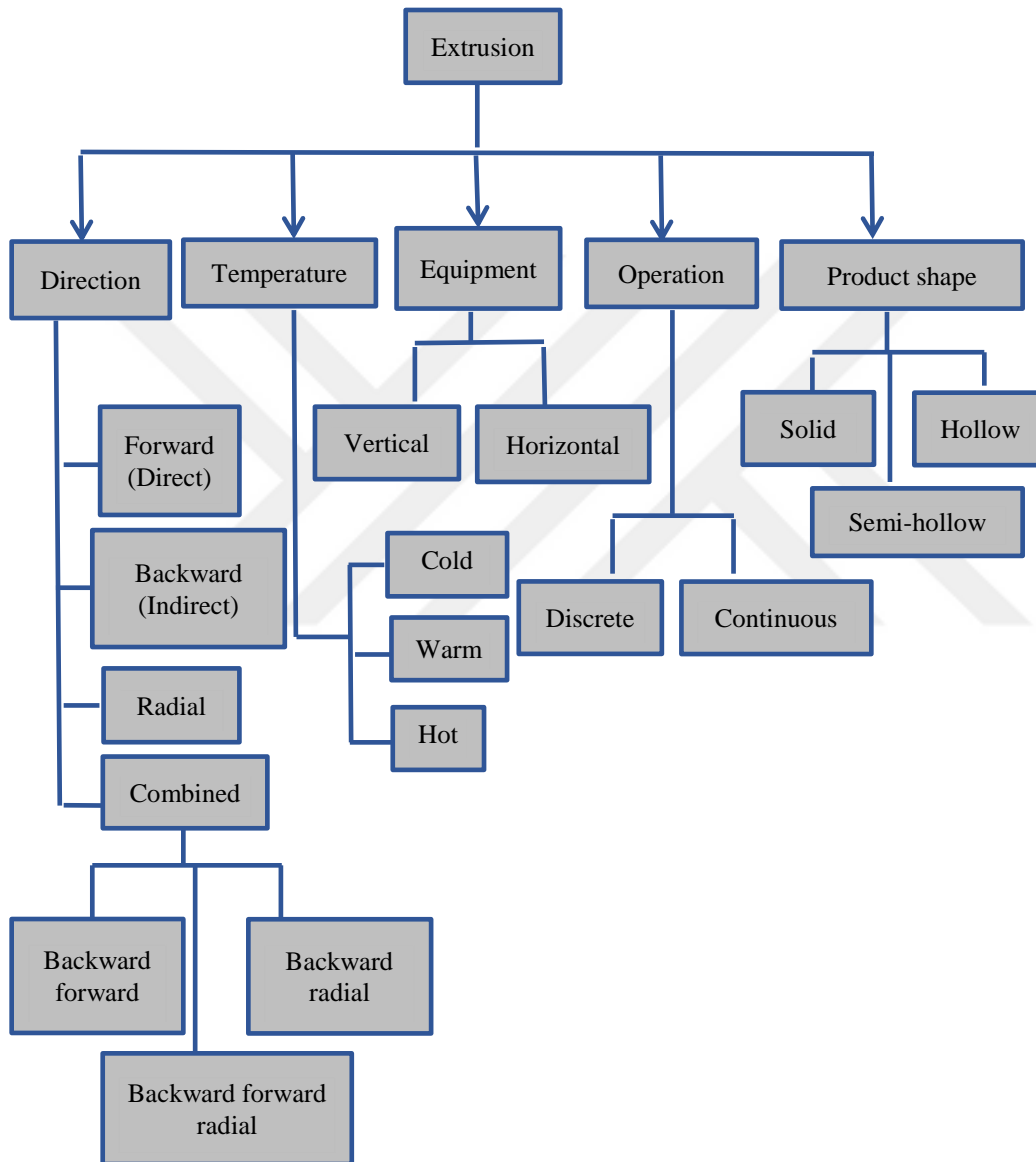


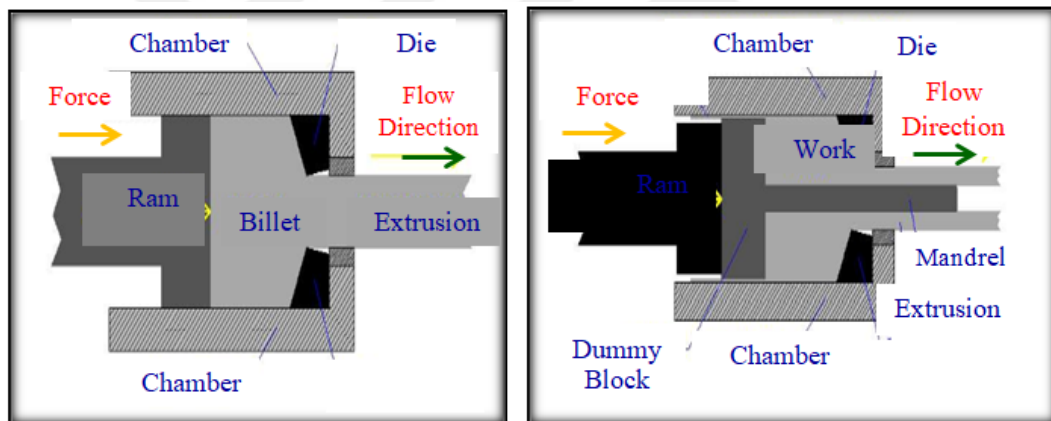
Figure 3.4: Classification of extrusions [3, 5, 7, 37, 46, 50]

3.4.1 Extrusion Direction

3.4.1.1 Forward Extrusion

Also known as direct extrusion, forward extrusion occurs when the work piece is put into a container and the punch presses the metal, allowing it to flow across the openings in a die in the same direction of the punch movement. The work piece moves forward relative to the container wall and this will increase the friction resistance (Figure 3.5a).

For hollow sections, the work piece is designed with a hole parallel to the main axis to allow the mandrel to pass through the material which flows across the clearance of the die (Figure 3.5b) [3].



(a) Solid part

(b) Hollow part

Figure 3.5: Forward extrusion process (direct extrusion) [51]

3.4.1.2 Backward Extrusion

Also known as indirect extrusion and reverse extrusion, backward extrusion occurs as the ram penetrates into the work piece, the metal is forced to flow through the clearance in a direction opposite to that of the motion of the ram (Figure 3.6a)

For hollow cross sections, the ram is pressed into the billet, forcing the material to flow around the ram to take a cup shape (Figure 3.6b) [46].

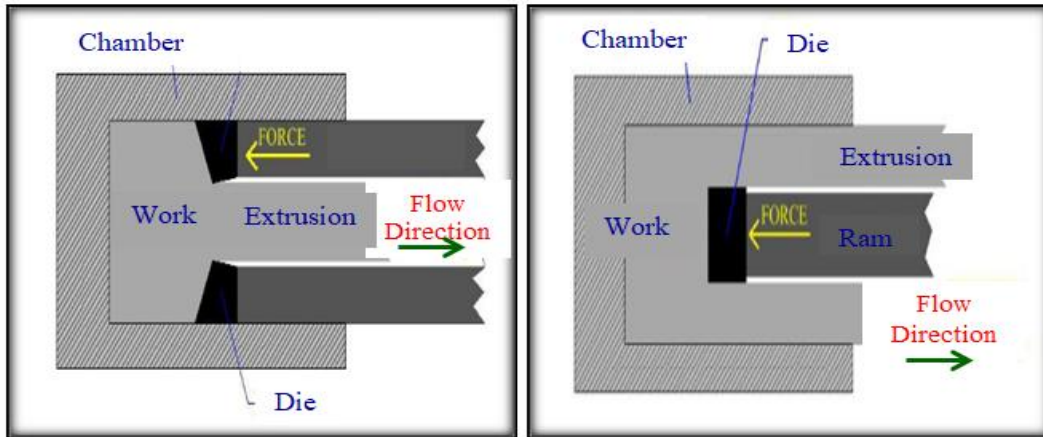


Figure 3.6: Backward Extrusion process (indirect extrusion) [51]

The types of hollow sections that can be extruded in forward or backward extrusion processes are shown in Figure 3.7.

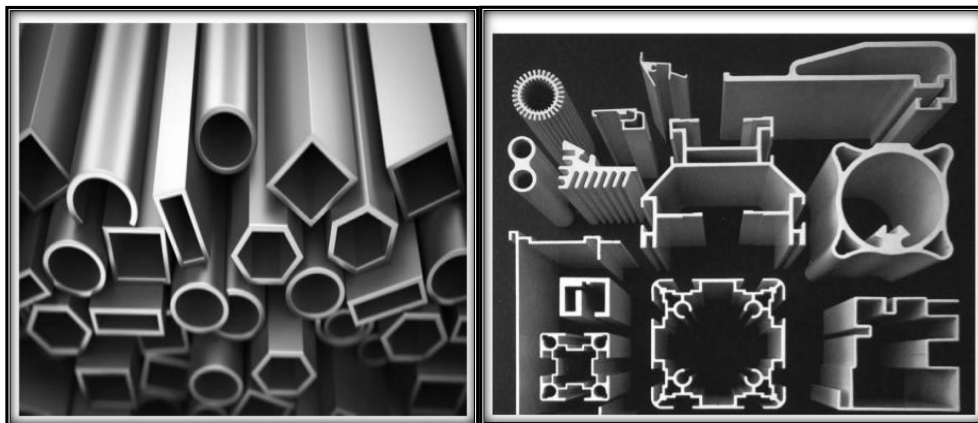


Figure 3.7: Some hollow and semi-hollow cross sections of extrusion [5, 46]

The differences between the direct and indirect extrusion pertain not only to the direction of the material movement relative to the ram motion but also to the friction, which is an important problem that occurs in direct extrusion. Because of contact being made in direct extrusion between the work piece and the surface with

the walls of the container as the billet is forced to slide, the friction resistance increases, and this needs more force for pressing (Figure 3.8a). In indirect extrusion, the billet is not forced to move relative to the container; therefore, there is no friction at the container walls and the ram force is therefore lower than the indirect extrusion (Figure 3.8b).

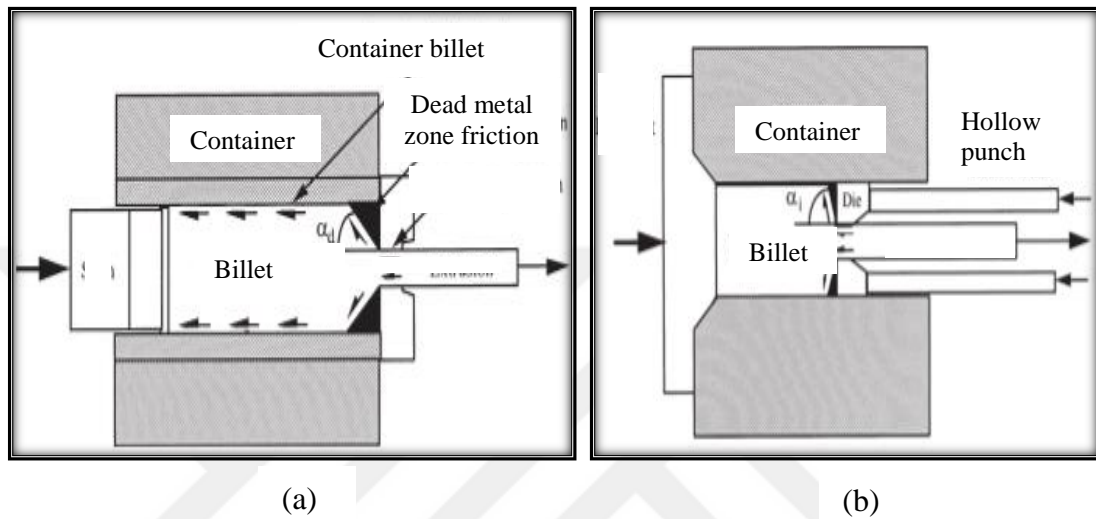


Figure 3.8: Effect of friction in (a) direct extrusion, and (b) indirect extrusion [5]

Limitations of indirect extrusion are (1) the lower rigidity of the hollow ram, and (2) the difficulty to support the extruded product when exiting from the die opening and the force required in direct extrusion being higher than that of indirect extrusion (Figure 3.9) [2].

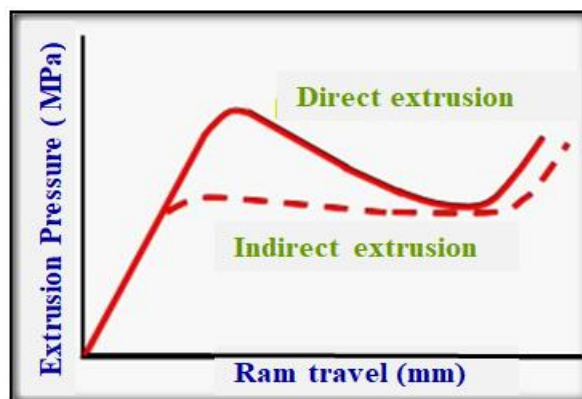


Figure 3.9: Relationship between direct and indirect extrusion pressure [5]

3.4.1.3 Radial Extrusion

The material moves in a lateral direction and as the ram penetrates into the work piece, the metal is forced to flow through the clearance of the lateral direction of the die (Figure 3.10).

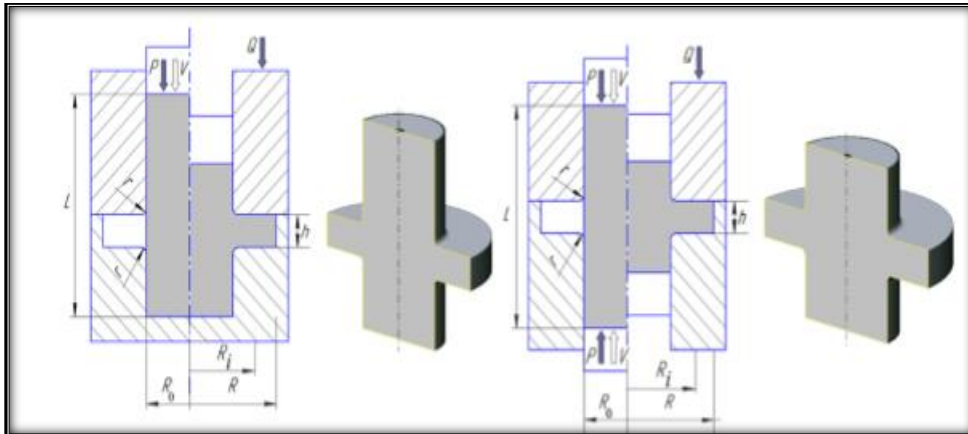


Figure 3.10: Radial extrusion [17]

3.4.2 Extrusion Temperature

3.4.2.1 Cold Extrusion

Cold extrusion is usually the method followed to produce discrete parts near net shape by pushing the work piece with the punch through the die at room temperature. This has more advantages than hot extrusion as strength increases and there is a good surface finish. It is also free from oxidation and has a good fit tolerance. Aluminum, copper, steel and their alloys can be cold extruded. Punch pressure depends on material flow, work piece shape, die design and friction. Two types of pressing are used in cold extrusion: (1) hydraulic pressing; and (2) mechanical pressing, which includes high alignment accuracy, good rigidity and long strokes. Generally, the mechanical method is better than the hydraulic because less maintenance is required in mass production. Tool design and product shape are limited in cold extrusion because of low material flow and work safety.

The alignment, friction, flow velocity, part shape simple die assembly, and distribution of forces are the most important points that should be taken into account in tool design. To achieve good accuracy of the dimensions of the work piece, it is necessary to depend on tool dimensions since tool wear is low in cold extrusion. Tool materials, compression, and direction of movement also have a strong influence on dimensional accuracy. The limitations of cold extrusion include the sticking between the billet and die, die fractures, tool alignment accuracy and lubricant built up [50].

3.4.2.2 Hot Extrusion

In the hot extrusion process, the work piece is heated to a temperature exceeding recrystallization prior to extrusion. The advantages of hot extrusion are: ability to produce complex shape, strength decreasing, ductility increasing, low force and power require. The limitations of this process include oxidation layers, the problems of lubrication at high temperatures and the loss of billet temperature upon contact with a cold die; therefore, pre-heating of the die should added to the process [46].

3.4.3 Extrusion Equipment

3.4.3.1 Horizontal Press Extrusion

The press in the extrusion process can be horizontal according to the work direction and axis and it is the most important and common type of extrusion. It provides easy use for workers but with large area for working, as shown in Figure 3.11.

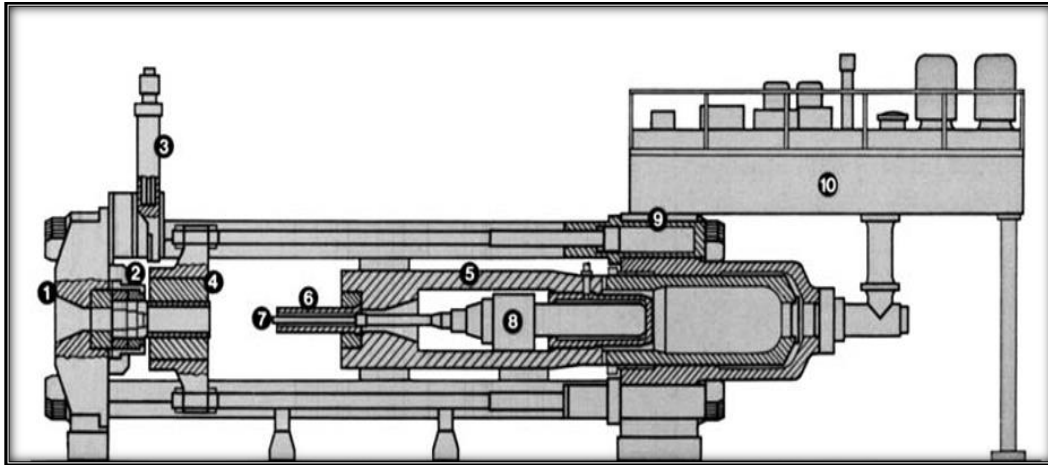


Figure 3.11: Horizontal extrusion [5]

3.4.3.2 Vertical Press Extrusion

In this situation, the press is put in a vertical direction depending on the orientation of the process and it takes less space in the work place. However, it is difficult to operate due to its height (Figure 3.12) [46].

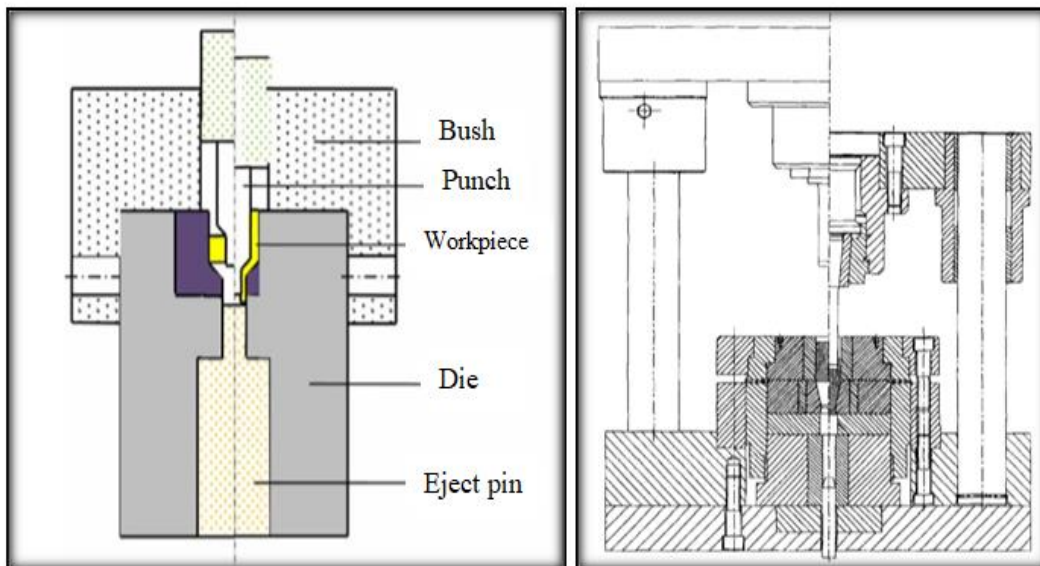


Figure 3.12: Vertical Extrusion [7, 37]

3.4.4 Extrusion Operations

3.4.4.1 Continuous Extrusion

Continuous extrusion is a process that works in a steady-state mode for an indeterminate time. Some processes are used to produce extremely long parts in one cycle with the parts being cut into many smaller parts (Figure 3.13).



Figure 3.13: Continuous extrusion products [5]

3.4.4.2 Discrete Extrusion

In this extrusion process, a single part is achieved in each cycle of work and stroke. Impact extrusion is one of discrete extrusion processes (Figure 3.14) [46].

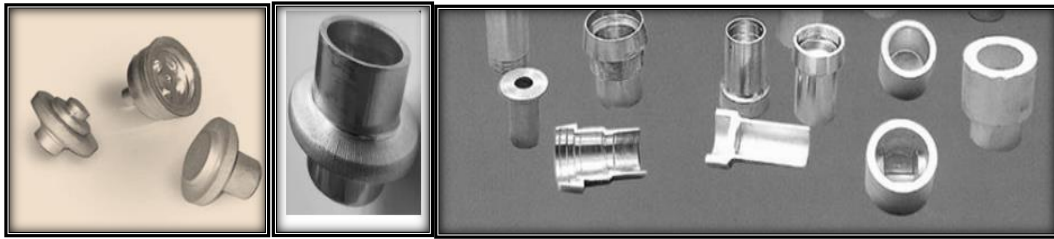


Figure 3.14: Discrete Extrusion products [4]

3.5 Special Forms of Extrusion

3.5.1 Impact Extrusion

This extrusion process produces individual parts at high speed and with shorter strokes than traditional extrusion processes. The differences are in force and pressure, which are applied as a shock on the billet while in classic extrusion, the pressing is achieved gradually (Figure 3.15) [6, 46].

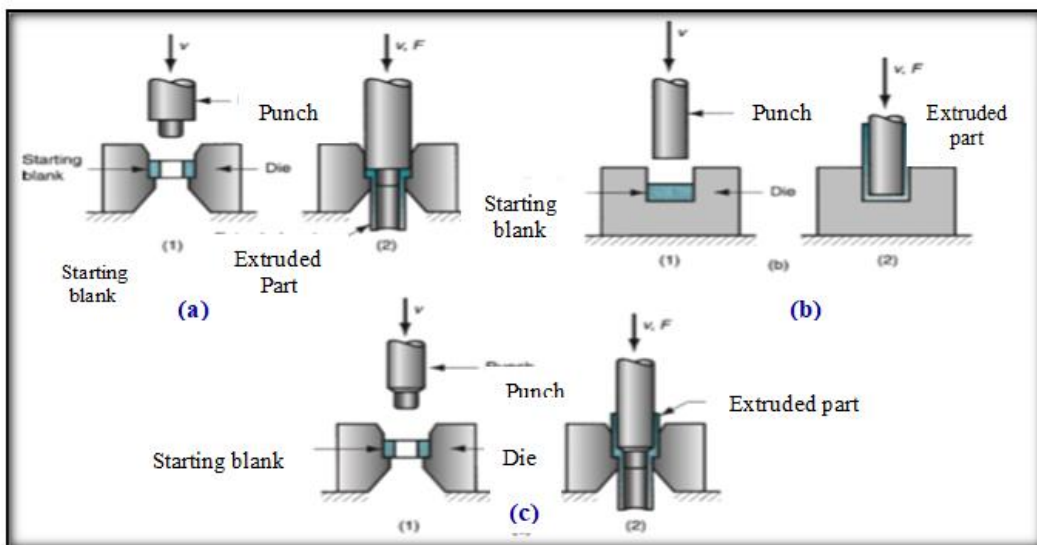


Figure 3.15: Impact extrusion process: (a) Forward, (b) Backward, and (c) Combined [46]

The shapes of the items produced by impact extrusion are restricted to being symmetric cross sections (Figure 3.16).



Figure 3.16: Impact extrusion products [6]

3.5.2 Hydrostatic Extrusion

Hydrostatic extrusion is used to avoid high friction influences between the billet and die wall in classic extrusion by surrounding the work piece with fluid and then applying the punch press to the work piece with the fluid indirectly. This process decreases the friction to the minimum and reduces the force required for deformation. This process is suitable only for direct extrusion and in this way, the force acts on all the surfaces of the billet (Figure 3.17).

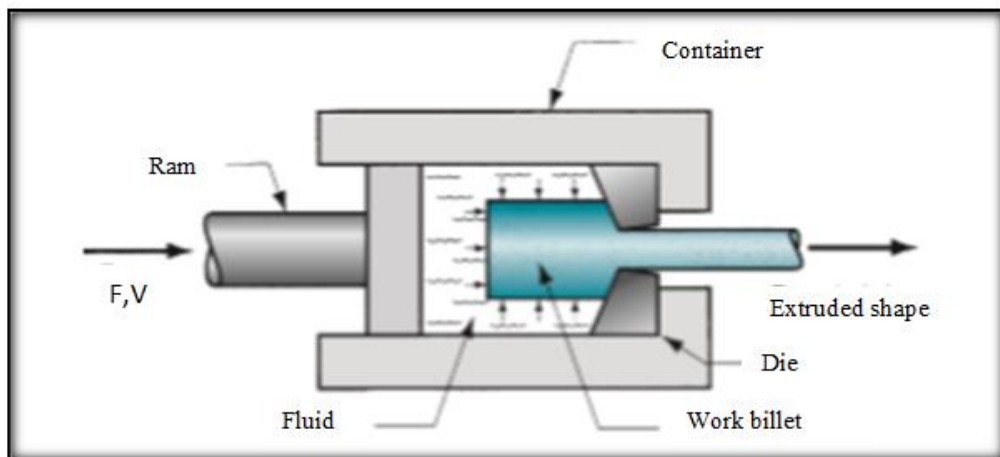


Figure 3.17: Hydrostatic extrusion [46]

3.6 Extrusion Products Defects

Some defects appear in extrusion products due to factors such as billet material and shape, process conditions and die geometry. The main defects include the following:

1- Center Crack

This type of crack is an internal defect that increases while stresses are occurring in the billet. The center crack occurs because of sharp angles in the die as well because of the extrusion ratio being very low and the presence of impurities in the billet metal (Figure 3.18a).

2- Piping

This appears only in forward extrusion processes that involve sink holes in the upper side of the billet (Figure 3.18b).

3- Surface Crack

This defect occurs due to high billet temperatures as a result of very high extrusion velocities, large friction factors and strain rates, which increases in relation to increases in the heat (Figure 3.18c).

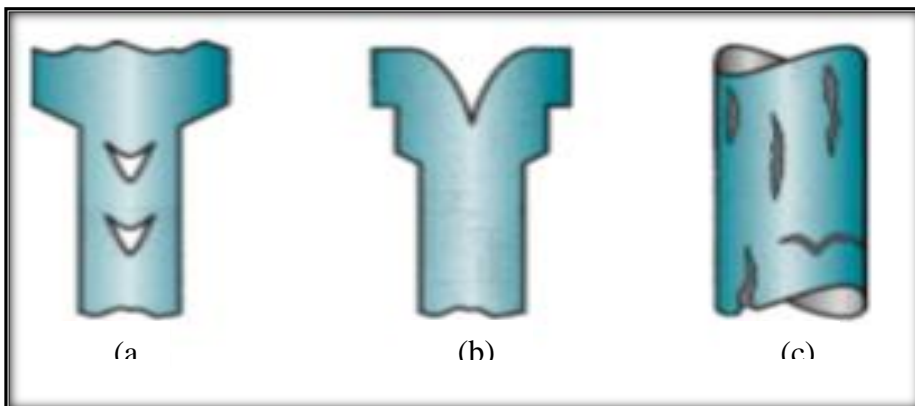


Figure 3.18: Extrusion product defects [46]

3.7 Combined Extrusion

In addition to the basic extrusion processes, there are a number of combined extrusion processes in which two or more basic extrusion processes occur simultaneously.

In this process, a round shaft can be extruded into different head shapes (triangular, square, pentagon, hexagon, gear) in more than one direction. Of importance in the combined extrusion process is the total energy required, which is less than that of backward or forward extrusion (Figure 3.19) [10].

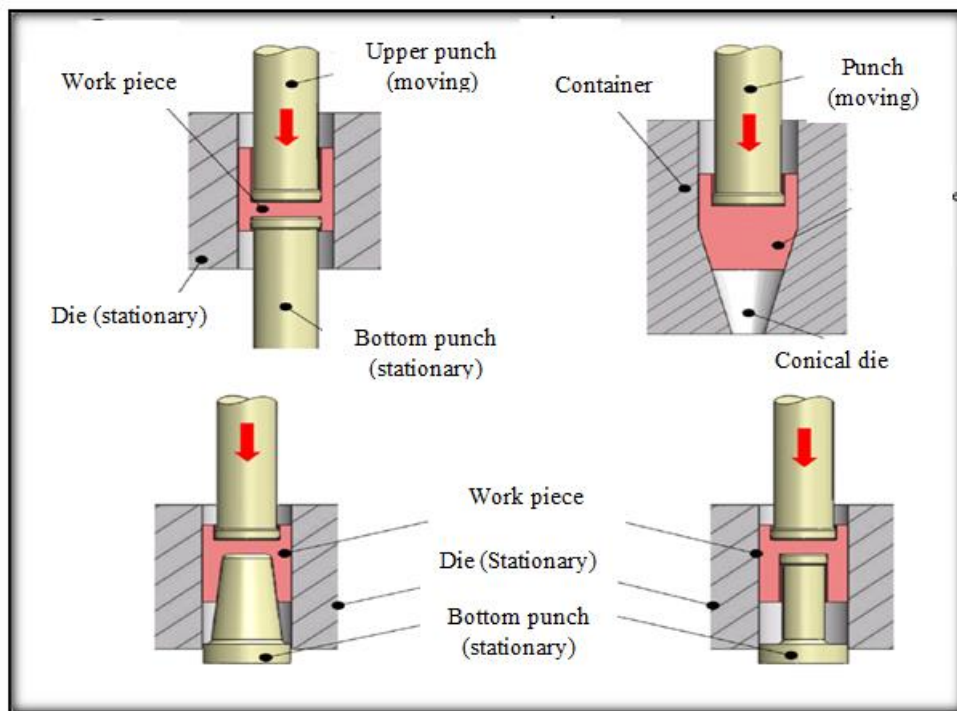


Figure 3.19: Combined extrusion [52]

3.7.1 Combined Forward-Backward Extrusion

The material flows in two directions by two presses in compression in backward and forward orientations (Figure 3.20).

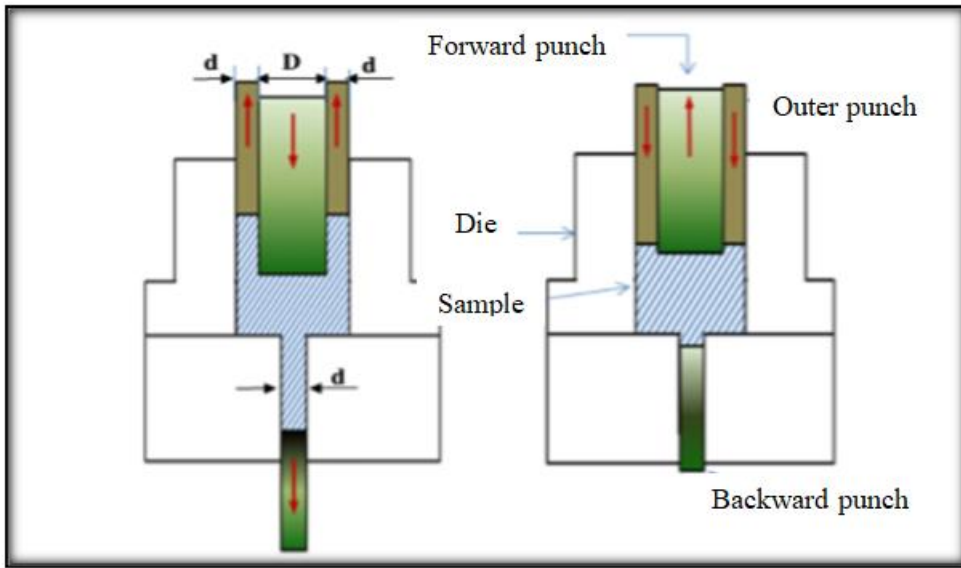


Figure 3.20: Combined forward-backward extrusion [30]

3.7.2 Combined Radial Forward-Backward Extrusion

Three directions of material flow move backward, forward and along radial axes such that the material fills the gaps in different directions by two pressing forces.

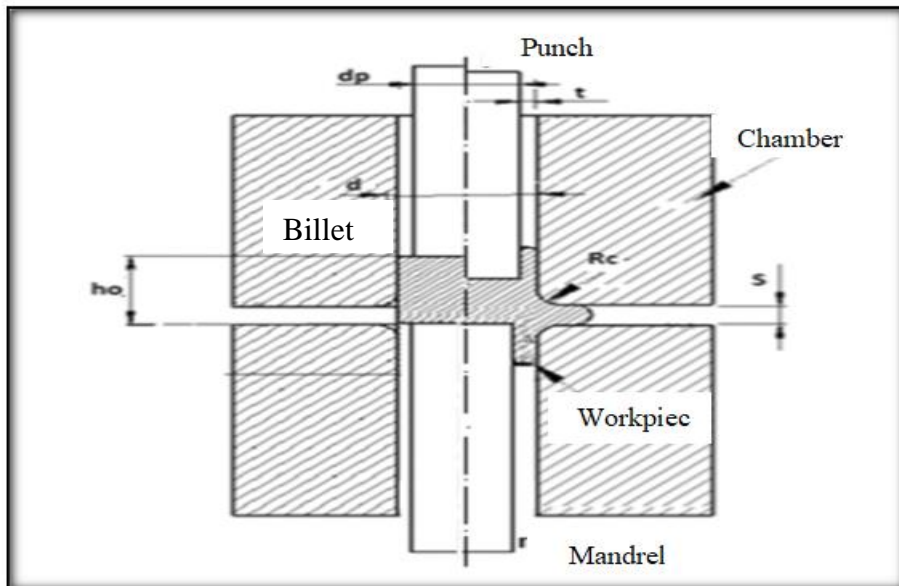


Figure 3.21: Combined radial forward-backward extrusion [32]

3.7.3 Combined Backward Radial Extrusion

It is a process that punches force the work piece to flow in backward direction through the die in the opposite direction of pressing and radial direction that fill the gap between upper and lower parts of the die [12].

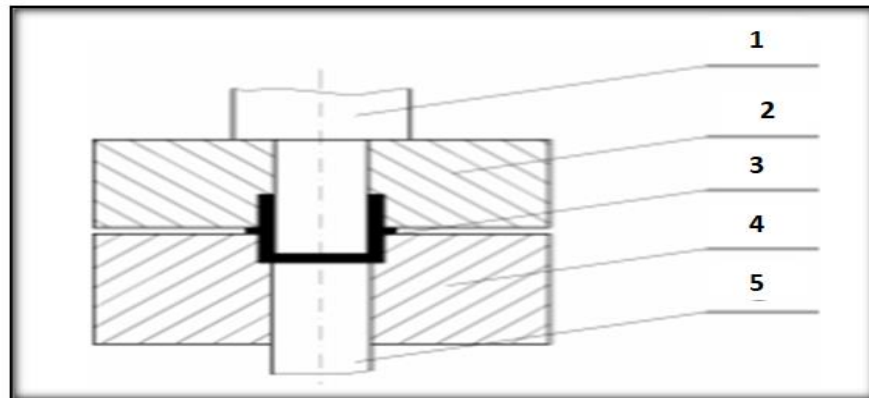


Figure 3.22: Combined backward radial extrusion: (1) punch, (2) die, (3) radial flow, (4) lower die, and (5) ejector [12]

3.8 Combined Extrusion Characteristics

3.8.1 Advantages of Combined Extrusion

- 1- Reducing the stages of the process.
- 2- Decreasing production cost.
- 3- Uniform residual stresses.
- 4- Improved mechanical properties.
- 5- Near net shape products.
- 6- Time savings.
- 7- High product quality.
- 8- Mass production.
- 9- More complex shapes. [53]

3.8.2 Combined Extrusion Products

The combined extrusion method enhances the efficiency of the manufacturing process by combining various operations to produce complex shapes at low cost. The method is used to produce parts of different shapes for many applications and uses [54]. Products manufactured through combined extrusion include automotive parts, agricultural instruments, aircraft, electrical parts, construction tools and defense equipment. Other applications include sharpened diameter solid shafts, tubular parts with multiple diameters, cylindrical, conical or other non-round holes, hollow parts with closed-end cupped parts with holes that are cylindrical, conical shapes, nuts and bolts, flanged shafts, box spanners, and male-female adapters. Some examples of applications are shown in Figure 3.23 [4].



Figure 3.23: Applications of the combined extrusion process [4]

3.8.3 Parameters Affecting the Combined Extrusion Process

- 1- Extrusion ratio.
- 2- Die and punch geometry.
- 3- Product shape.
- 4- Punch velocity.
- 5- Process conditions.
- 6- Work piece and die temperature.
- 7- Lubrication. [3]

3.9 Severe Plastic Deformation (SPD)

Sever Plastic Deformation (SPD) is defined as a technology of materials processing with large plastic strains and deformation which depends on strain distribution through the continuity of sliding lines. The deformation can be either simple shear or pure shear. SPD can also be defined as a process of metal working when being under intense hydrostatic pressure to obtain a large strain without important changes in total dimensions to produce large grain refinement. In normal metal forming processes, large strains occur during either hot working or cold working, such as when forging, rolling and drawing. It is significant to know the deformation mode during SPD, which depends on the properties of stress and strain when a coupling of processes occurs. [55]

In metal forming processes, a type of severe plastic deformation at a shear zone occurs during combined backward-forward extrusion with different metal flow directions and high amount of load that produces material with ultrafine grains and with increased strength (Figure 3.24).

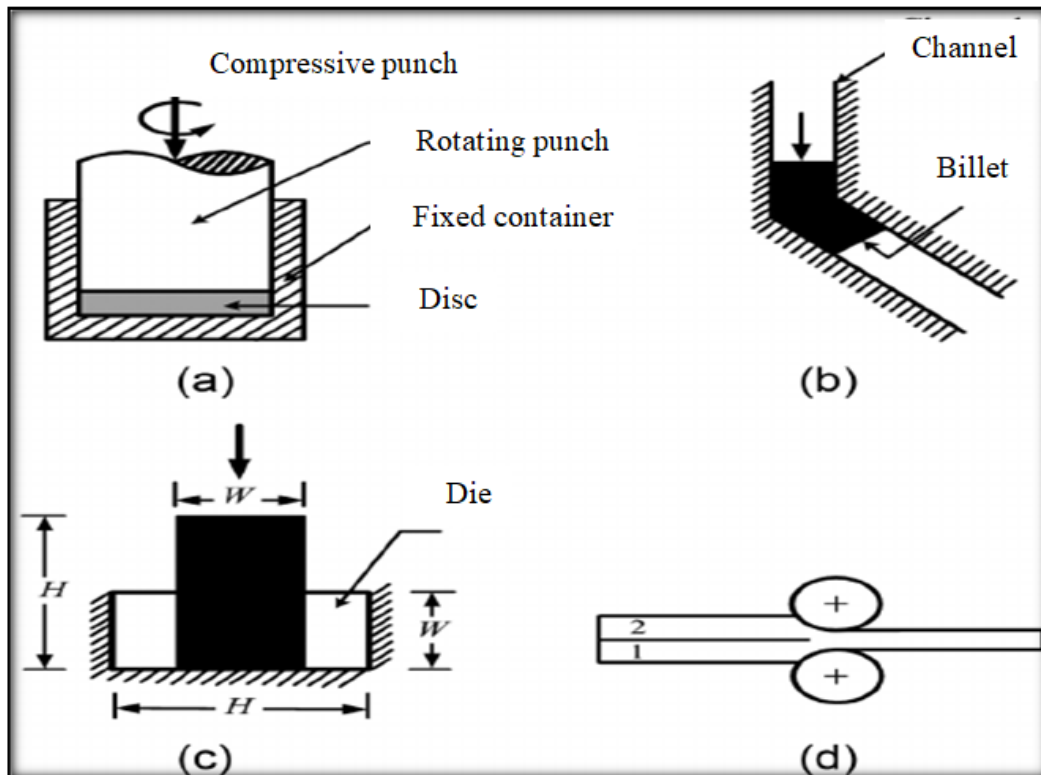


Figure 3.24: Types of severe plastic deformation processes: (a) High-pressure torsion, (b) equal channel angular extrusion, (c) cyclic closed-die forging, and (d) accumulated roll bonding. [56]

The significance of metal forming processes of combined extrusion came from its ability to produce complex parts with high dimensional accuracy, good surface finish, increased mechanical properties through an ultrafine grain and low material waste (Figure 25). It is important in this process to estimate the load required to deform the billet according to another process condition.

The combined extrusion can produce more complex corners than traditional processes in manufacturing. Of most importance is that the pressing and its reaction between the work piece and die surfaces during this process is enhanced to form compressive stresses that increase fatigue resistance [57].

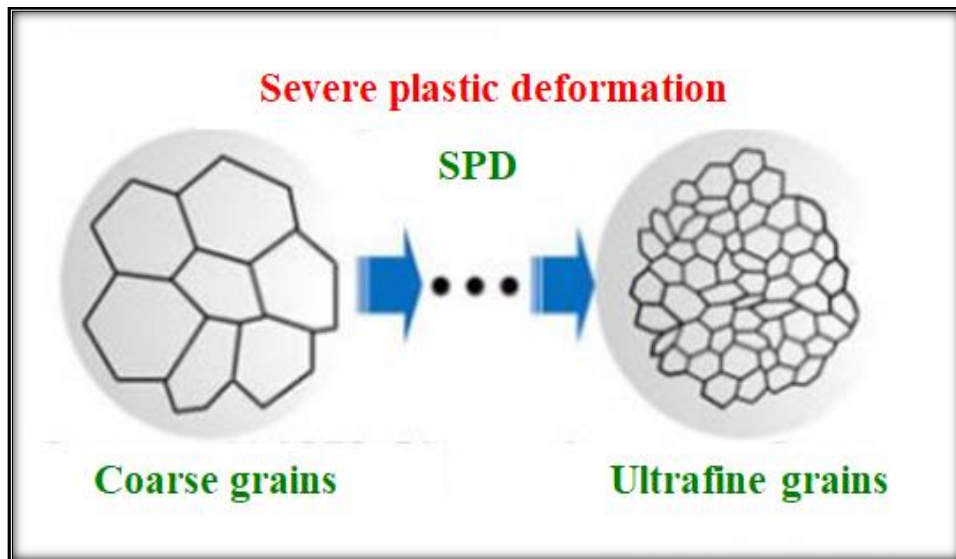


Figure 3.25: Effect of severe plastic deformation (SPD) on grain size [58]

A number of advantages can be gained from combined extrusion, such as the velocity of the metal flow in two directions being controlled using a device that supports the drag to increase the efficiency of the process. However, the load required in combined extrusion is less than that of other normal extrusion processes. [59]

3.10 Residual Stresses

MetAl-forming processes usually generate non-homogeneous plastic deformation in the work piece so that the final product is left in a state of residual stress. To increase fatigue resistance and restrict crack growth, tensile stress should be avoided by encouraging compressive stress, which can be done with any residual stresses. While no load is applied, these residual stresses are in equilibrium. They are at rest from a prior process on the part; therefore, they are called residual stresses and they are similar to the mean stress that appears after the manufacturing process (Figure 3.26).

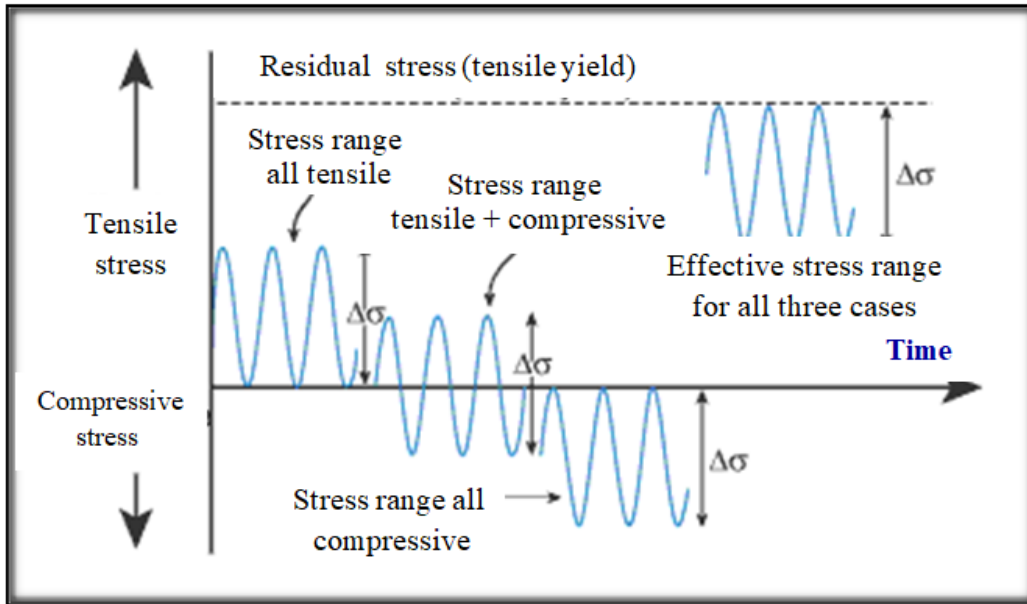


Figure 3.26: Effect of residual stresses on stress range [60]

Residual stresses are defined as the stress available in the parts in the absence of applying any forces. These stresses exist after deformation during mechanical processes such as strains occurring due to non-homogeneous cooling and heating, non-uniform plastic deformation and irregular thermal expansion. The amount and type of residual stress rely on part history and part material properties [61].

To calculate the residual stresses in parts, a total stress analysis of the work piece during the process should be calculated using elastic plastic analysis [62].

3.10.1 Effects of Residual Stresses

Residual stresses can affect the mechanical conduct by:

- 1- Influencing the structure and dimension of the part
- 2- Enhancing the growing of cracks on the surface of the part
- 3- Decreasing the resistance of cracks and increasing the probability of fatigue



Figure 3.27: Effect of residual stresses on mechanical behavior [63]

3.10.2 Causes of Residual Stresses

In manufacturing processes, a material is exposed to different changes that include deformation, properties modification, shape transformation, machining, and temperature changes. These processes cause residual stresses in the material, or they are already available in the part before any process and they can be increased during the service of the part. These residual surface reasons can be arranged according to the following:

- 1- Volume variation and transformation in phases.
- 2- Plastic deformation through non-uniform flow.
- 3- Heating and cooling rates processes. [24]

3.10.3 Types of Residual Stresses

Residual stresses can be classified according to force direction into two types:

- 1- Tension residual stresses, which are undesirable because they increase the probability of fatigue occurrence. They are formed by a number of processes including grinding, bending and torsion. Tensile stresses cause stress corrosion cracking.
- 2- Compressive residual stresses, which are desirable because they retard the formation and growth of cracks that are subjected to cyclic loading and thus enhance fatigue resistance and increase stress corrosion cracking resistance. Laser peening and low plasticity burnishing processes can form compressive stresses which cold work or strain harden the material. This balances the worse influences of tensile stresses.

The aim is always to form compressive stresses at the surface of parts to improve fatigue resistance and prevent cracks [64].

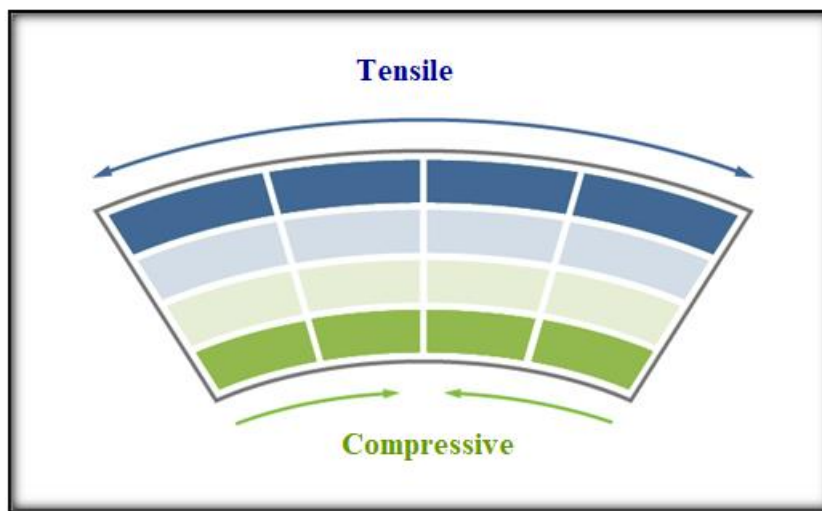


Figure 3.28: Tensile and compressive of stresses [65]

Residual stresses affect a material's structure and properties such that the stability of its dimensions, the corrosion probability and fatigue resistance can change. These effects lead to additional cost for repairs and replacement of parts.

3.10.4 Classification of Residual Stresses

It is important to know the history of a part and the type of processes through which it had passed before selecting the type of residual stress test. These residual stresses can be classified into three types according to their regions (Figure 3.29).

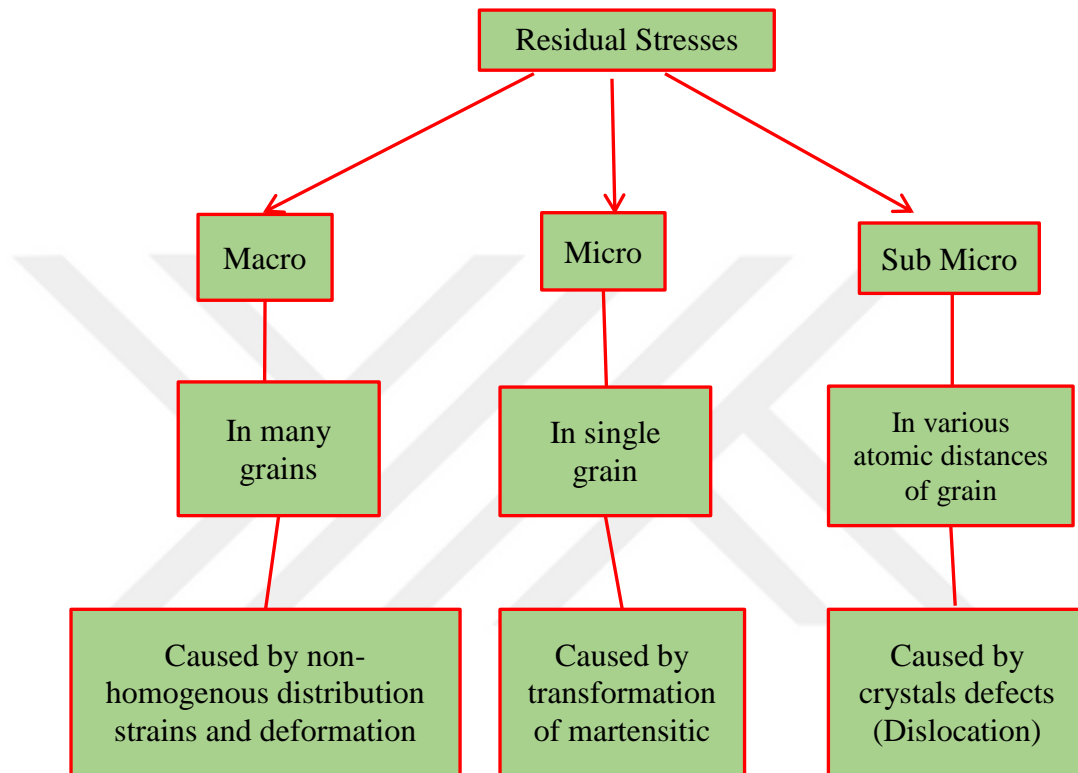


Figure 3.29: Classification of residual stresses [24, 65]

Residual stresses remain in a part after passing through processes or they can occur during service loading, which results in non-homogenous plastic deformation. Macro residual stresses occur in many grains because in homogeneous treatment, whereas micro type stresses occur in individual grains but can have various sizes which are occur because of the differences in volume between martensite and austenite. Therefore, during conversion between phases, this type of residual stress appears. Sub micro stresses can exist because of grain defects such as dislocations and spaces [65].

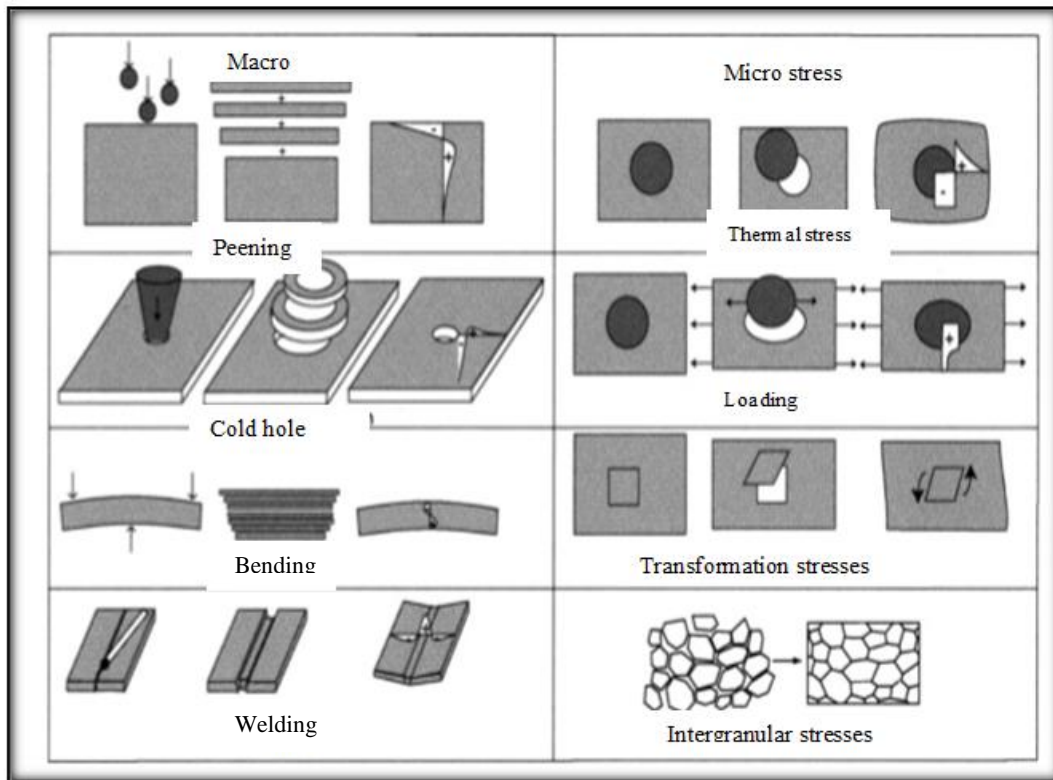


Figure 3.30: Types of residual stress through different processes [66]

3.10.5 Methods of Removing Residual Stresses

A load can be controlled to achieve compressive stresses in the surface to avoid cracks, which can be done following a number of methods, including:

- (1) Heat treatment: an annealing process to form local yielding which decreases or removes residual stresses.
- (2) Shot peening: a high velocity shot on the surface of a part to achieve local plastic yield that expands in comparison to the internal regions.

Cold working residual stresses are kept in the part, but for hot working, residual stresses are removed because of the heat effect. [67]

3.10.6 Methods of Measuring Residual Stresses

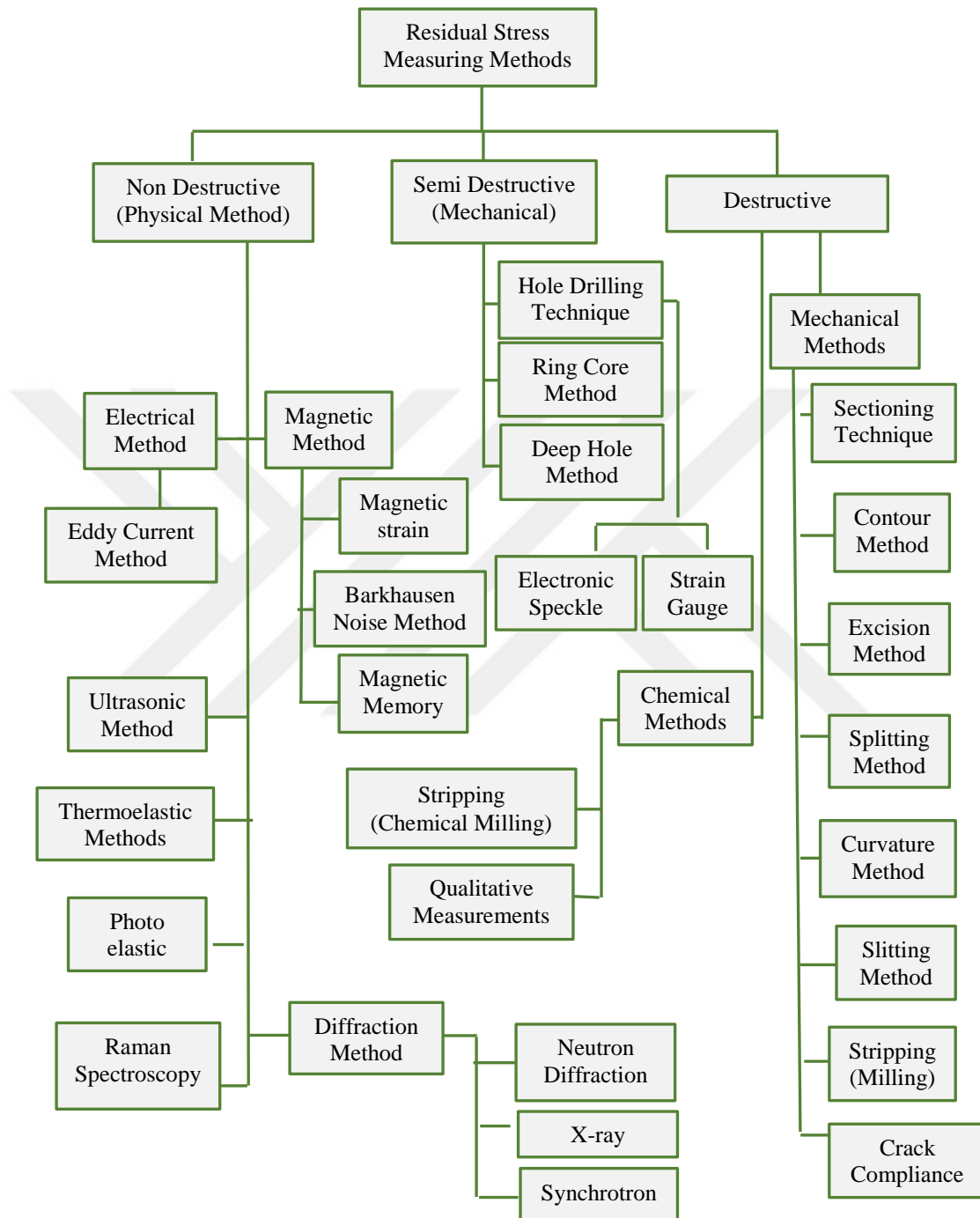


Figure 3.31: Methods of measuring residual stresses [24, 66, 68-71]

3.10.6.1 Non-Destructive Methods

These methods are also called physical methods and are used to measure residual stresses without destroying the part during measurement. Non-destructive methods include the following:

1. Magnetic Methods

These depend on magnetic induction and the movement of the magnetic domain. Stresses encourage magnetic isotropy, turning the field far from the utilized orientation. One is able to observe a few turnings in the part plane by using a sensor coil. Some of the magnetic methods include:

- 1- Magnetic strain
- 2- Barkhausen noise method
- 3- Magnetic Memory [68]

2. Electrical Method

The electrical method includes an eddy current test involving the application of eddy currents on the tested part and revealing any variation in electrical conductivity and allowance in the magnetic field by observing the resistance of the coil. It is considered to be a fast and low cost method of testing which is more suitable than the magnetic method. [68]

3. Ultrasonic Method

Also known as the refracted longitudinal wave method, the ultrasonic method can be used for different types of materials with various thicknesses. The procedure depends on the influence of sonic elasticity such that variations in ultrasonic velocity can be observed in the wave path of the part experiencing stress. [24, 66]

4. Thermoelastic Method

The thermoelastic method is able to distinguish the existence of stresses by observing the minute differences in temperature due to elastic distortion in a tested part. An infrared copier can show a chart of calorific changes which indicate stress changes [68].

5. Photo Elastic Method

The photo elastic method is used with transparent material when observing the differences in light velocities for materials with stresses. According to the path length notification, it can distinguish the existence of stress [66-68].

6. Raman Spectroscopy

Raman spectroscopy is a method of finding the vibrational modes of molecules by using the elastic scattering of photons. An X-ray is sometimes used and when laser light interacts through the photons of the laser, the laser energy move in the upper or lower direction.[71].

7. Diffraction Methods

There are three types of diffraction method:

- 1- Neutron Diffraction
- 2- X-ray
- 3- Synchrotron

These methods can be followed to measure and record residual stresses through polycrystalline materials. [72] The methods depend on measuring elastic deformation, which leads to varying the spaces between the planes and measuring the strain. Bragg's Law is then used to calculate the stress.

X-ray diffraction is used to measure the stresses on the surface of a material. It depends on elastic strain that gives atomic planes a metallic crystal structure and can determine the stresses [24].

3.10.6.2 Semi-Destructive Methods

This set of methods, also known as mechanical methods, are used to measure the stress on a material with few distortions or little destruction without harming any of the sides of a part. An analysis is performed for any stress relaxation in the part while eliminating the material. The relaxation leads to deformation, which can give indications of any residual stresses. Semi-destructive methods can be divided into three types:

- 1- Hole drilling.
- 2- Deep hole.
- 3- Ring core. [73, 74]

3.10.6.3 Destructive Methods

In measuring with this type of method, the part will be completely destroyed to determine the residual stresses in the material. All the methods are indirect methods that use another quantity such as strain or displacement to calculate the residual stresses.

Destructive methods can be divided thus:

A- Mechanical Methods

These include many types of testing methods that depend on stress relaxation to calculate the residual stresses. They are classified thus:

- 1- Sectioning Technique

- 2- Contour Method
- 3- Excision Method
- 4- Splitting Method
- 5- Curvature Method
- 6- Slitting Method
- 7- Stripping (Milling)
- 8- Crack Compliance [75, 76]

B- Chemical Methods

- 1- Stripping (chemical milling)
- 2- Qualitative Measurements [69]

3.11 Extrusion Analysis

There are many parameters affecting the extrusion process which can be calculated and defined as follows:

1- Extrusion Ratio (r_x)

$$r_x = \frac{A_0}{A_f} \quad (1)$$

where r_x = the extrusion ratio, A_0 = the first cross section area of the work piece (mm^2), and A_f = the cross section area after extrusion (mm^2).

2- True Strain (ϵ)

$$\epsilon = \ln r_x \quad (2)$$

3- Punch Pressure (p)

$$P = \bar{Y}_f \ln r_x \quad (3)$$

where \bar{Y}_f = the average of the flow stress when deformation occurs (MPa).

4- Strain During Extrusion

$$\epsilon_x = a + b \ln r_x \quad (4)$$

where ϵ_x = the strain of extrusion, and a and b = constants depending on the die geometry.

5- Pressure of Indirect Extrusion

$$P = \bar{Y}_f \epsilon_x \quad (5)$$

6- Pressure of Direct Extrusion

The friction here has a great influence such that it increases the pressure required.

$$\frac{p_f}{4} \pi D_o^2 = \mu p_c \pi D_o L \quad (6)$$

where p_f = the pressure used to pass the friction (MPa), μ = the friction coefficient, and p_c = the pressure required to push the work piece against the die wall (MPa).

7- Shear Yield strength

$$Y_s = \frac{\bar{Y}_f}{2} \quad (7)$$

where Y_s = shear yield strength (MPa).

$$p_f = \bar{Y}_f \frac{2L}{D_o} \quad (8)$$

where L = the length of the work piece prepared for extrusion (mm), and D = the work piece diameter (mm).

8- Ram Pressure

$$P = \bar{Y}_f \left(\varepsilon_{x+\frac{2L}{D_0}} \right) \quad (9)$$

9- Punch Force

$$F = p/A_0 \quad (10)$$

10- Power

$$P^{\circ} = F v \quad (11)$$

where P° = power (J/s) and v = punch velocity (mm/s) [46]

11- Stresses

While plastic deformation is occurring, the pressing of the punches and application of forces on the billets cause an internal force on the deformed parts, which is called stress. These stresses can be classified as (1) mean stress, (2) Principle Stress, and (3) Effective stress.

3.11.1 Theoretical Analysis

For theoretical analysis, the method that is used to determine the residual stresses depends on the relationship between strain and stress.

3.11.2 Constitutive Equations

The shape and volume are changed when external force is applied and increases in these forces lead to increases in the strains that appear on the deformed part. Therefore, there is always a relationship between the stresses and strains by an equation called the **constitutive equation**.

For visco-plastic deformation, plastic deformation is too high when compared with elastic deformation, so the last one is neglected and all the strains are considered to be plastic strains.

In this state, the constitutive equations become **Levy misses equations**:

$$\dot{\epsilon}_{ij} = \frac{3}{2} \frac{\bar{\epsilon}}{\bar{\sigma}} \cdot \dot{\sigma}_{ij}. \quad (12)$$

where $\bar{\sigma}$ = effective stress, $\bar{\epsilon}$ = the rate of effective deformation, $\dot{\epsilon}_{ij}$ = the rate of strain tensor, and $\dot{\sigma}_{ij}$ = the stress deviator [77].

3.11.3 Experimental Work

Diffraction can occur as X-rays from crystalline materials according to Bragg's Law:

$$\lambda = 2 d_{hkl} \sin \theta \quad (13)$$

where d_{hkl} = the inter planar spacing, and λ = the X-ray wavelength.

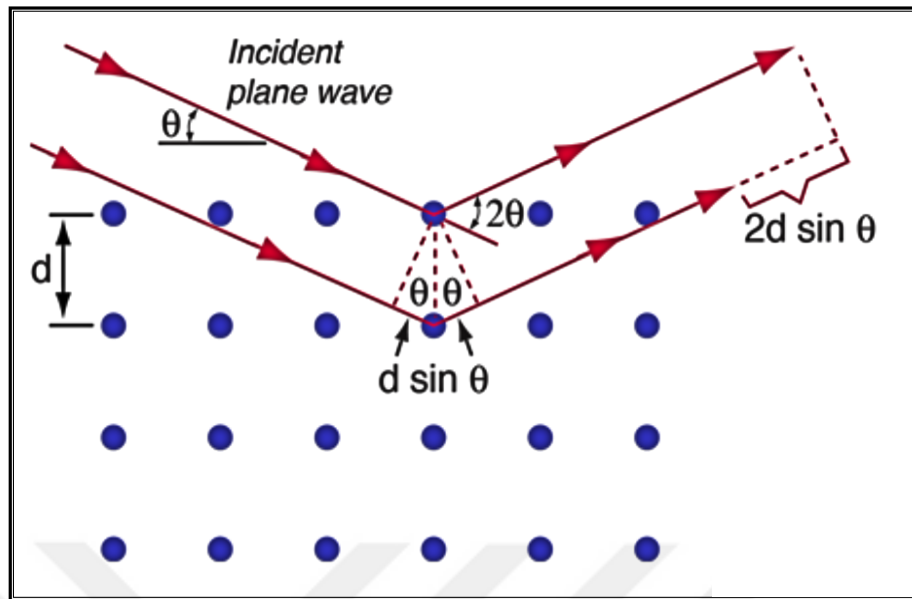


Figure 3.32: X-ray diffraction at the residual stresses [78]

To determine the time of the part life, it can be interact the defects through the part and stress during stress applied.

All service stress is determined by adding the applied stress and residual stresses. These residual stresses are generated from many changes, such as (1) plastic deformation, (2) phase transformation and (3) heat changing. These can occur after processes such as machining, welding, casting and different heat treatments.

Residual stresses can be either useful or harmful depending on whether they are compressive stresses that can help for fatigue resistance or tension stresses that increase fatigue resistance [79].

During the method of measurement, the crystallographic plane uses inter planar spacing (D_{hkl}) that includes large angles greater than 120° . To begin measuring, the part should be rotated around the axis normal to its surface.

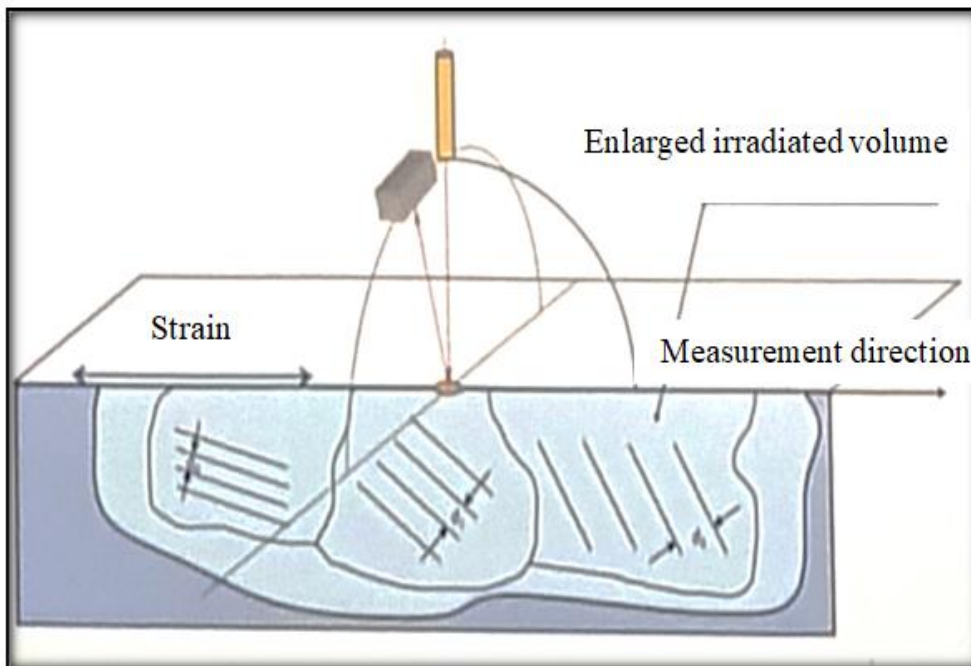
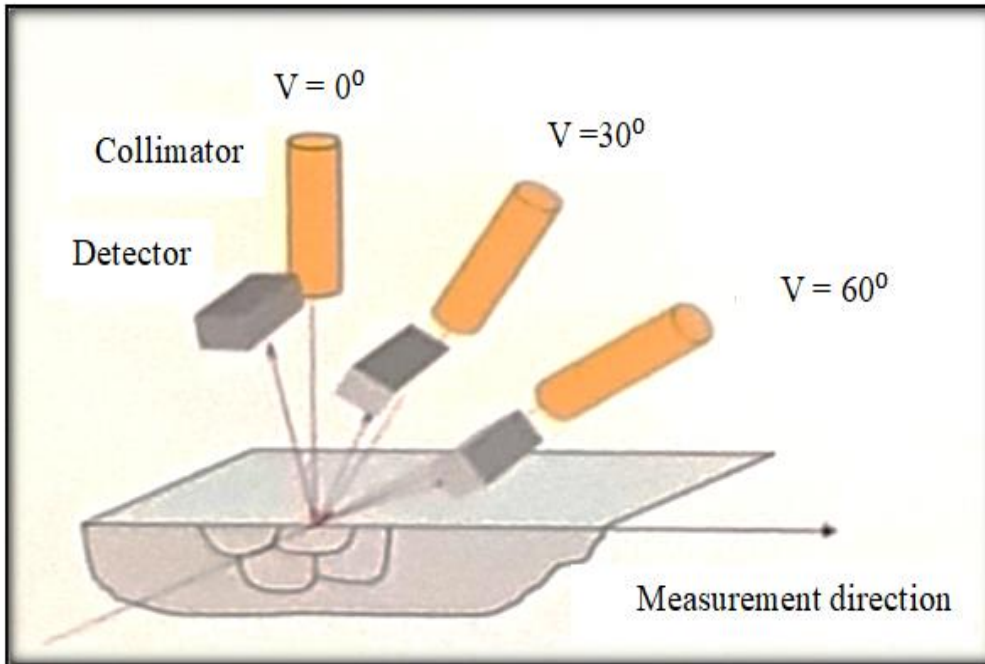


Figure 3.33: Residual stress measurement method [80, 81]

CHAPTER 4

NUMERICAL ANALYSIS PROCESS

4.1 Introduction

In recent years, great changes and evolution have occurred for metal forming processes, the most important of which is the utilization of computers and a variety of software to modify the way processes occur and the method of planning, design and implementation.

Software applications and numerical analysis have made significant differences in the industry in general and in metal forming processes in particular.

Simulation processes have many advantages, one of which is the increase in efficiency of any metal forming process. The most important benefits of simulation are the increase in the process velocity that reduces the process time, the process becoming easier by predicting accurate results and making any necessary modifications to designs and boundary conditions before commencing any experimental work. Other benefits include the improvement of many modern procedures, increasing tool and die design efficiency, reducing material waste by increasing its utilization, and better final product quality and reductions in the cost of production.

When a process would depend on worker experience to find faults, it would, with a great consumption of time, reduce the efficiency of the process and increase manufacturing expenses. New software helps to analyze the process and its properties to predict suitable die designs with optimal results, which leads to the possibility of obtaining optimal conditions to fast track experimental work and facilitate procedures. Many finite element methods are used for this purpose, such as DEFORM or ABAQUS methods and QForm [12].

Metal forming is attractive, especially with increases in product shape complexity and with strict production requirements. Before development of the finite element analysis simulation program, these metal forming processes were performed with many trial and error steps to try new die designs with much time being lost in order to obtain optimal process conditions and product quality. All these factors would inevitably lead to increases in production costs. Therefore, software nowadays is enthusiastically applied to decrease production expenditure and time consumption and increase dimensional accuracy in the final part [4].

General finite element analysis passes through three steps, as shown in Figure 4.1

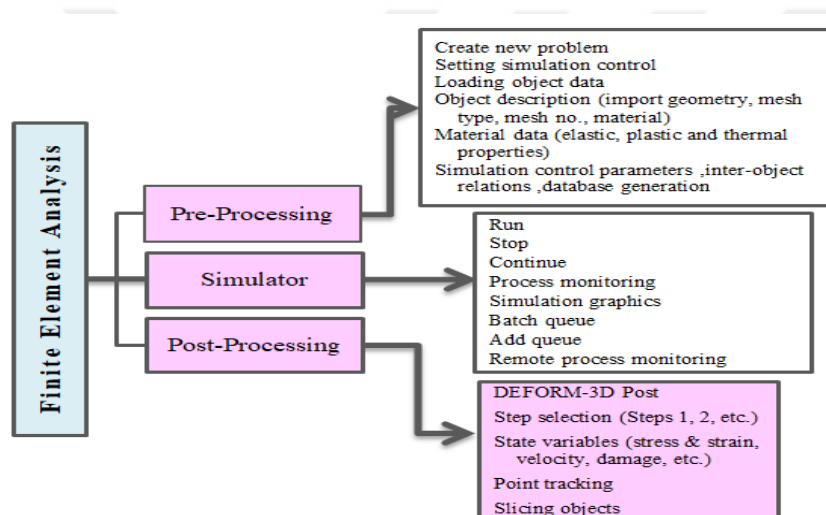


Figure 4.1: General steps to solve problems with the FEM simulation [4]

4.2 Q Form Software

QForm software has the capability of predicting and analyzing metal forming processes, very notably forging and extrusion, and it has excellent applications in the manufacturing process field [18].

QForm V9 is a major development for modern paths in metal forming simulation software. This program can be considered a good reference to continue for further change and advancement in the numerical analysis field, particularly in metal forming. The software has a unique data framework and a clear interface that

increases the speed and simplification of analysis. Moreover, the software has the ability to work in different applications between servers and remote users [77].

4.3 Numerical Analysis

In this study, a QForm simulation is used to predict the values of power, stress, strain temperature and load for the combined extrusion process by investigating the effect of velocity and pressure on the residual stress using the Levy Misses equation as a relation between plastic strain and stress. In spite of using many simulation methods on different forming processes, the aluminum extrusion process numerical analysis is still under investigation, especially for complicated shapes, thin parts, high reduction areas and sharp edges and corner shapes [82].

4.4 Method

In this study, the combined backward-forward extrusion process is used to produce aluminum parts with hollow polygonal shapes. One side is a hexagonal shape produced by backward extrusion and other side is a square shape produced by forward extrusion.

4.4.1 Cases of the Study

According to the requirements, the study demonstrates the effects of two parameters on the residual stresses that formed in the product after combined extrusion:

- 1- Velocity: The study used three values of velocity by duplicating the velocity in each step.
- 2- Pressure: Three values of pressure were applied using different cross sectional areas of the punches because the force was constant.

$$P = F/A$$

4.4.2 Types of Punch

In this study, to achieve the desired product shape, two types of punch should be used to press the work piece and deform it in this combined extrusion process.

- 1- Square punch (for forward extrusion to produce a square sided shape).
- 2- Hexagonal punch (for backward extrusion to produce a hexagonal sided shape).

For the rate of area reduction = RA, punch cross section areas will decrease by 10% in each case.

4.4.3 Punch and Billet Dimensions

1- Square Punches

Table 4.1: Square Punch Dimensions

Cases	Rate of Reduction	Length of side mm (L)	Diameter (D) mm	Area (A) mm ²	Reduction area (RA)
1		12	12	144	68%
2	Decrease 10%	11.4	11.4	130	71%
3	Decrease 20%	10.7	10.7	115	74%

2- Hexagonal Punches

Table 4.2: Hexagonal Punch Dimensions

Cases	Rate of Reduction	Length of side mm (L)	Diameter (D) mm	Area (A) mm ²	Reduction area (RA)
1		10.9	19	313	31%
2	Decrease 10%	10.4	18	281	38%
3	Decrease 20%	9.8	17	250	44%

3- Billets

Table 4.3: Billet Dimensions

Cases	Volume mm ³	Diameter mm	Height mm	Area mm ²
1	7068	24	15.62	452
2	7800	24	17.24	452
3	8538	24	18.87	452

4.4.4 Boundary Condition

Table 4.4: Boundary condition of the process

Type of working	Cold work
Material	Al6061
Type of press	Hydraulic press
Lubrication	With lubrication
Maximum Force	450 kN
Work piece temperature	20°C°
Environment temperature	20°C

Input Parameters

1- Pressure 2- Velocity

Table 4.5: Velocity and pressure values for the three cases of the process

Case	Velocity (mm/s)	Pressure (kN/mm ²)
1	0.25	1.4
2	0.5	1.6
3	1	1.8

Output Parameters

1- Temperature 2- Stress 3- Power 4- Load

4.4.5 Material Chemical Compositions

4.4.5.1 Billet Material

Aluminum Alloy 6061 is a heat treatable wrought alloy which has many properties, including good corrosion resistance, ease of fabrication, good mechanical properties, high machinability, and sufficient ability to be welded. It has wide use in various applications, especially in extrusion, forging and rolling because of its versatility.

Table 4.6: Chemical composition of billet material of commercial Al 6061 [83, 84]

Composition	Mg	Si	Al	Fe	Cu	Zn	Mn	Ti	Cr	Other, each
Wt%	0.4-0.8	0.4-0.8	95.8-98.6	0.7	0.15-0.40	0.25	0.15	0.25	0.04-0.35	Max 0.05

Table 4.7: Chemical composition of billet material of Al 6061 from test

Composition	Mg	Si	Al	Fe	Cu	Zn	Mn	Ti	Cr	Other, each
Wt%	0.85	0.80	96.7	0.6	0.29	0.29	0.08	0.04	0.14	0.045

4.4.5.2 Die Material

Table 4.8: Chemical composition of die and punch materials (tool steel) [85, 86]

Composition	C	Mn	Cr	Fe	Mo	Si	V
Wt%	0.40	0.40	5.25	others	1.35	1.00	1.00

4.5 Die and Product Design

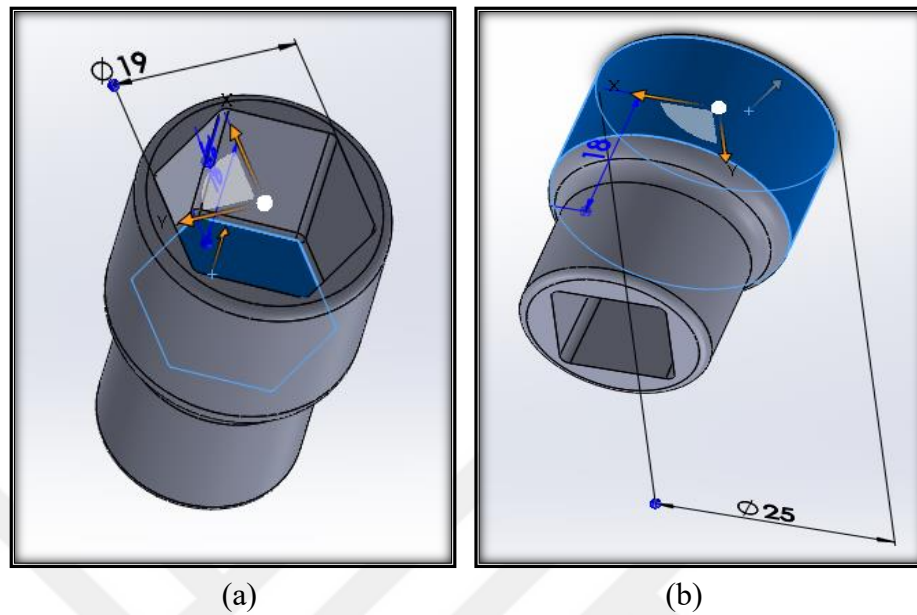


Figure 4.2: Final product shape: (a) Hexagonal side shape produce by backward extrusion; (b) Square side shape produced by forward extrusion

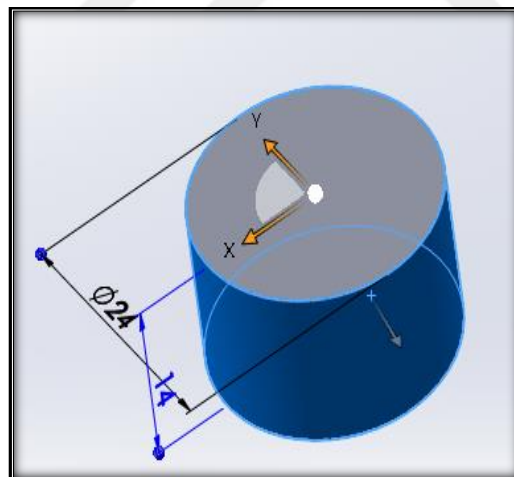


Figure 4.3: Work piece shape

In the extrusion process, the values of pressure and speed are very high such that there is a need for special die finishing and suitable lubrication with a low friction factor. Wear occurs on the die surface because of high velocity and pressure that cause increases in stress and wear. Therefore, mineral oil lubrication is used to reduce the friction and produce good die surfaces for better product quality [87]. In

the extrusion process, for mass production with high accuracy requirements, it is important to know the steps of work piece deformation and the effect of the die shape and its surface finish [88].

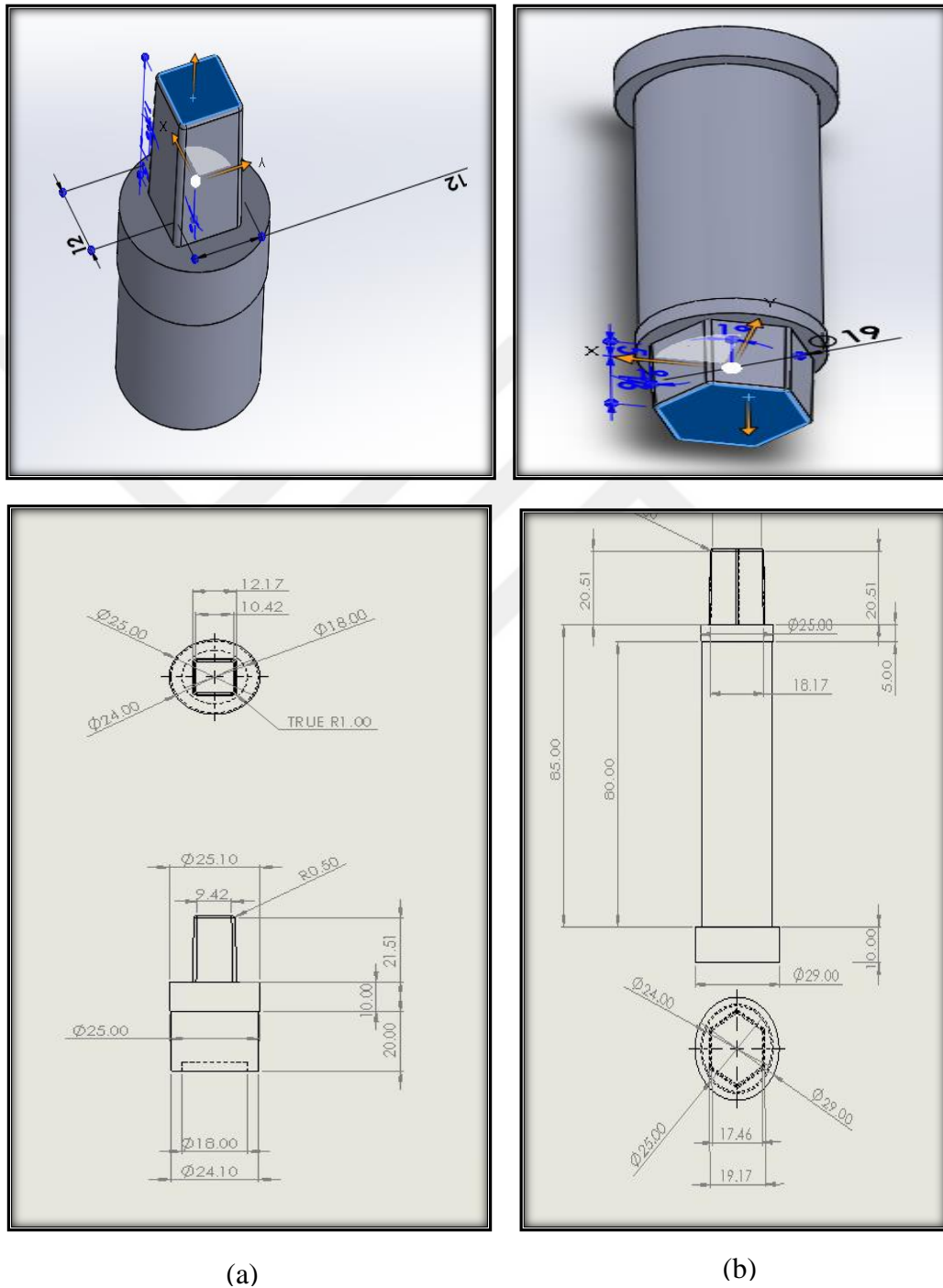


Figure 4.4: Punches: (a) Lower square punch for forward extrusion; (b) Upper hexagonal punch for backward extrusion

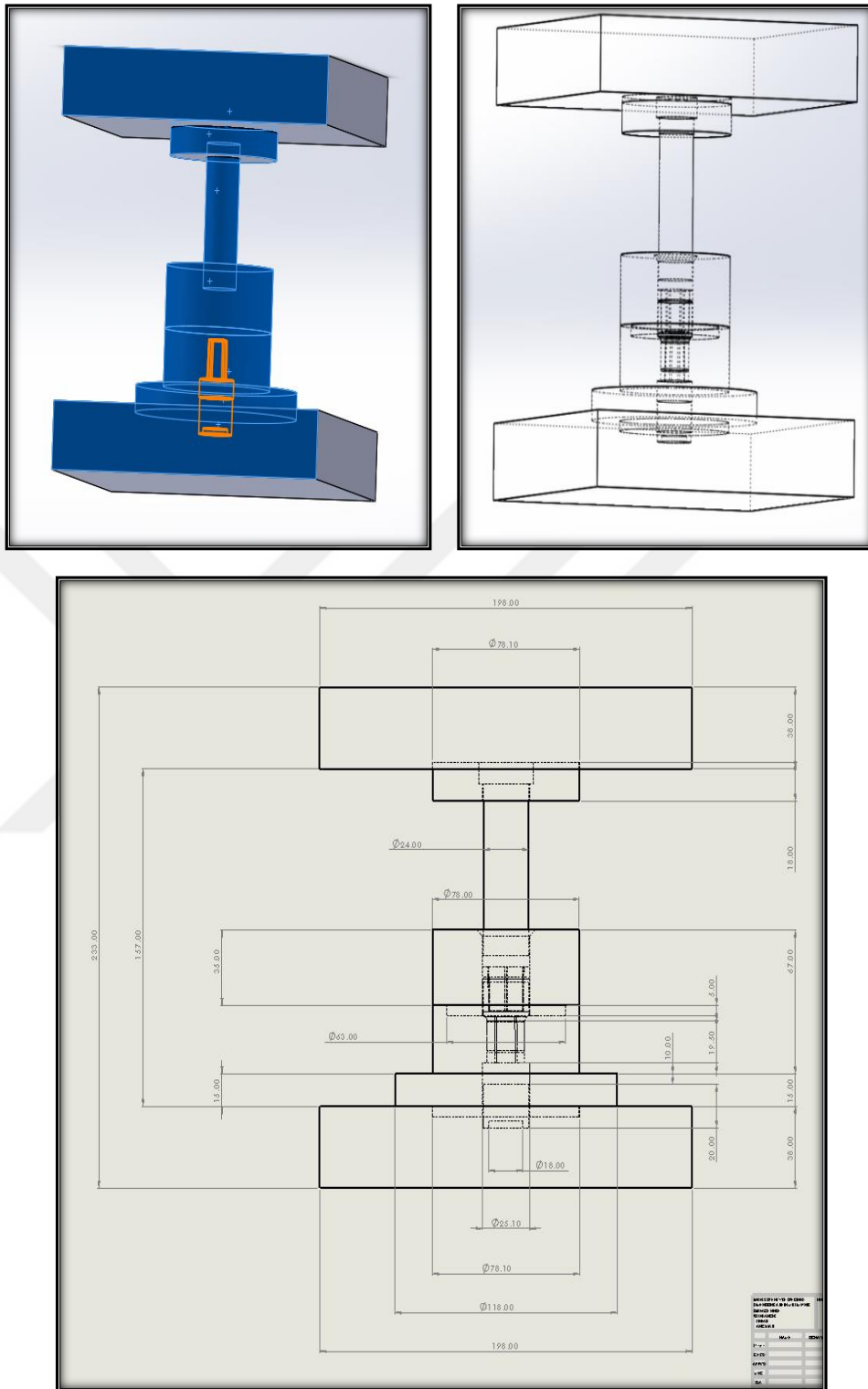


Figure 4.5: Shape of the die assembly of combined backward-forward extrusion

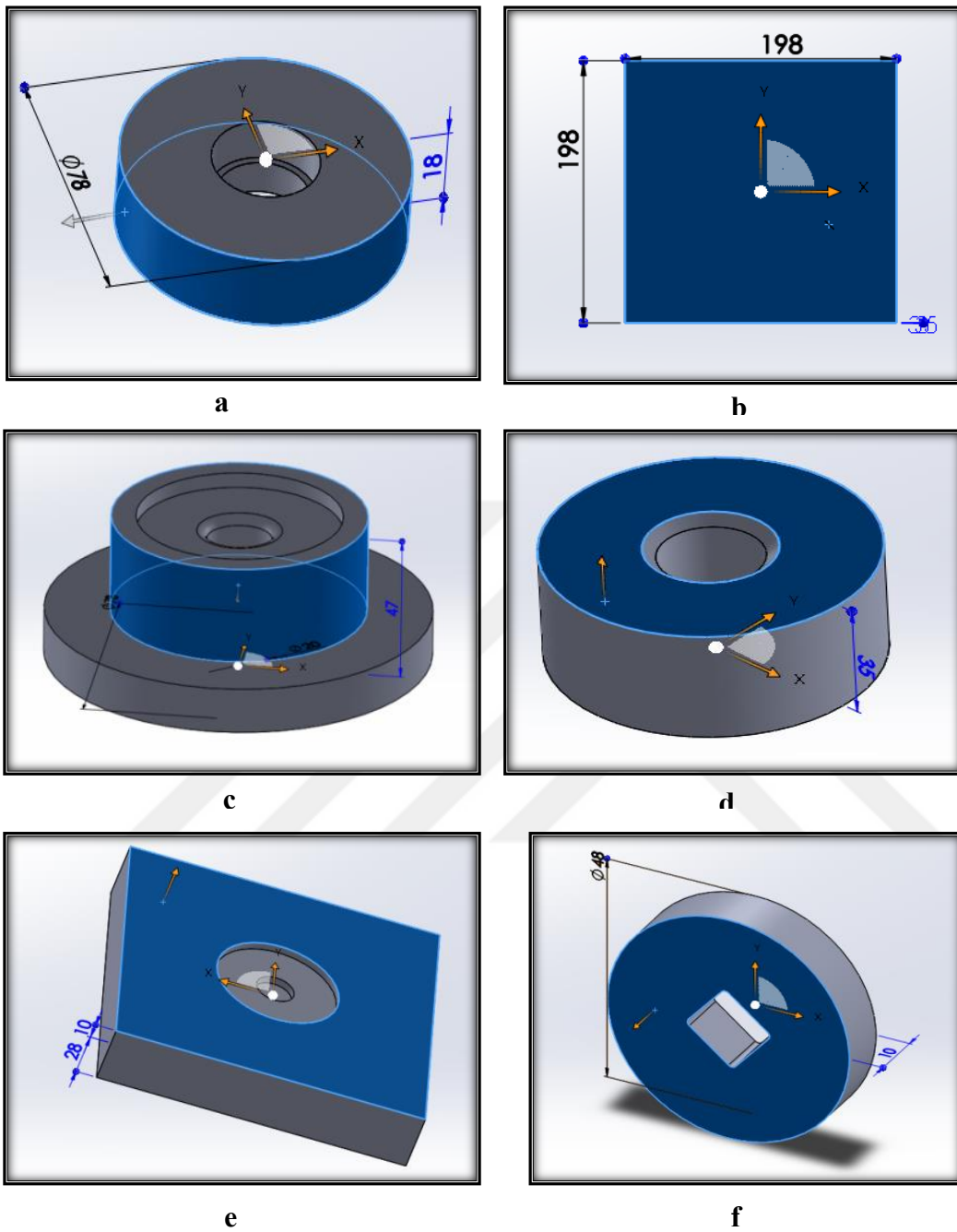


Figure 4.6: Parts of the die: (a) Upper punch holder; (b) Top and bottom plate; (c) Lower holder; (d) Lower billet holder; (e) Ejector; (f) Bottom plate

The design of the die for the extrusion process can be considered more an art more than a science, especially for complex shapes that include many details and various cross-sectional areas. Therefore, a design's success and development depends on the preceding works and practices and can lead to additional costs because of trial

and error, which makes simulation programs necessary to avoid faults. Generally, the most important step is the die filing followed by the next important step of the steady state step at the end of the process, when the product shape is finished with its properties [89].

The importance of the extrusion die comes from its control of all of the process efficiency due to the influence of the die on product quality and production expenses. The complication of the extrusion process and the various geometries of extruded parts with the growth for more complicated shapes makes the accuracy of die design the first requirement for the economic success of the extrusion process [90].

4.6 Simulation Analysis

The analysis of numerical solution includes 2D work because of the symmetry of the die and product shape. The following figures show quarter views of the die and billet deformation. The work page shows all the requirements to analyze the forming process by insert the following :

- (1) The project that involves assigning for the process and sub process names that can be achieved step by step through different analysis .
- (2) Operation which means the process chossing such as forging, rolling and extrusion .
- (3) Boundary conditions of the process which includes the environment temperature (air temperature) .
- (4) Workpiece selection and that is consists of material , microstructure and temperature .
- (5) Tool parameters , in which the lubrication condition, nominal velocity , maximum load and motion direction should be added .

Numerical analysis were performed to optimize the work and results.



Figure 4.7: Home page of the Q Form software

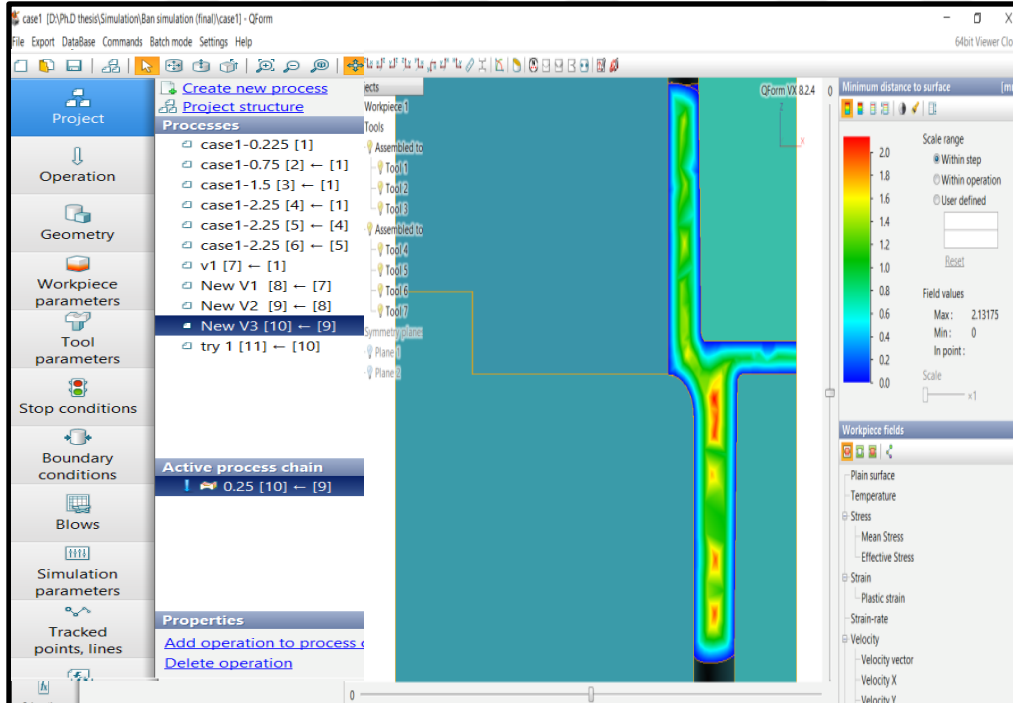
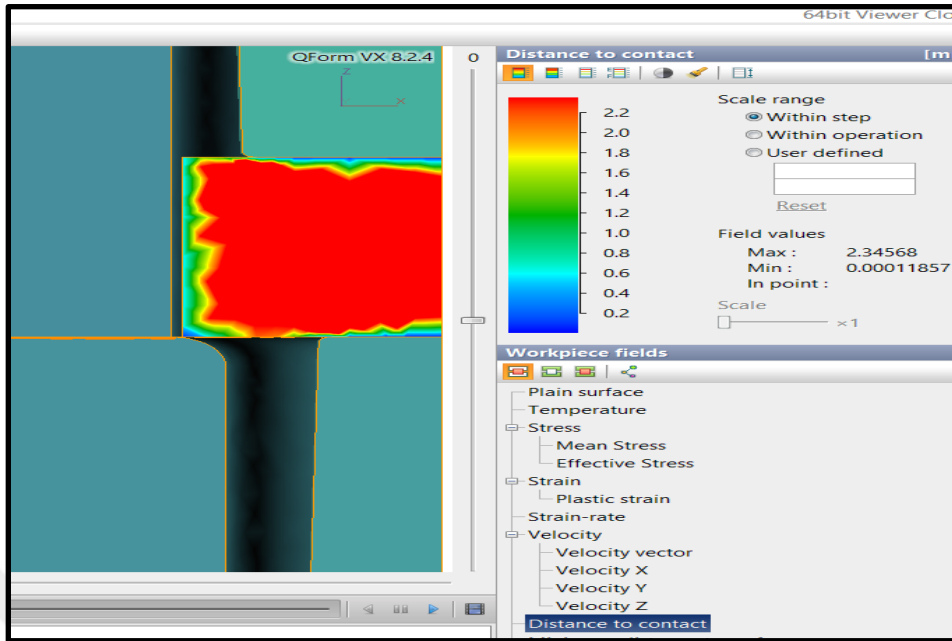
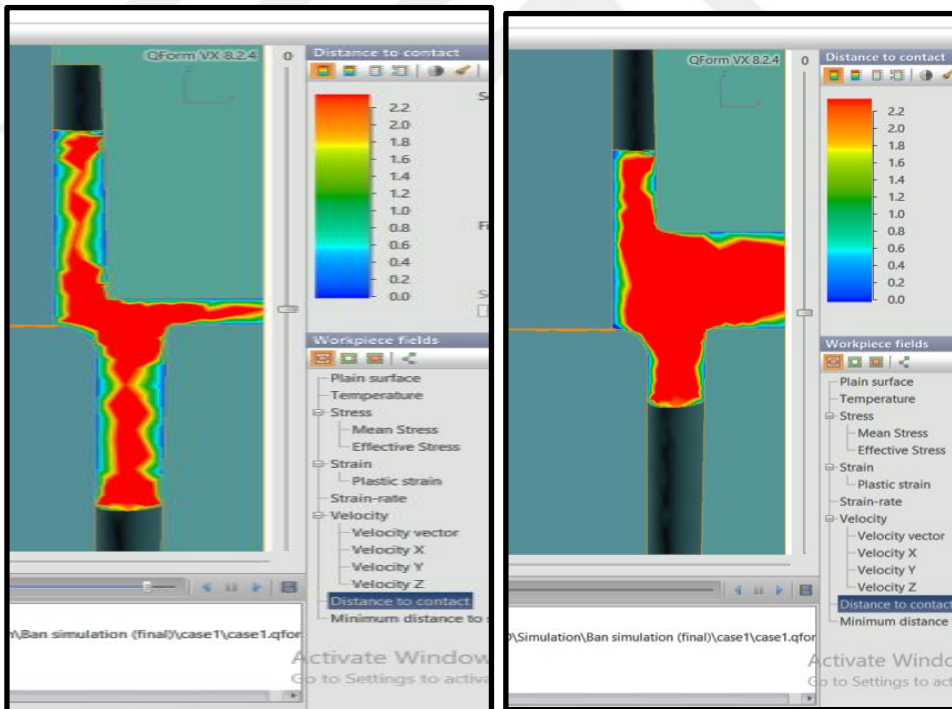


Figure 4.8: Work page of the Q Form software



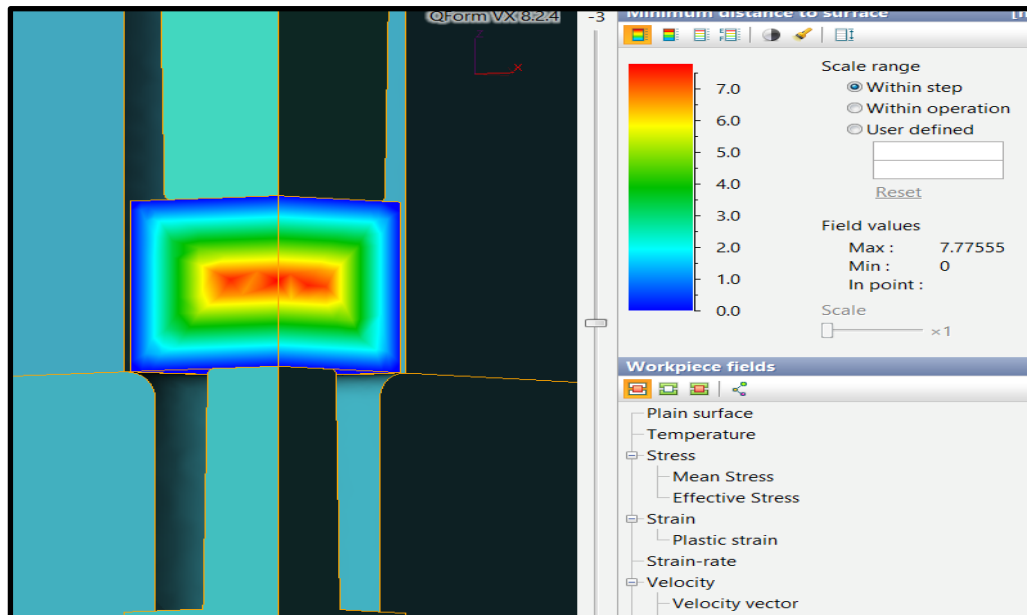
(a)



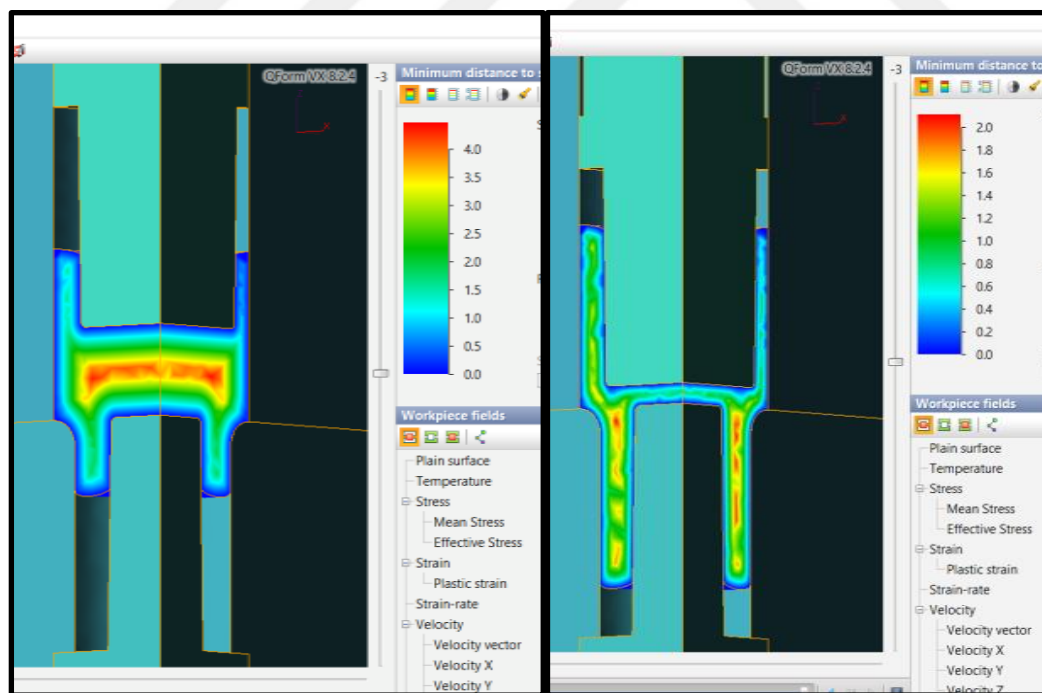
(b)

Figure 4.9: The Q Form simulation for the quarter view of die and sample:
 (a) Billet before deformation; (b) The billet after deformation

The halves of the geometry can be also taken from the QForm software after the simulations for each of the temperature, distance to contact, and strain and stresses with the range of values.



(a)



(b)

Figure 4.10: Q Form simulation for the half view of the die and sample: (a) Billet before deformation; (b) Billet after deformation

CHAPTER 5

EXPERIMENTAL WORK

5.1 Introduction

In this chapter, an investigation of the experimental work is presented to show the influence of velocity and pressure on the residual stresses for billets of aluminum alloy 6061 to produce polygonal hollow shapes with the combined backward-forward extrusion process. The procedure of manufacturing and production for the required part shape is explained. Extrusion is described as big release faces and thermal mellowing by applying large strain changes. Important parameters, such as pressure, process condition, material, flow properties and defect causes, should be clearly discussed when discussing extrusion [91].

In this experimental work, the discussion includes the following:

- 1- Steps of die manufacturing and die parts.
- 2- Aluminum Alloy 6061 work piece preparation.
- 3- Press machine control and process condition.
- 4- Product outputs.
- 5- Results.

5.2 The Experimental Procedure

1. Material selection for the work piece, punches and extrusion die.
2. Finding the chemical compositions of the work piece, punch and die materials.
3. Manufacturing the die for the combined backward-forward extrusion process.

4. Manufacturing punches for the process.
5. Assigning the process parameters.
6. Implementation of the combined backward-forward extrusion process.
7. Solving problems that cause parts to be produced with defects.
8. Applying tests for the products: residual stresses, hardness and microstructure.

5.3 Experimental Work (Methodology)

- 1- Backward extrusion is represented by an externally moving punch to produce hexagonal cross sections.
- 2- Forward extrusion is represented by an internally constant die to produce square cross sections.
- 3- Manufacturing the following parts:
 - Upper punch with a hexagonal shaped section for the backward extrusion direction.
 - Lower punch with a square cross section shaped section for the forward extrusion direction.
 - The other parts of the die that are used to support the punches and the billets in this process.
- 4- Billet preparation with required dimensions.
- 5- Press preparation with ability to change velocity and force with a maximum load of 450 kN to complete the process.

5.3.1 Material

5.3.1.1 Selection of the Work Piece Material

The material of the work piece used in this study for the extrusion process was Aluminum Alloy 6061, which can be used because of its excellent and good properties that are suitable for the extrusion process.

5.3.1.2 General Al 6061 Characteristics

Typical properties of Aluminum Alloy 6061 include:

- Medium to high strength.
- Good toughness.
- Good surface finish.
- Excellent corrosion resistance to atmospheric conditions.
- Good corrosion resistance to sea water.
- Can be anodized.
- Good weldability
- Good workability.
- Wide availability.

5.3.1.3 Billet Preparation

Rods of Aluminum Alloy 6061 are used to prepare the billets according to the required diameter and heights, lathe was used for turning the rods to diameter $D = 24\text{mm}$ with using of lubrication to reduce the effect of residual stresses and heat generation during working. The cutting machine was used to divided the rods to the required workpiece heights which are divided to three groups according to the process three cases of different punches cross sectional area as shown in Figure 5.1



Figure 5.1: Billet preparation

5.3.1.4 Billet Dimensions

Three types of billet sets are prepared according to the process conditions and cases suitable for the pressure cases and hexagonal with square punches that classify the workpieces to three heights and one constant cross section diameter .

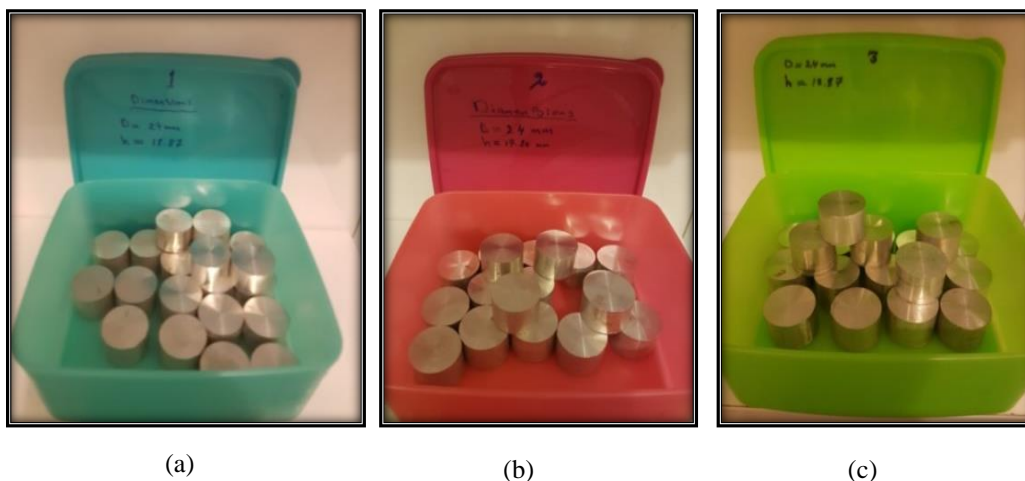


Figure 5.2: Final aluminum billets (a) Case 1 $h = 15.62$ mm $D = 24$ mm (b) Case 2 $h = 17.24$ mm $D = 24$ mm (c) Case 3 $h = 18.87$ mm $D = 24$ mm

5.3.1.5 Billet Heat Treatment

Annealing heat treatment at 500°C for 1 hour is done for the final billets to reduce their hardness and increase their formability and ductility followed by decreasing the power and load because of the cold forming process. As a result, the billets hardness decreases from 114 HB to 38 HB.



Figure 5.3: Annealing heat treatment for billets

5.4 Press Machine

To perform the extrusion process, a computerized hydraulic press machine was used. The press provided a load of up to 450 kN, as well as velocity control for the punches, 500-mm piston stroke and 4 kW of power.

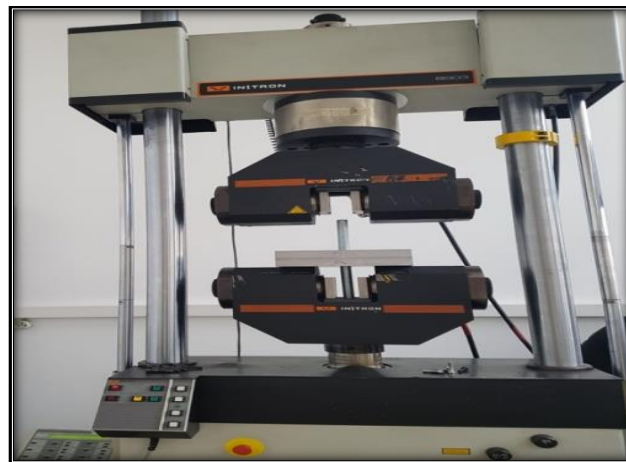


Figure 5.4: Tensile test machine

5.5 Die Manufacturing

5.5.1 Die Parts



Figure 5.5: Die parts



Figure 5.6: Final die

5.5.2 Punch Types

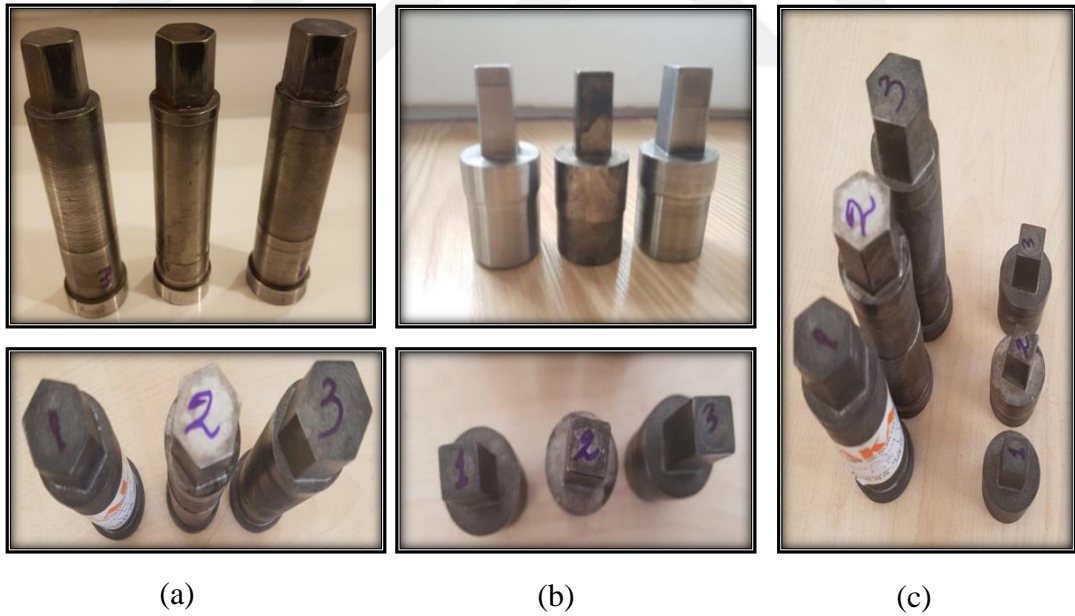


Figure 5.7: Punches: (a) Hexagonal, (b) Square, and (c) all sets

5.6 Experimental Work

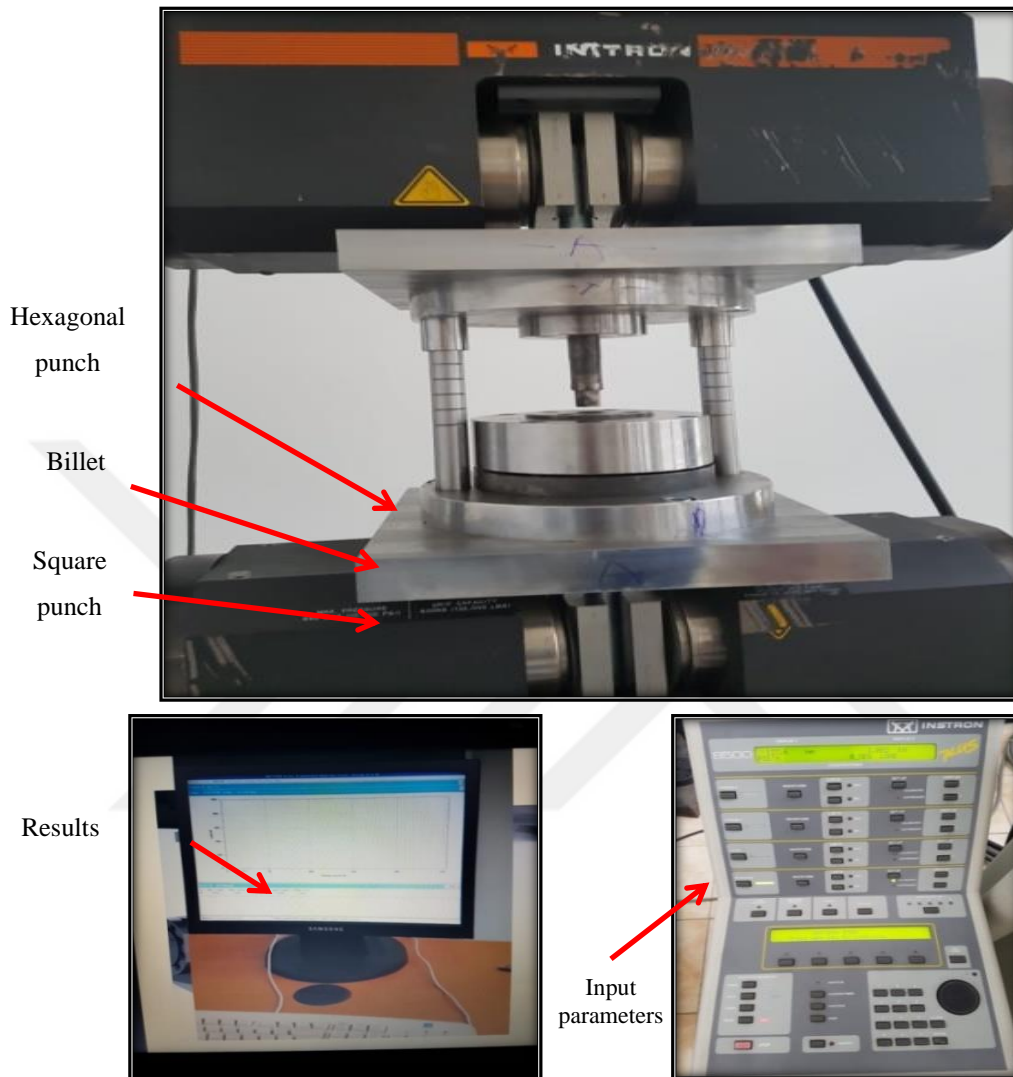


Figure 5.8: Combined extrusion process press, die and work piece setting

Friction is one of the important problems during any process of metal forming and is complicated to evaluate as it depends on the work piece and process condition. [92] Different types of lubrication are used in the extrusion process depending on the work piece material and other process parameters. Some of these lubricants may include vegetable oils others are mineral oils. [93] In this study, a type of mineral oil (MOLY KOTE D321) was used due to its high efficiency at high temperatures and forces.



Figure 5.9: Combined extrusion process: lubrication for the die and billets

5.6.1 Product Shape



(a)

(b)

Figure 5.10: Product inside die: (a) hexagonal side, (b) square side



Figure 5.11: Final product shape

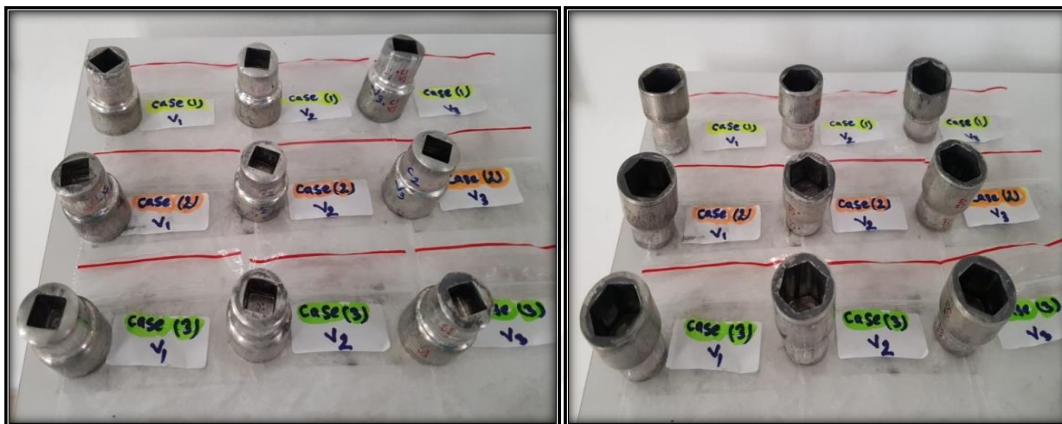


Figure 5.12: Samples for all cases: (a) Square side shape by forward extrusion; (b) Hexagonal side shape by backward extrusion

5.7 Process Defects

5.7.1 Product Defects

- a- Sample broken into two halves.
- b- Flashes on the top and sides of the backward extrusion of hexagonal shape.
- c- Flakes.
- d- Non-uniform surfaces.
- e- Welded the sample with punch after process.
- f- Sharp edges between two halves of die .

g- Large thickness (dimensions not uniform).

h- Surface cracks.

i- Shape not completed.



Figure 5.13: Product defects

5.7.2 Punch Defects

Punch defects are divided into two types:

a- Buckling

b- Broken

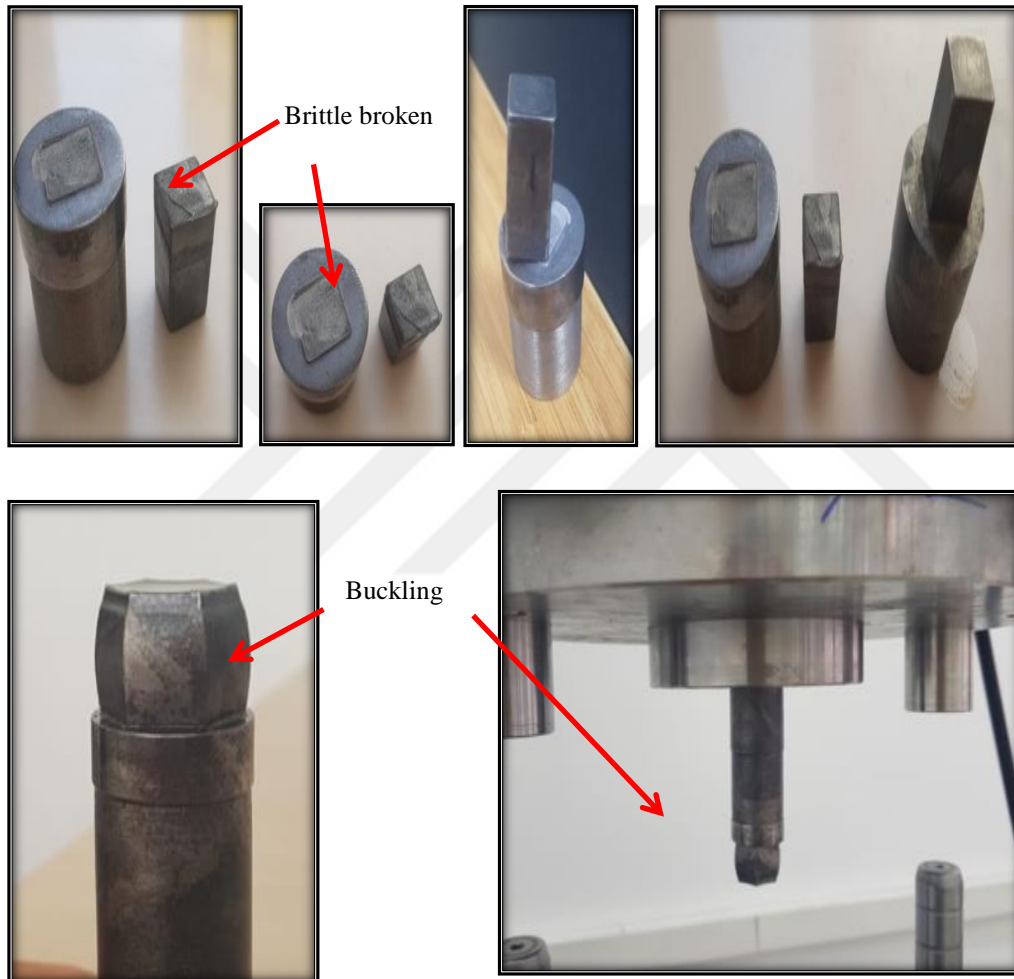


Figure 5.14: Punch defects

5.7.3 Defect Causes

In both cases of product and punch defects, there are many reasons affecting and leading to these faults. These can be avoided by reducing or removing these causes.

- 1- Die design faults in two parts.
- 2- Low punch hardness.
- 3- High billet hardness.
- 4- High velocities.
- 5- No lubrication use.
- 6- High residual stress.
- 7- Non-uniform plastic deformation.
- 8- Non-centering of the punch.
- 9- Applying insufficient loads.

5.8 Samples Preparing for Tests

5.8.1 Samples Cutting

The samples were cut into two halves using the EDM (electrical discharge machine). Two metal parts were submerged in an insulating liquid and connected to a source of current which was switched on and off automatically depending on the parameters set on the controller. When the current was switched on, electric tension was created between the two metal parts. When the two parts were brought together to within a fraction of an inch, the electrical tension would discharge and a spark would jump across. Where it struck, the metal would be heated to the point of melting.

The temperature of the process during the cutting was $T = 8000^{\circ}\text{C}$, which is equal to $T = 15000^{\circ}\text{F}$.

Sometimes problems occur during cutting such as non equal halves , not complete cutting and wire cut because of some mistakes during setting , so the process is repeated many times to achieve equal good halves of the workpiece .

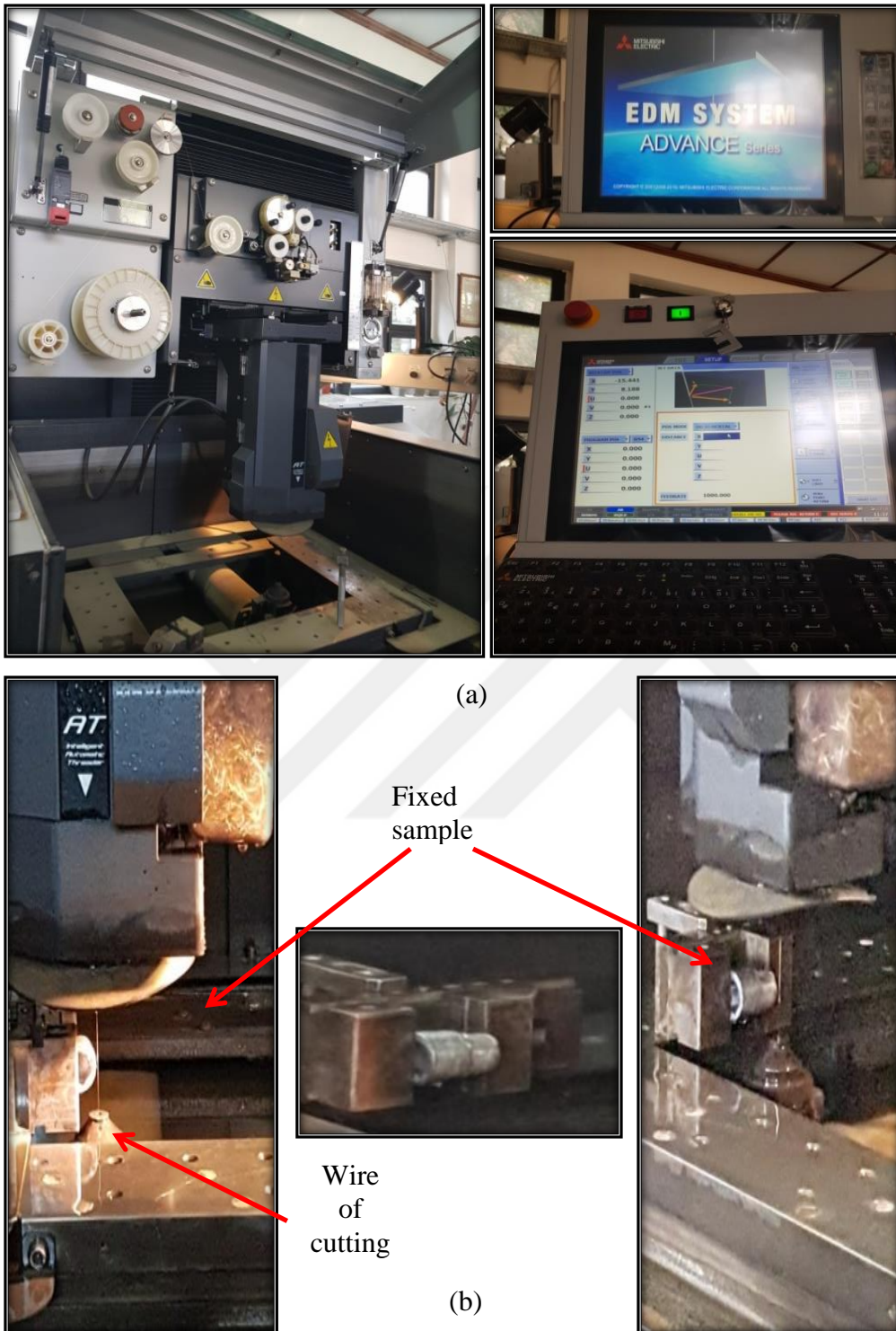


Figure 5.15: (a) EDM machine for samples cutting; (b) Sample fixing in EDM machine.



Figure 5.16: Two halves of samples

5.8.2 Samples Molding

Metallurgy Laboratory

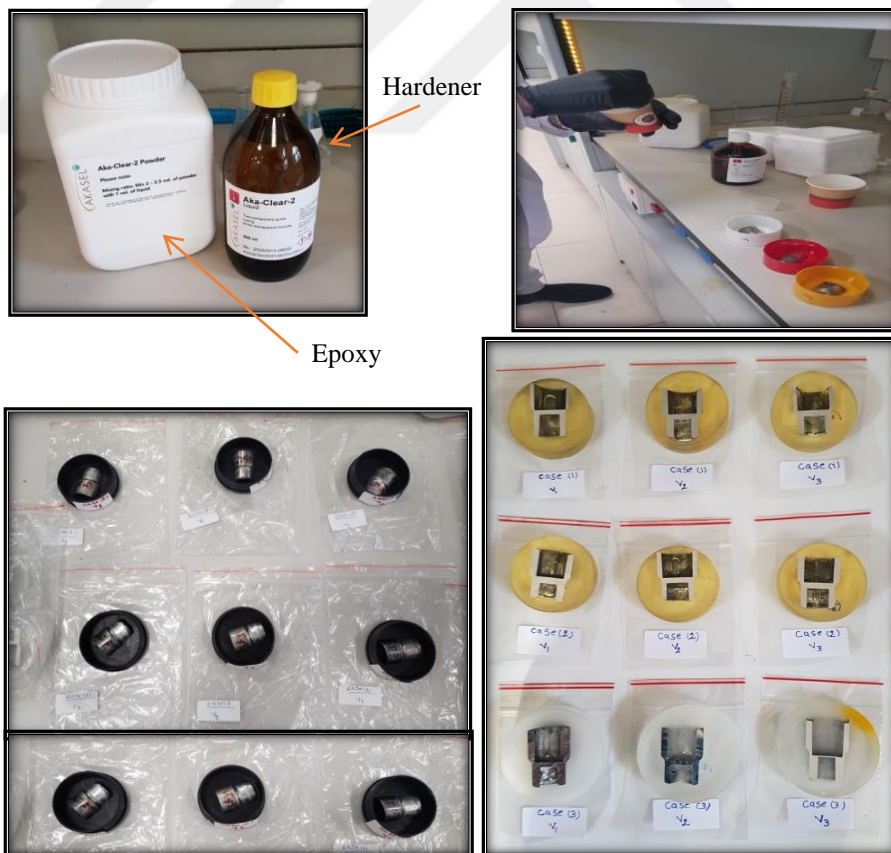


Figure 5.17: Molded samples

5.8.3 Samples Grinding

- 1- Grinding with paper 600 + water (5 minutes).
- 2- Grinding with paper 800 +water (5 minutes).
- 3- Grinding with paper 1200 + water (5 minutes).
- 4- Clean with $\text{CH}_3\text{CH}(\text{OH})\text{CH}_3$.
- 5- Dry with air.

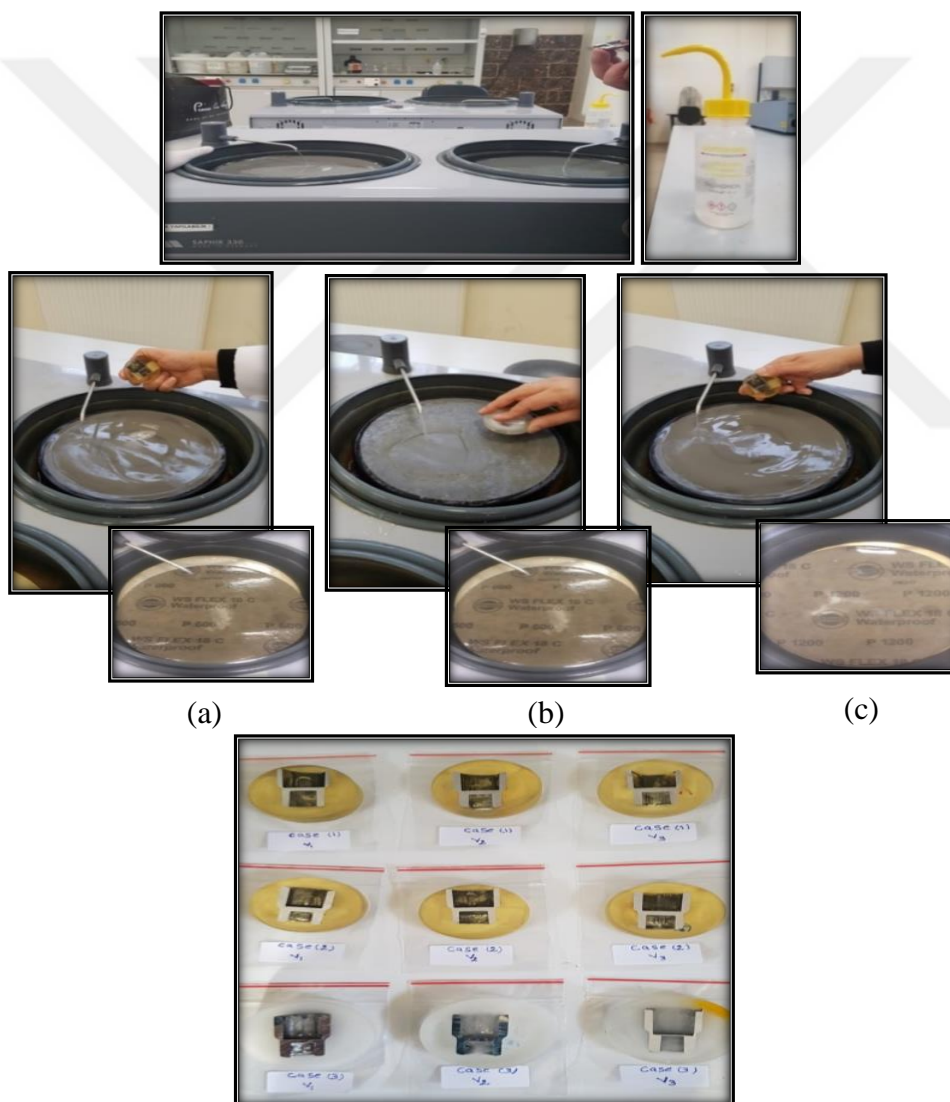


Figure 5.18: Sample Grinding with (a) P 600; (b) P 800; (c) P 1200; and (d) Final grinding samples

5.8.4 Samples Polishing

- A- 6 μm with Dia Doublo Mono 6 μm 500 mL (10 minutes)
- B- 3 μm with Dia Doublo Mono 3 μm 500 mL 3130 (15 minutes)
- C- 1 μm with Dia Doublo Mono 1 μm 500 mL 3120 (10 minutes)
- D- 0.25 μm with colloida silica (5 minutes).



(d)



Figure 5.19: Sample polishing steps: (a) 6 μm , (b) 3 μm , (c) 1 μm , and (d) 0.25 μm

5.8.5 Sample Etching

For sample etching for the macrostructure and microstructure, the following chemicals were used:

5.8.5.1 Macrostructure Etching

- 1- 15 mL HF (hydrofluoric acid).
- 2- 45 mL HCL (hydrochloric acid).
- 3- 15 mL HNO₃ (nitric acid).
- 4- 25 mL pure water [94, 95].

5.8.5.2 Microstructure Etching

- 1- 2 mL HF (hydrofluoric acid).
- 2- 45 mL HCl (hydrochloric acid).
- 3- 5 mL HNO₃ (nitric acid).
- 4- 190 mL pure water [96, 97].

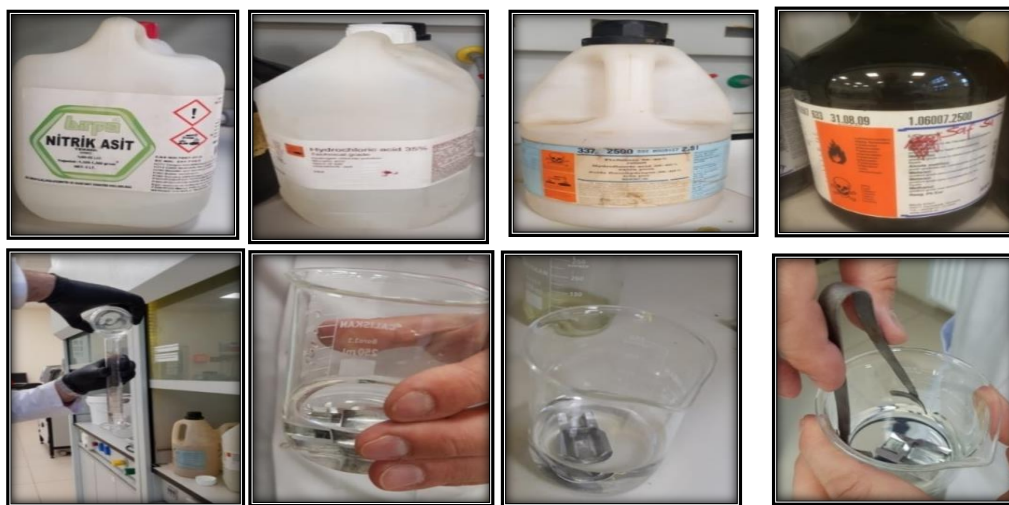


Figure 5.20: Sample etching

5.9 Tests

5.9.1 Macrostructure Test (Optical Micro Scope)

The macrostructure test was done for the 9 samples of three cases:

- 1- Case 1 ($P1 = 1.4 \text{ kN/mm}^2$)
- 2- Case 2 ($P2 = 1.6 \text{ kN/mm}^2$)
- 3- Case 3 ($P3 = 1.8 \text{ kN/mm}^2$)

In each case three velocities are used $V1 = 0.25 \text{ mm/s}$, $V2 = 0.5 \text{ mm/s}$ and $V3 = 1 \text{ mm/s}$.

The test was applied to different regions on the sample, as shown in Figure 5.21

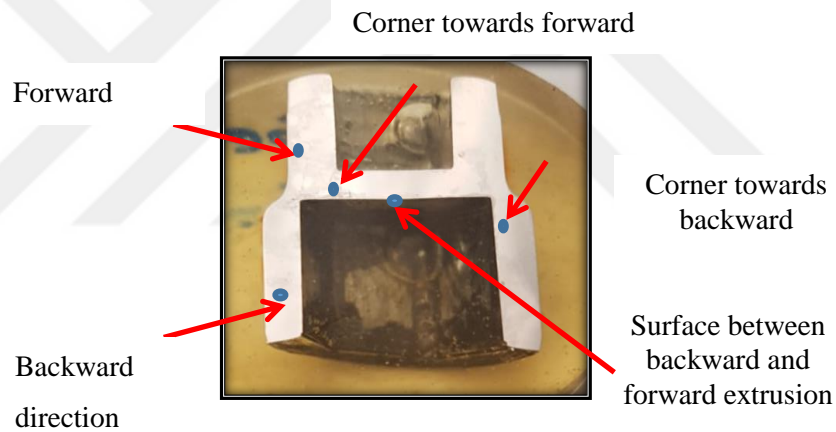


Figure 5.21: Sample regions

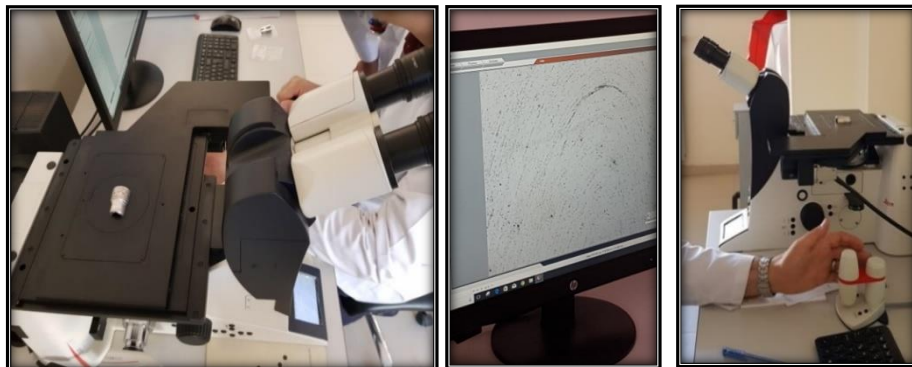


Figure 5.22: Macro structure test (optical test)

5.9.2 Microstructure Test (Stereo Macro Scope)

DM4 M and DM6 M Microscopes from Leica Microsystems were used for the microstructure test.



Figure 5.23: Samples micro structure test (stereo test)

5.9.3 Residual Stress Test

The XRD 3003 TPS X-ray diffraction system was used to measure residual stresses at different points of the parts. This method used fixed penetration; however, a number of errors can occur because of the non-uniform control of penetration. The measurement depends on samples being lean and strain free with crystallographic texture analysis [98]. X-rays are dispersed with a polycrystalline solid to produce a diffracted beam with the measurement of angles using Bragg's Law [99].

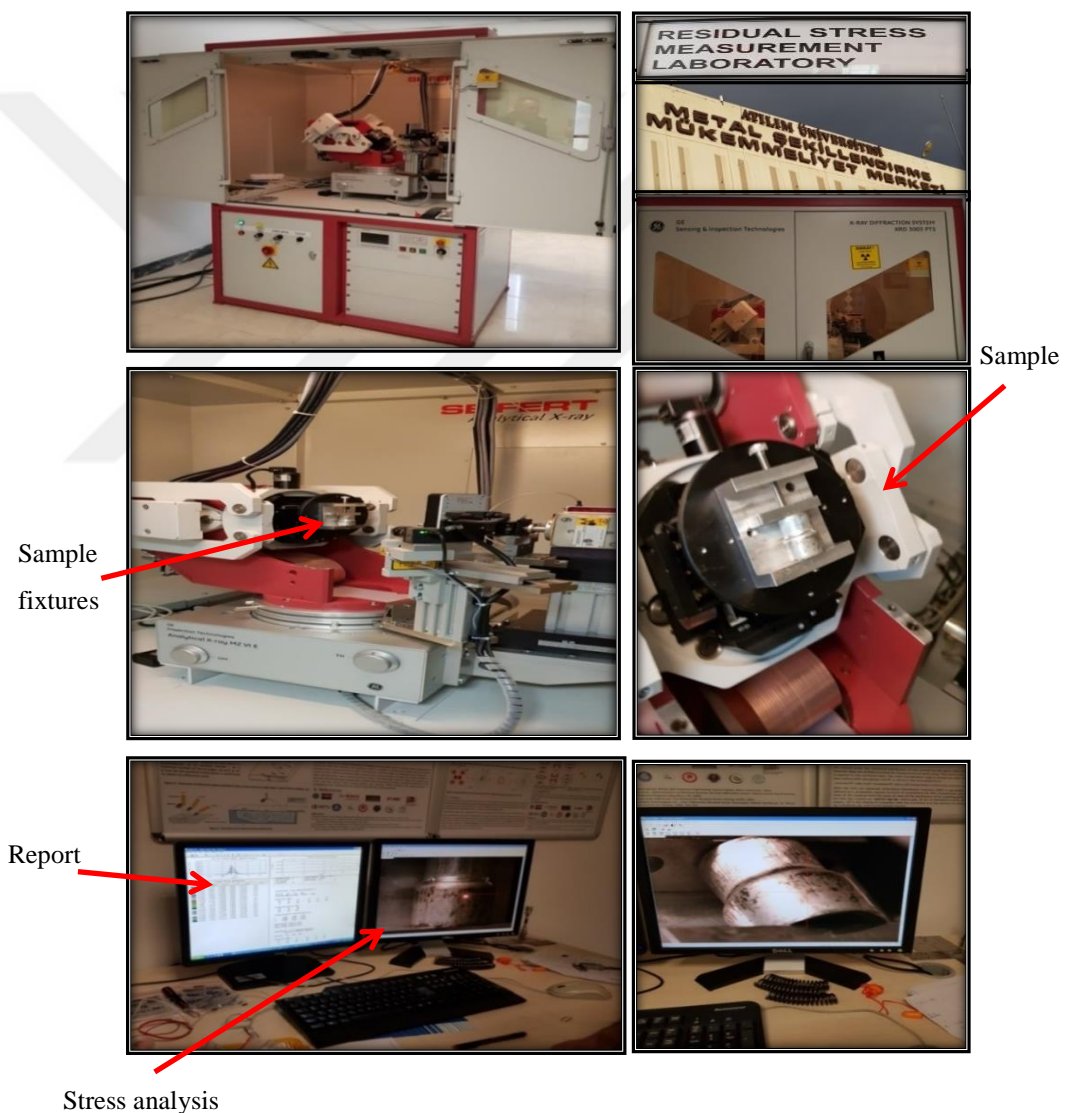


Figure 5.24: Residual stress test machine

5.9.4 Hardness Test

The HMV SHIMADZU micro hardness tester was used to measure the sample hardness with a Vickers indenter with load $p = 200 \text{ g}$ and time $t = 10 \text{ s}$.

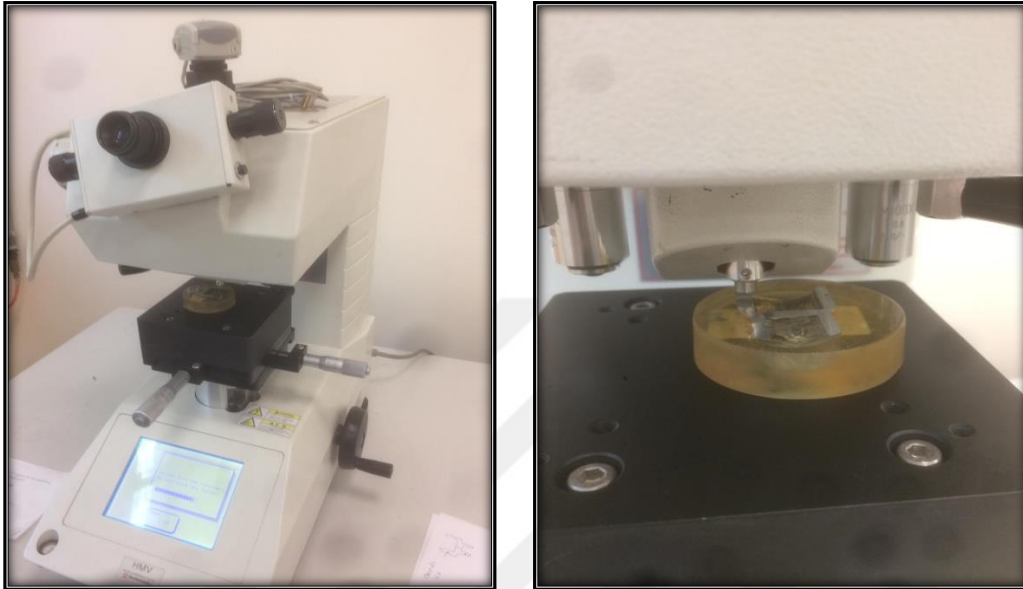


Figure 5.25: Hardness Vickers tester



Figure 5.26: Hardness impact and score

CHAPTER 6

RESULTS AND DISCUSSION

6.1 Simulation Results

6.1.1 Stress Distribution

Numerical analysis was performed to predict the residual stress distribution along the die during combined backward-forward extrusion processes using three velocities with three constant pressures to deform cylindrical billets of Aluminum Alloy 6061 [100]. The hexagon shaped side was produced using backward extrusion and the square shaped side was produced using forward extrusion. Mineral oil was selected as the lubricant in the hydraulic press.

The QForm simulation showed the regions of stress concentration and predicted the values of the residual stresses along the work piece and product. The punch in the forward extrusion process with the square shape was stationary down the die, while the punch in the backward extrusion process moved from the upper part of the die. The stress distribution for the first case of constant pressure (P1) with V1, V2, V3 for the quarter of the shape is shown in the following figures.

The Q Form results window show scale of stress values with different colours from the minimum to the maximum value to the right side of the shape . In addition, the quarter of the product shape is demonstrated with the stress distribution along the part . The stresses on this method can be mean stress or effective stress while strains that are taken from this numerical analysis are plastic strain and strain rate .

The product appears in this window inside the die parts and it is possible to hide any parts of the tools and leave the product only .

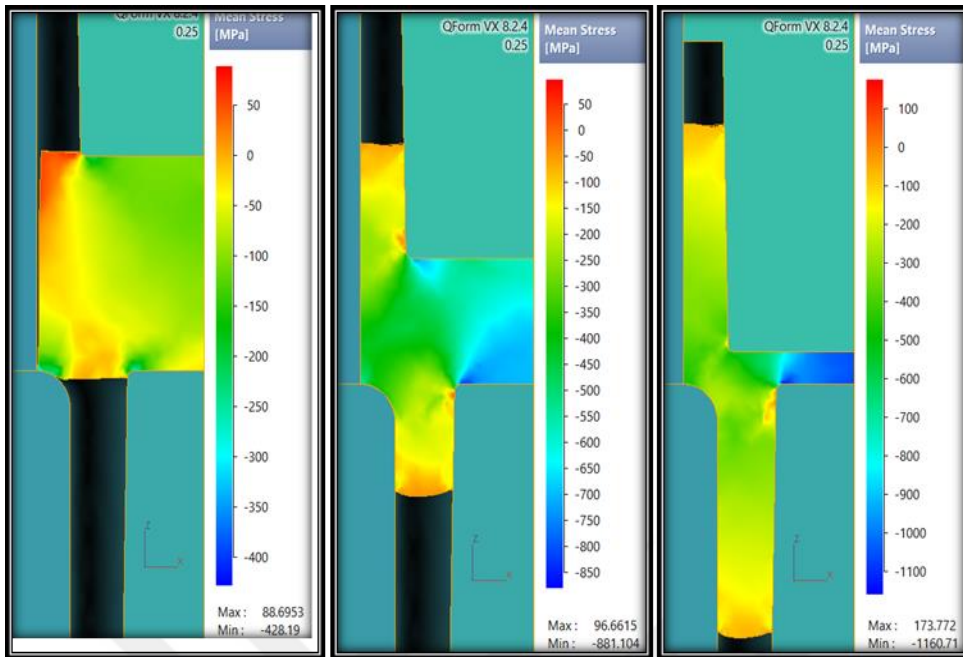


Figure 6.1: Mean stress distribution steps for case 1 ($P1 = 1.4 \text{ kN/mm}^2$) at $V1 = 0.25 \text{ mm/s}$

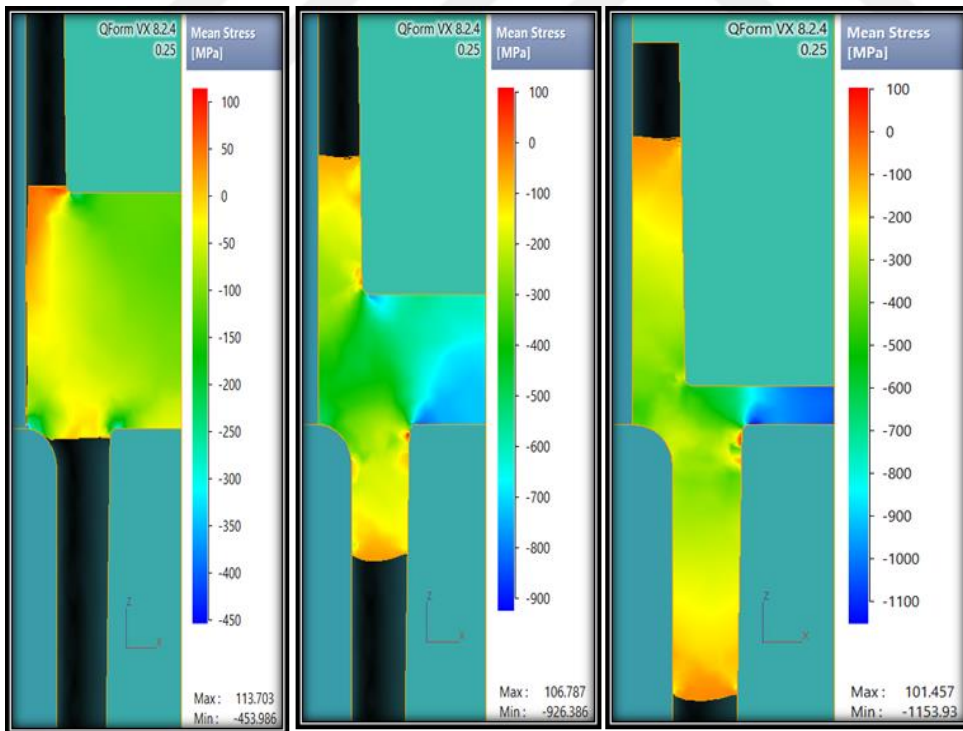


Figure 6.2: Mean stress distribution steps for case 1 ($P1 = 1.4 \text{ kN/mm}^2$) at $V2 = 0.5 \text{ mm/s}$

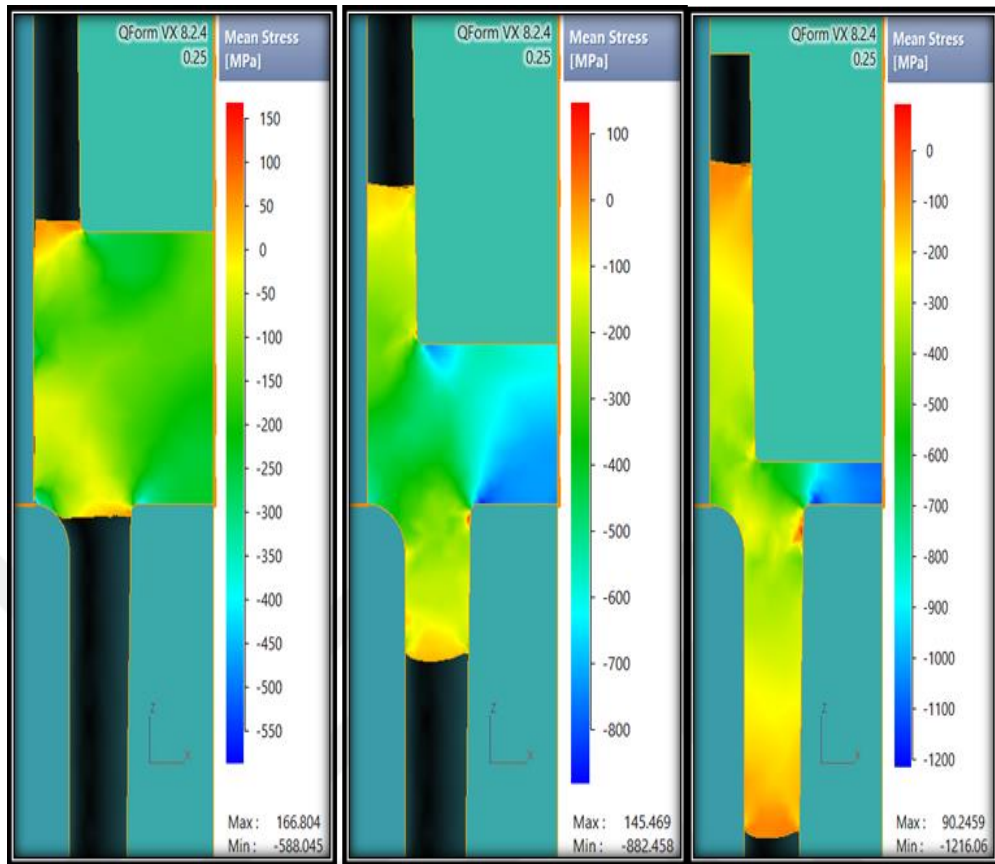


Figure 6.3: Mean stress distribution steps for case 1 ($P1 = 1.4 \text{ kN/mm}^2$) for $V3 = 1 \text{ mm/s}$

The numerical analysis for the residual stresses shows high values at each sharp edge in the die, especially in the forward and backward direction movement. This occurs because of the high friction at that regions and the turbulent flow due the sudden cross sections changing. In the beginning of the pressing, the highest stress values concentrate at the contact area between the punch and work piece until the end of deformation. They then appear at the sharp edges. An increasing velocity leads to an increase in the stresses at constant pressure. The regions with the blue color refer to the minimum stress values. The best stress distribution occurs at the middle velocity value of $V2 = 0.5 \text{ mm/s}$ because it ensures low stress with good deformation conditions.

6.1.1.1 Stress Relations at Constant Pressures

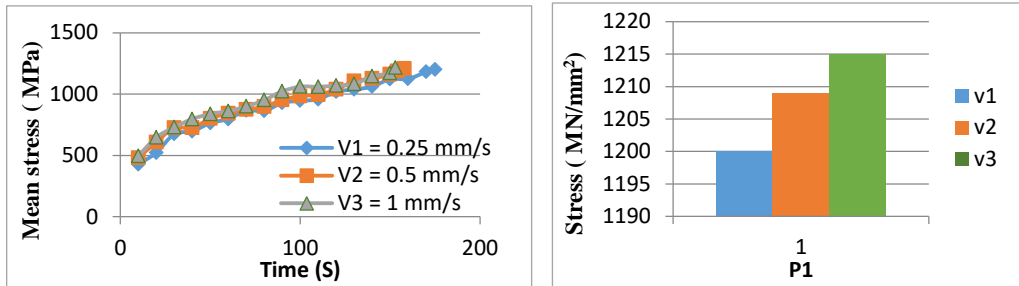


Figure 6.4: Mean stresses for $V1 = 0.25 \text{ mm/s}$, $V2 = 0.5 \text{ mm/s}$ and $V3 = 1 \text{ mm/s}$ with constant pressure $P1 = 1.4 \text{ kN/mm}^2$

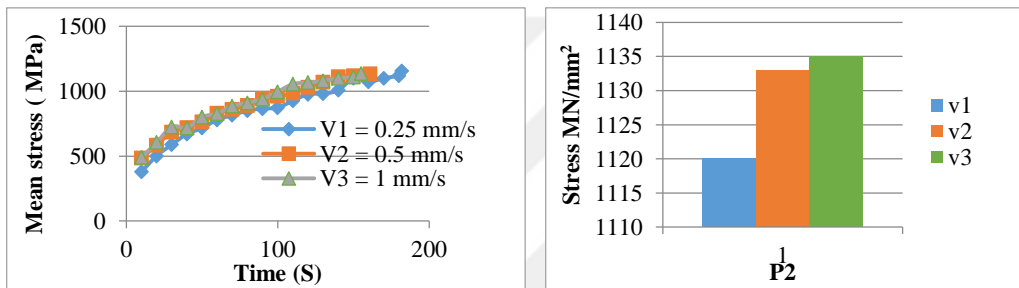


Figure 6.5: Mean stresses for $V1 = 0.25 \text{ mm/s}$, $V2 = 0.5 \text{ mm/s}$ and $V3 = 1 \text{ mm/s}$ with constant pressure $P2 = 1.6 \text{ kN/mm}^2$

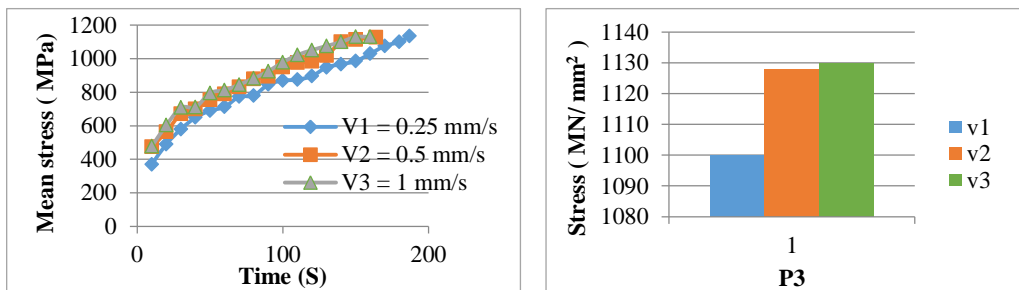


Figure 6.6: Mean stresses for $V1 = 0.25 \text{ mm/s}$, $V2 = 0.5 \text{ mm/s}$ and $V3 = 1 \text{ mm/s}$ with constant pressure $P3 = 1.8 \text{ kN/mm}^2$

From the figure above, it is seen that at a constant pressure, the increase of velocity from $V1 = 0.25 \text{ mm/s}$ to $V3 = 1 \text{ mm/s}$ leads to an increase in the residual stresses from 1,200 MPa to 1,215 MPa at $P1 = 1.4 \text{ kN/mm}^2$, 1,120 MPa to 1,135 MPa at $P2 = 1.6 \text{ kN/mm}^2$ and 1,100 to 1,130 kN/mm^2 at $P3 = 1.8 \text{ kN/mm}^2$. Therefore, the highest stresses of 1,215 MPa occur at $V3 = 1 \text{ mm/s}$ and minimum pressure of $P1 = 1.4 \text{ kN/mm}^2$.

6.1.1.2 Stress Relations at Constant Velocity

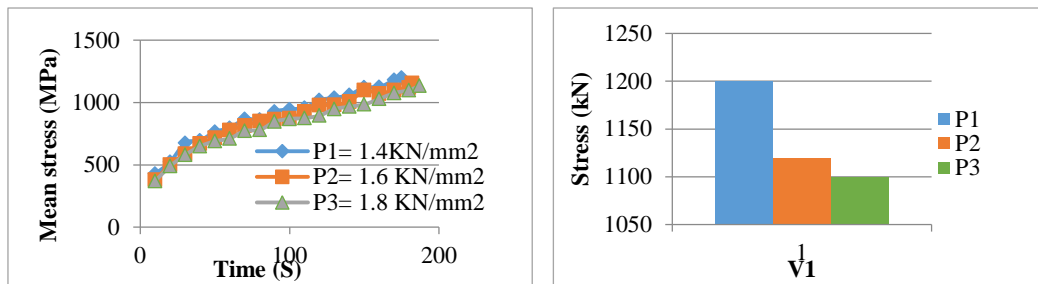


Figure 6.7: Mean stresses for $P1 = 1.4 \text{ kN/mm}^2$, $P2 = 1.6 \text{ kN/mm}^2$ and $P3 = 1.8 \text{ kN/mm}^2$ with constant velocity $V1 = 0.25 \text{ mm/s}$

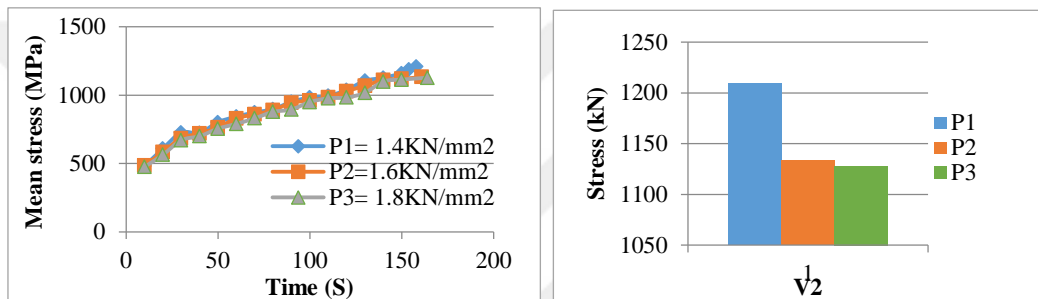


Figure 6.8: Mean stresses for $P1 = 1.4 \text{ kN/mm}^2$, $P2 = 1.6 \text{ kN/mm}^2$ and $P3 = 1.8 \text{ kN/mm}^2$ with constant velocity $V2 = 0.5 \text{ mm/s}$

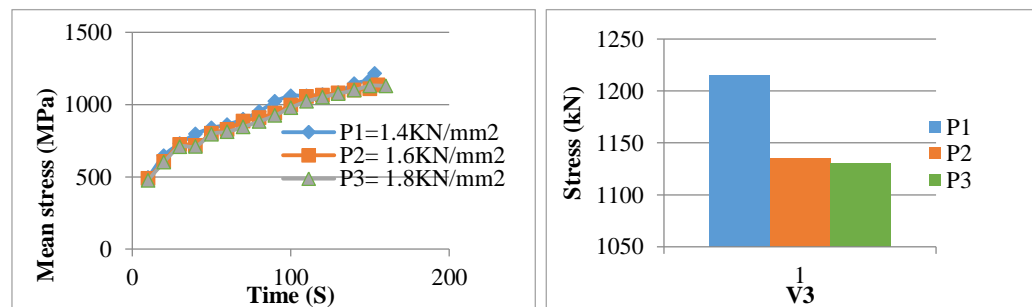


Figure 6.9: Mean stresses for $P1 = 1.4 \text{ kN/mm}^2$, $P2 = 1.6 \text{ kN/mm}^2$ and $P3 = 1.8 \text{ kN/mm}^2$ with constant velocity $V3 = 1 \text{ mm/s}$

The residual stresses decrease with increasing pressure, as seen in Figures 6.7, 6.8 and 6.9. When the punch pressure increase, the force can exceed the friction force and reduce the effects of the stresses that are kept on the part. The stresses increase from the beginning of the deformation due to the change of billet shape and increasing temperature. The stresses reach the highest value at the end of deformation process.

6.1.2 Temperature Distribution

The work piece temperature and environment temperature was 20°C and the process was carried out using lubrication to avoid sharp increases of temperature during deformation and to reduce the load and power required for extrusion. The temperature distribution revealed many regions of high temperature and others with low temperatures depending on the contact surfaces. The yellow color shows the highest temperature rates while the red and black colors indicate the minimum temperatures. The upper and lower punches are shown by coming into contact with the work piece from the first movement to the final product shape and the end of the process. Three velocities were used to clarify the temperature distribution in each point on the work piece, as shown in the figures below.

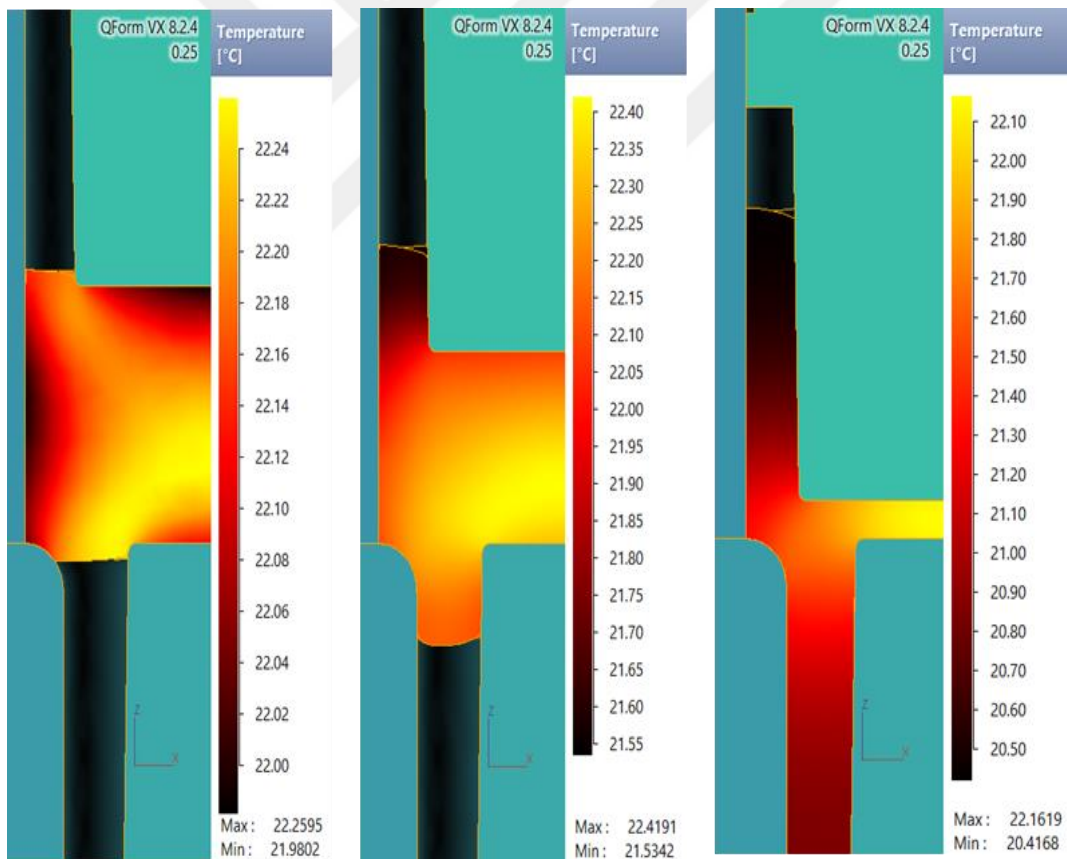


Figure 6.10: Temperature distribution along the work piece for P1 = 1.4 kN and V1 = 0.25 mm/s

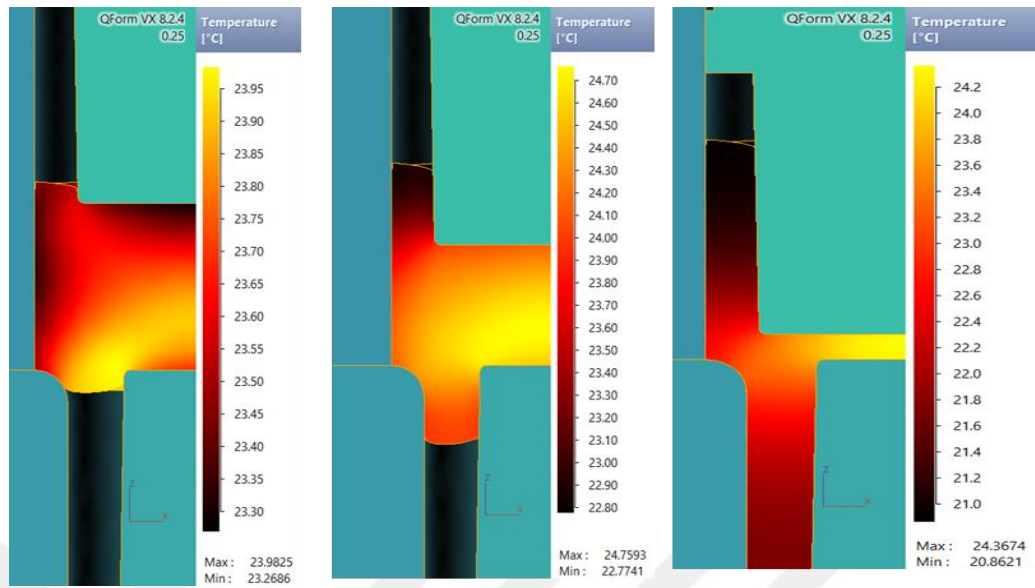


Figure 6.11: Temperature distribution along the work piece for $P1 = 1.4 \text{ kN}$ and $V2 = 0.5 \text{ mm/s}$

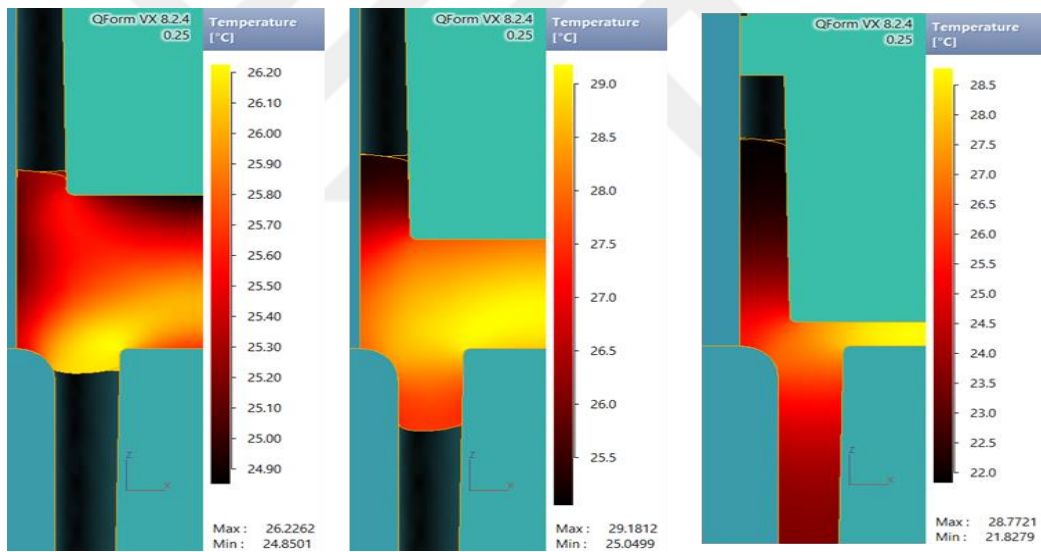


Figure 6.12: Temperature distribution along the work piece for $P1 = 1.4 \text{ kN}$ and $V3 = 1 \text{ mm/s}$

The figures show that the temperatures increased during the beginning of deformation and higher values were on the corner of the backward extrusion because of the higher friction effects in this region due to the opposite directions of the metal movement that led to heat generation. The minimum temperatures appeared at the forward region where the metal moved in the same direction as the pressing.

6.1.2.1 Temperatures Relations at Constant Pressure

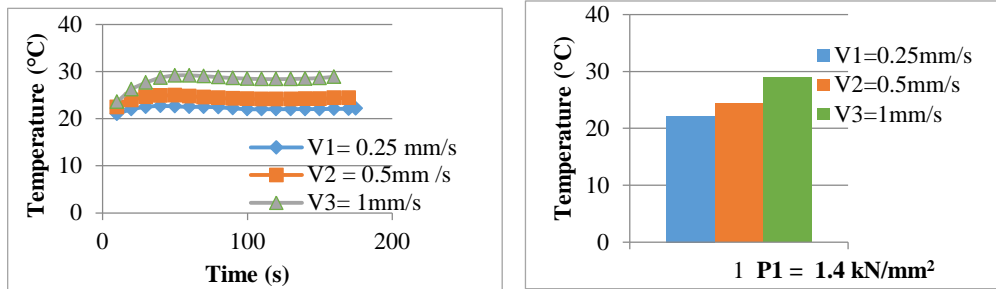


Figure 6.13: Temperature for V1 = 0.25 mm/s, V2 = 0.5 mm/s and V3 = 1 mm/s with constant pressure P1 = 1.4 kN/mm²

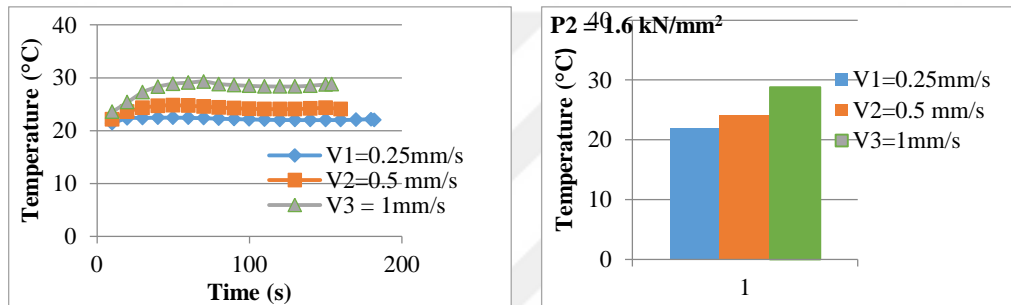


Figure 6.14: Temperature for V1 = 0.25 mm/s, V2 = 0.5 mm/s and V3 = 1 mm/s with constant pressure P2 = 1.6 kN/mm²

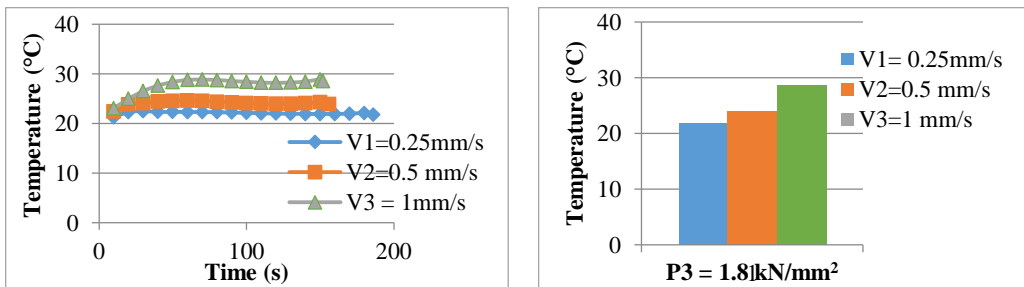


Figure 6.15: Temperature for V1 = 0.25 mm/s, V2 = 0.5 mm/s, V3 = 1 mm/s with constant pressure P3 = 1.8 kN/mm²

From the relationship between the temperature and time at constant pressure, the curves show an increase at the first deformation because of the high forces required to change the billet shape and volume. The temperature tended to be constant because of little change to the shape occurring due to punch pressing reducing the friction forces. Increasing velocities led to an increase in friction and temperature values.

6.1.2.2 Temperatures Relations at Constant Velocity

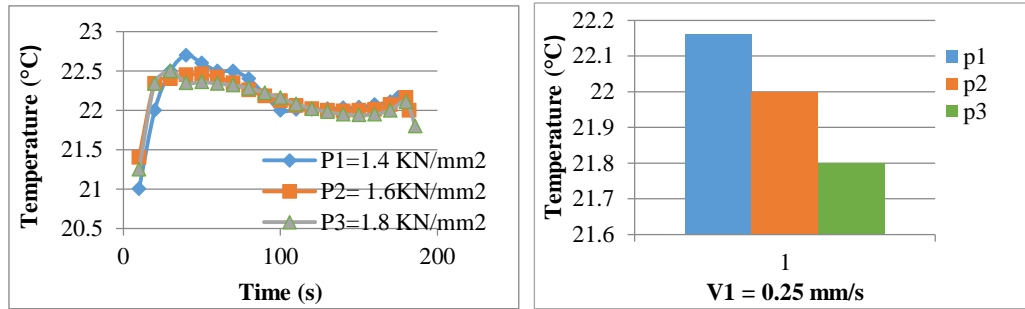


Figure 6.16: Temperatures for P1 = 1.4 kN/mm², P2 = 1.6 kN/mm² and P3 = 1.8 kN/mm² with constant velocity V1 = 0.25mm/s

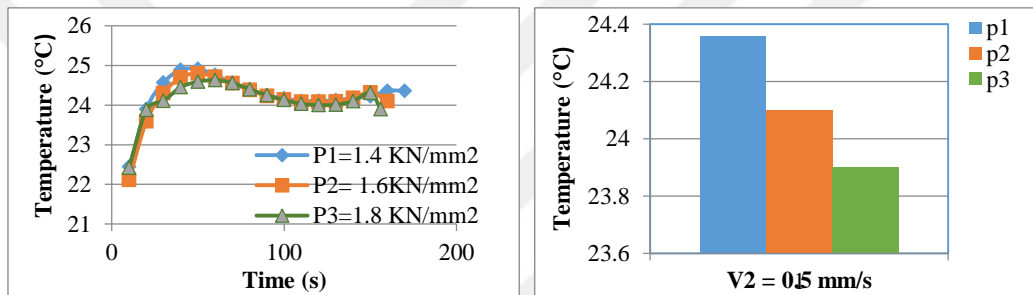


Figure 6.17: Temperatures for P1 = 1.4 kN/mm², P2 = 1.6 kN/mm² and P3 = 1.8 kN/mm² with constant velocity V2 = 0.5mm/s

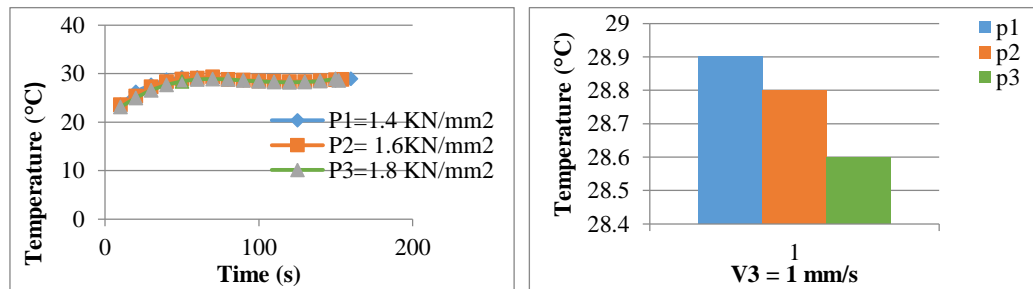


Figure 6.18: Temperatures for P1 = 1.4 kN/mm², P2 = 1.6 kN/mm² and P3 = 1.8 kN/mm² with constant velocity V3 = 1 mm/s

The figures show the decrease of temperature with pressures increasing at constant velocity as high pressures reduce the effect of friction forces and a reduction of heat. The temperatures show large increases at the beginning of deformation followed by a reduction with temperatures nearly constant because of the reduction of the forces required after the yield stress due to the increase of the slip systems during plastic deformation.

6.1.3 Process Time

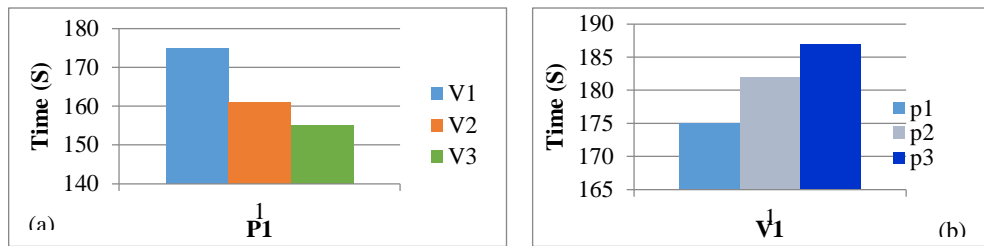


Figure 6.19: (a) Time for $V1 = 0.25$ mm/s, $V2 = 0.5$ mm/s and $V3 = 1$ mm/s with constant pressure $P1 = 1.4$ kN/mm²; (b) Time for $P1 = 1.4$ kN/mm², $P2 = 1.6$ kN/mm² and $P3 = 1.8$ kN/mm² with constant velocity $V1 = 0.25$ mm/s

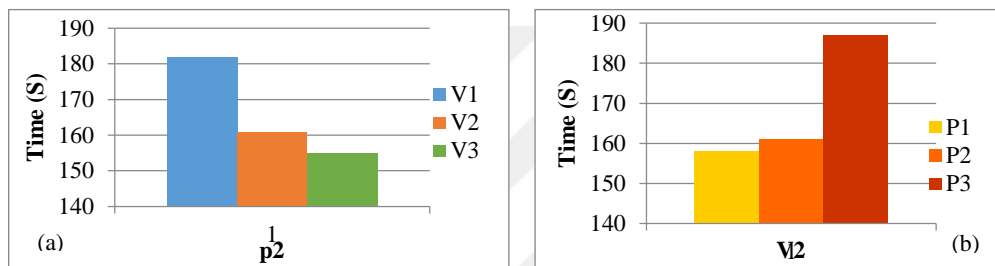


Figure 6.20: (a) Time for $V1 = 0.25$ mm/s, $V2 = 0.5$ mm/s and $V3 = 1$ mm/s with constant pressure $P2 = 1.6$ kN/mm²; (b) Time for $P1 = 1.4$ kN/mm², $P2 = 1.6$ kN/mm² and $P3 = 1.8$ kN/mm² with constant velocity $V2 = 0.5$ mm/s

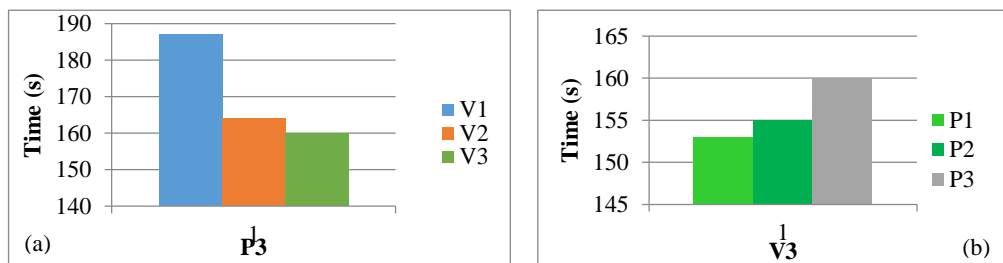


Figure 6.21: (a) Time for $V1 = 0.25$ mm/s, $V2 = 0.5$ mm/s and $V3 = 1$ mm/s with constant pressure $P3 = 1.8$ kN/mm²; (b) Time for $P1 = 1.4$ kN/mm², $P2 = 1.6$ kN/mm² and $P3 = 1.8$ kN/mm² with constant velocity $V3 = 1$ mm/s

The (a) figures above show that the time decreased with the velocity increasing at constant pressures such that the deformation finished faster but the stresses increased due to friction and increasing heat. The (b) figures show increases in process times with pressure increases with a constant velocity because high pressure means a low cross-sectional area of the punch which needs more time to deform the work piece.

6.1.4 Load

6.1.4.1 At Constant Pressure

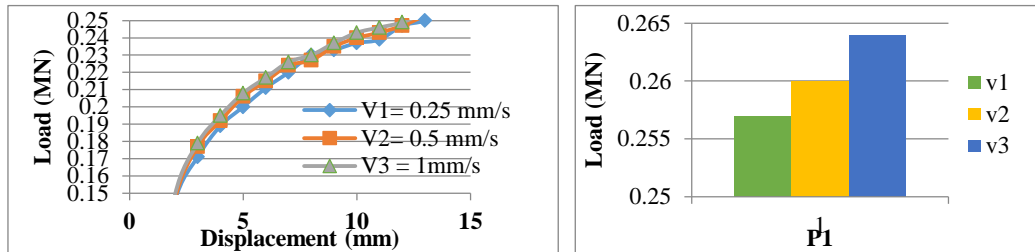


Figure 6.22: Loads for V1 = 0.25 mm/s, V2 = 0.5 mm/s and V3 = 1 mm/s with constant pressure P1 = 1.4 kN/mm²

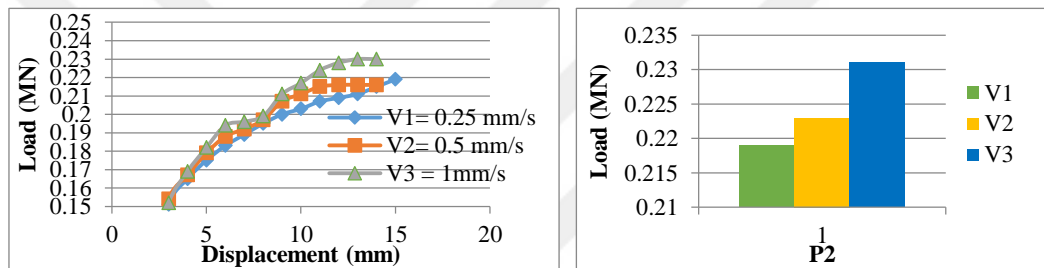


Figure 6.23: Loads for V1 = 0.25 mm/s, V2 = 0.5 mm/s and V3 = 1 mm/s with constant pressure P2 = 1.6 kN/mm²

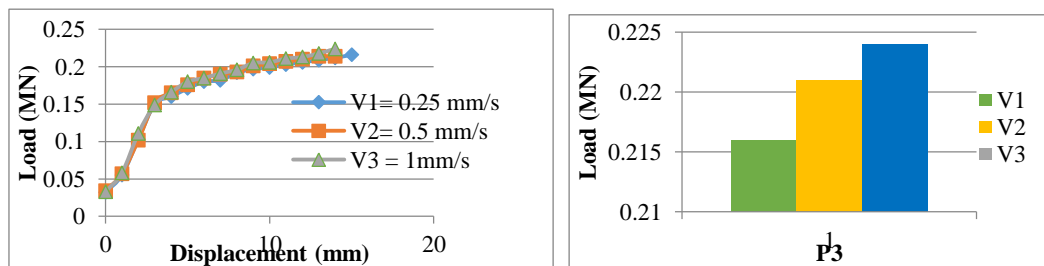


Figure 6.24: Loads for V1 = 0.25 mm/s, V2 = 0.5 mm/s and V3 = 1 mm/s with constant pressure P3 = 1.8 kN/mm²

Increasing velocity at a constant pressure leads to an increased load being required in order to achieve the deformation and end of the process. The load has a sharp increase at the beginning of the process to change the volume and shape of the billet and to exceed elastic deformation to the plastic region followed by a smooth increase occurring and the load tending to decrease by increasing the slip systems at that region. The highest load value was 0.264 MN at V3 = 1 mm/s.

6.1.4.2 At Constant Velocity

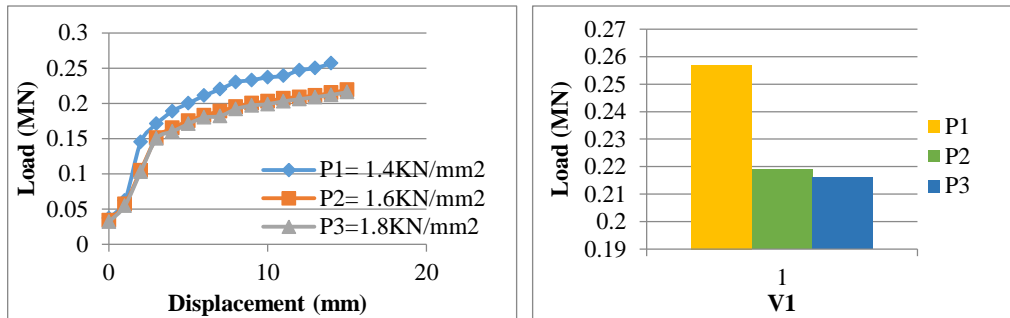


Figure 6.25: Loads for P1 = 1.4 kN/mm², P2 = 1.6 kN/mm² and P3 = 1.8 kN/mm² with constant velocity V1 = 0.25 mm/s

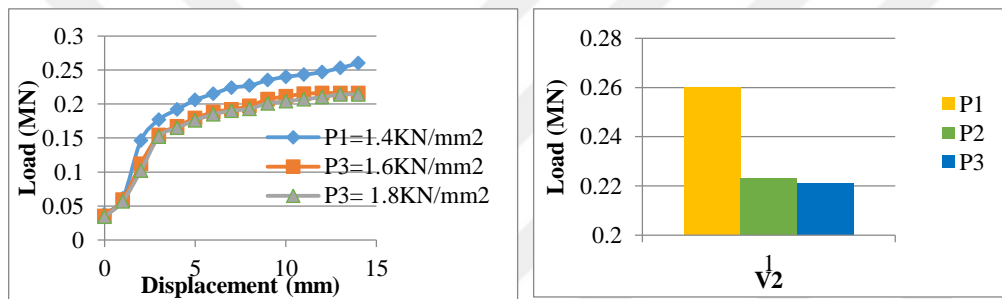


Figure 6.26: Loads for P1 = 1.4 kN/mm², P2 = 1.6 kN/mm² and P3 = 1.8 kN/mm² with constant velocity V2 = 0.5 mm/s

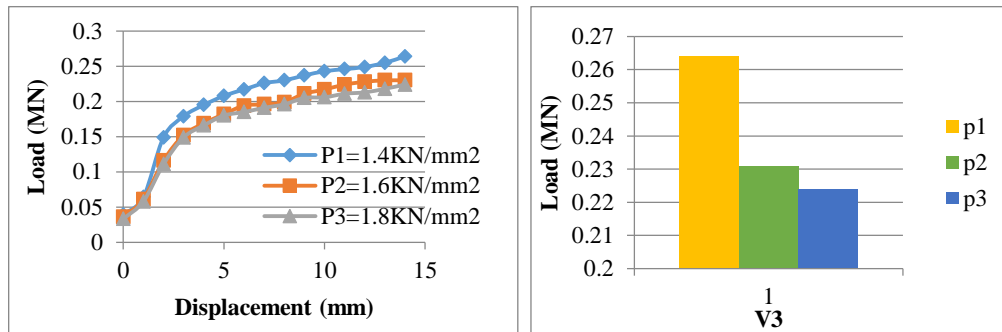


Figure 6.27: Loads for P1 = 1.4 kN/mm², P2 = 1.6 kN/mm² and P3 = 1.8 kN/mm² with constant velocity V3 = 1 mm/s

For a constant velocity, increasing the pressure gives a reduction on the load because of the reduction of the friction force effects that low pressure needs for high forces and more time to exceed the friction force and deform the billet plastically. On the other hand, high pressure involves low cross-sectional areas of the punch which needs less time to deform and reduce the load.

6.2 Experimental Results

6.2.1 Macrostructure Test (Optical Micro Scope)

1. Case 1 Constant Pressure $P1 = 1.4 \text{ kN/mm}^2$

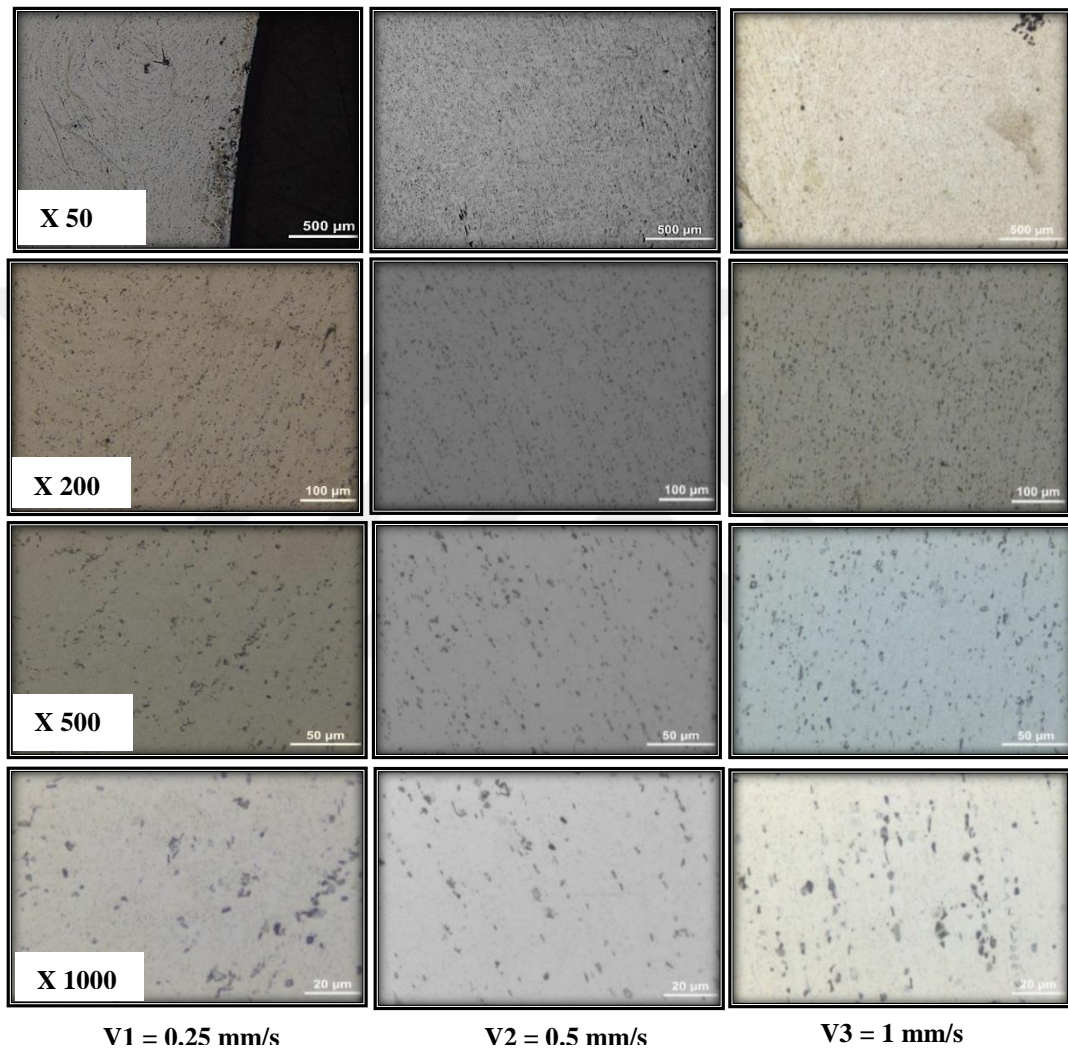


Figure 6.28: Backward view points of the sample for different velocities

The macrostructure test is achieved for the products of different velocity and pressure conditions. Figure 6.28 shows four magnification types for the backward region of the product at $P1 = 1.4 \text{ kN/mm}^2$. It is shown that increasing the velocity decreases the swirls and circulation and increases the homogeneity of the flow.

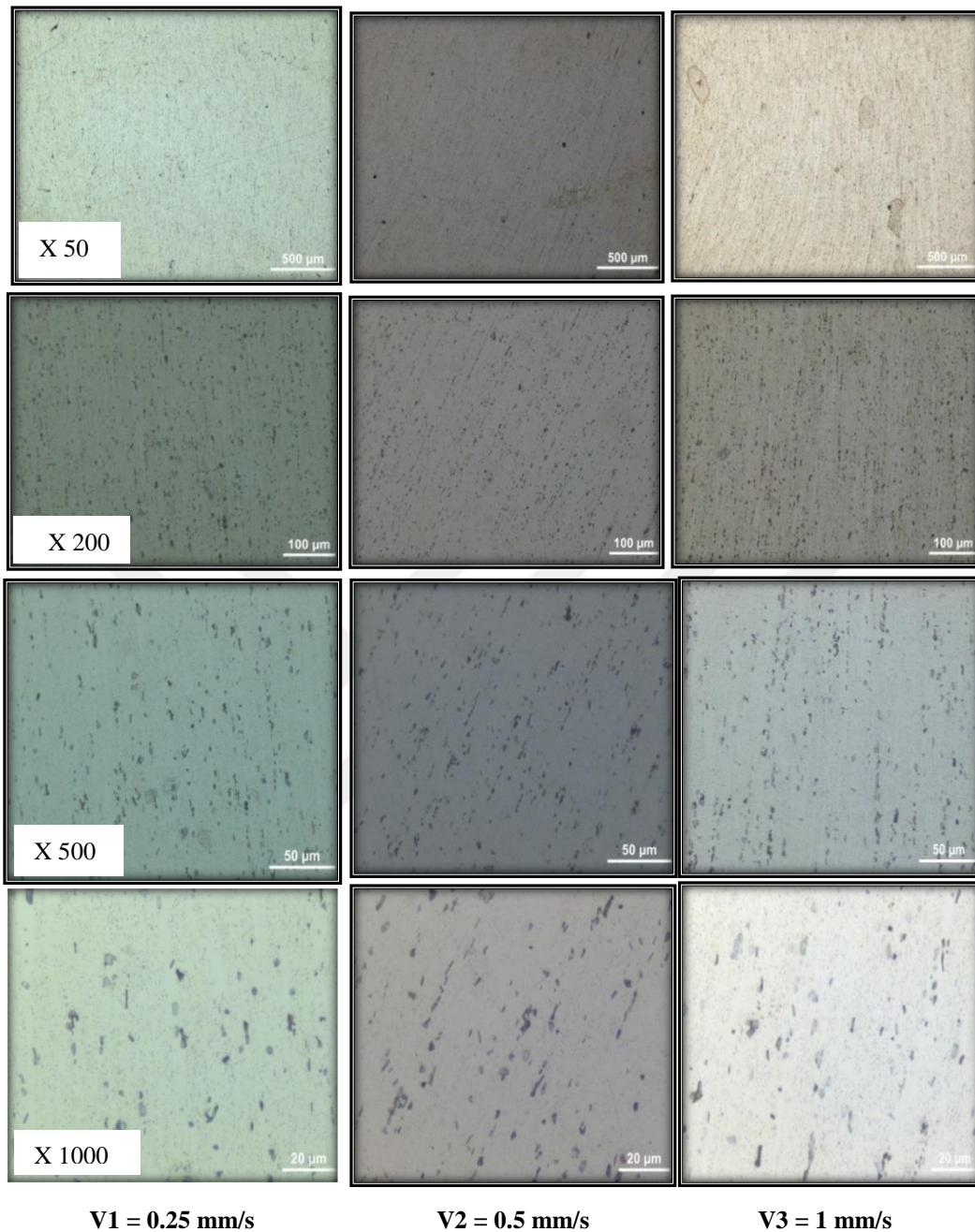


Figure 6.29: Forward viewpoints of the sample for different velocities

At the forward regions, the results of the macrostructure show fewer swirls and more uniform lines than the backward regions of Figure 6.28 because of the opposite direction effect of the backward punch and metal movement that increases the swirls.

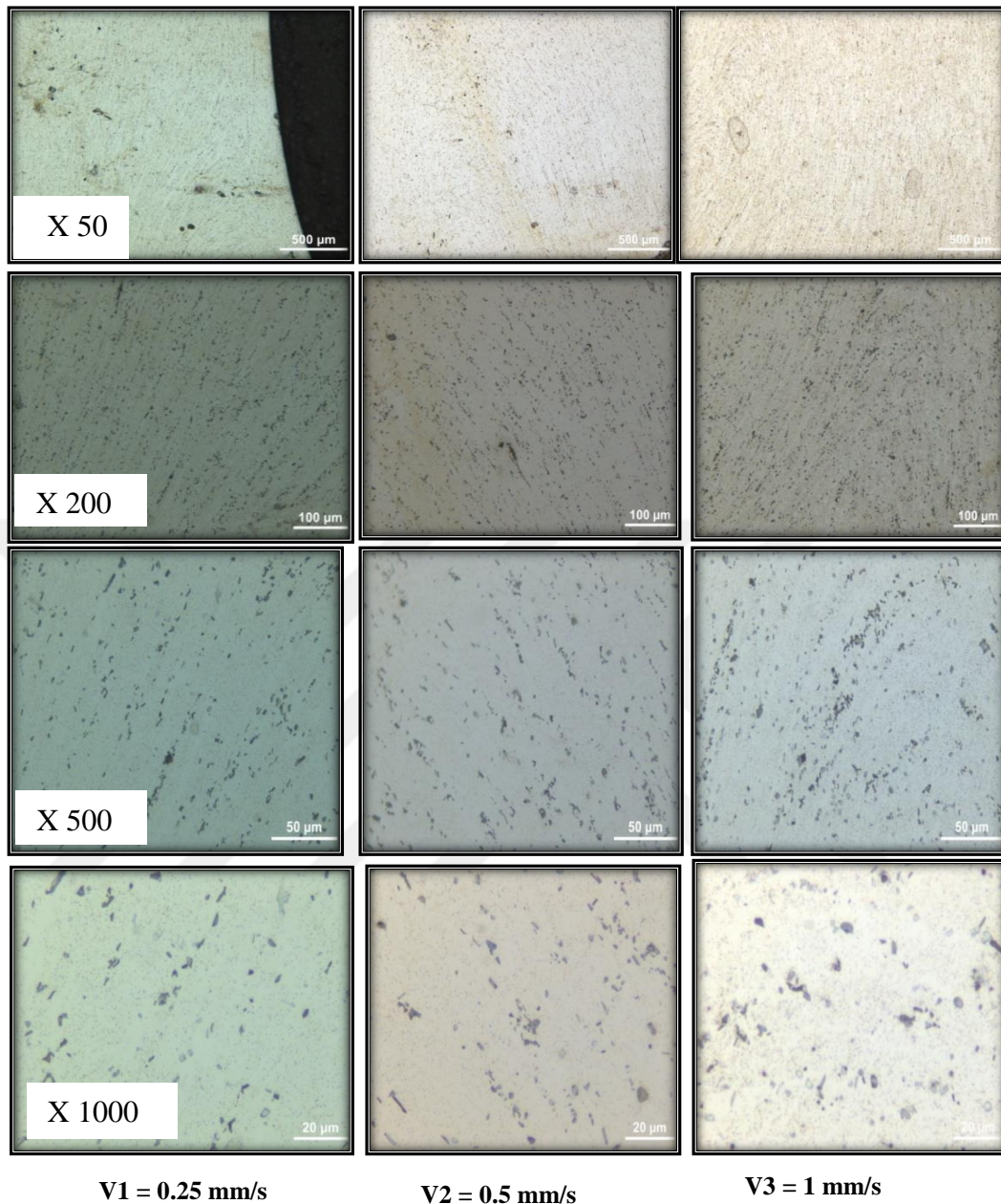


Figure 6.30: Corner towards the backward viewpoints of the sample for different velocities

The figure above includes the macrostructure at the corner of the metal movement from the middle towards the backward region. This involves high circulation and swirls because of the sudden changes in the direction of the flow and the narrow region with the influence of the opposite movement of flow during backward extrusion.

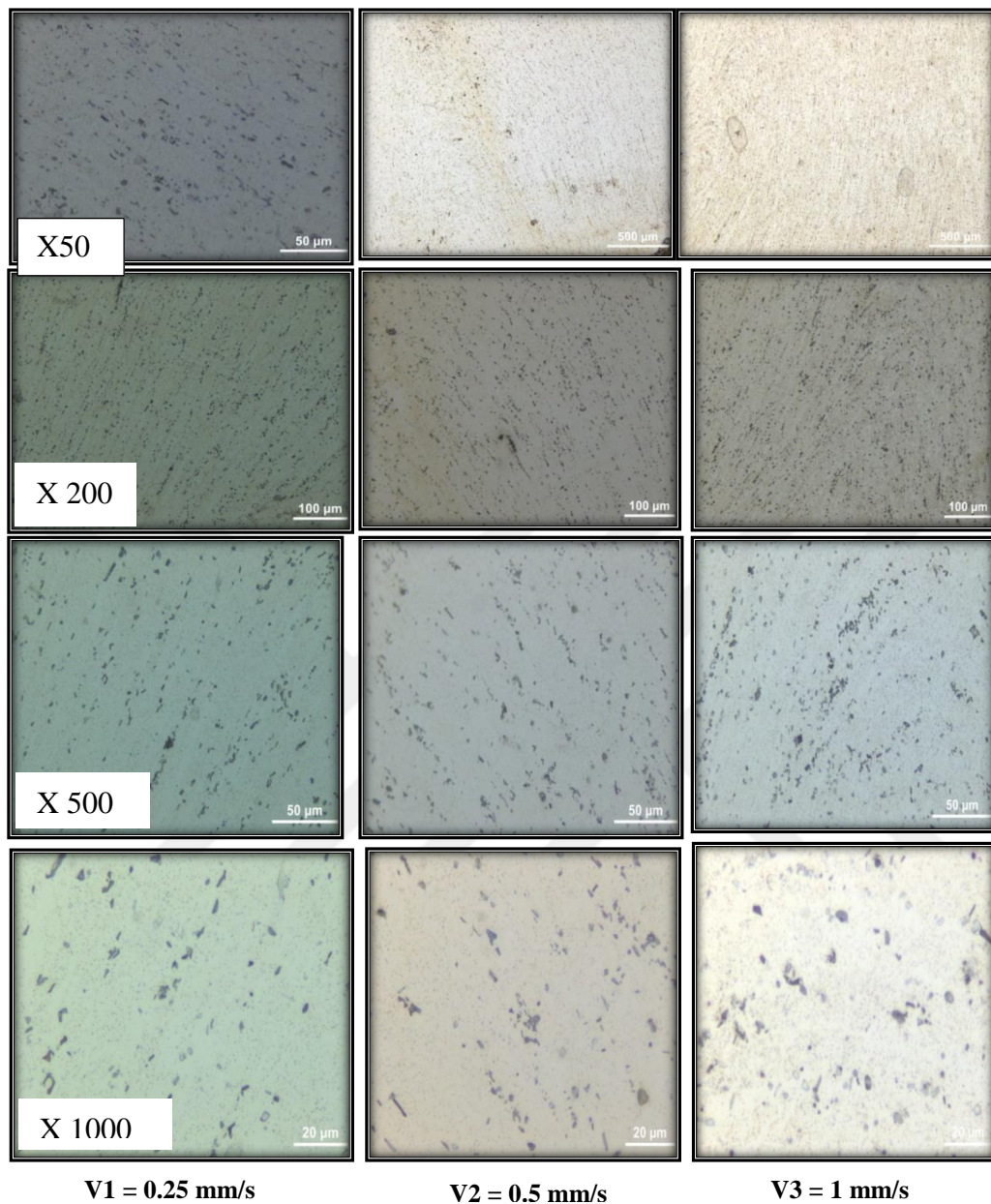


Figure 6.31: Corner towards the forward viewpoints of the sample for different velocities

Figure 6.31 shows the macrostructure at the region of the corner towards the forward extrusion with high circulation and random lines, especially at $V1 = 0.25 \text{ mm/s}$. This increases the friction force effects and reduces uniform homogeneity. At a maximum velocity of $V3 = 1 \text{ mm/s}$, the flow becomes steadier with uniform lines.

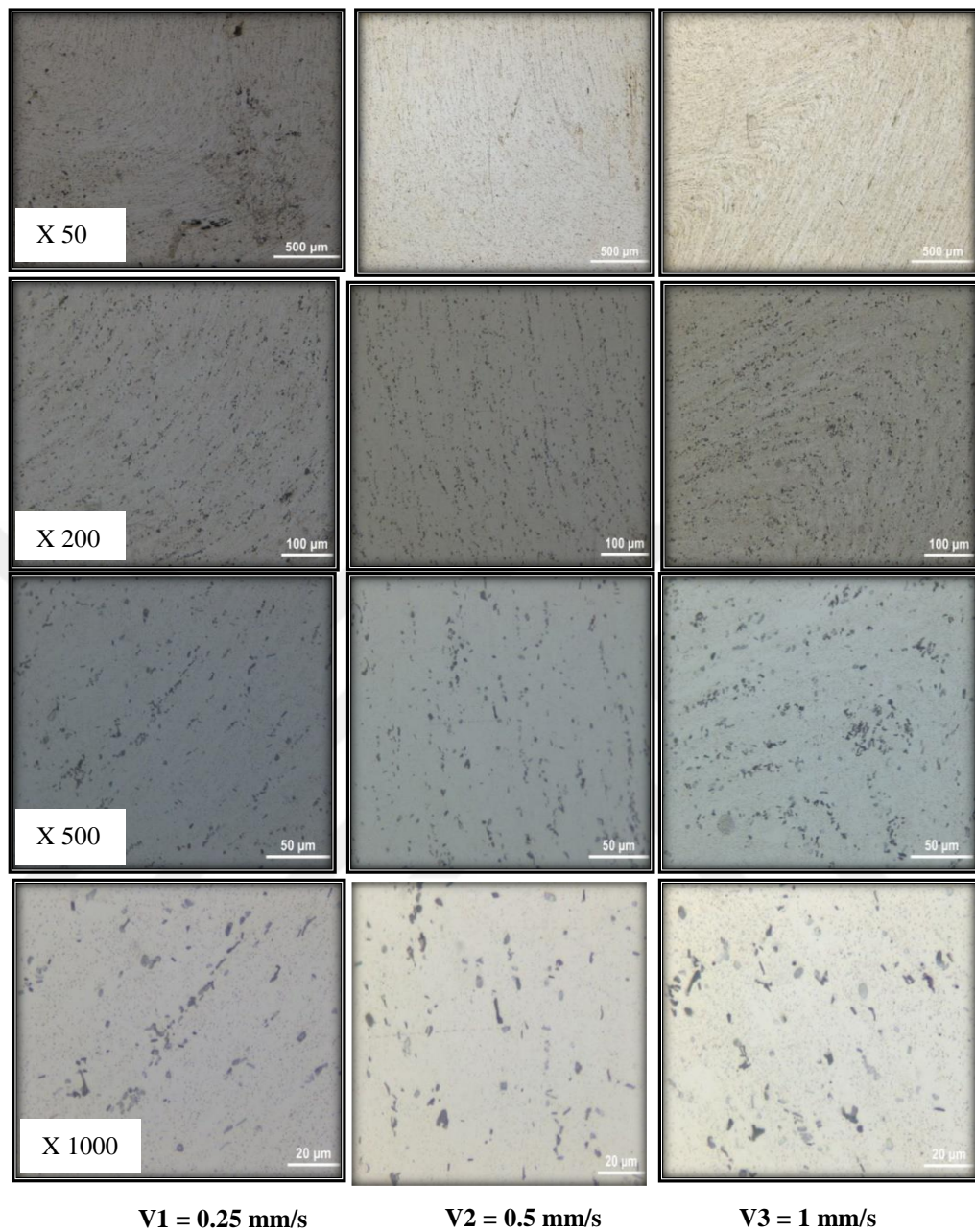


Figure 6.32: Surface center between backward and forward extrusion for different velocities

A region between the backward and forward extrusion is a narrow region and includes four corners and directions of metal movement that have sudden shape changes. Figure 6.32 shows random lines and swirls at different punch velocities and especially at the low velocity of $V1 = 0.25 \text{ mm/s}$.

2. Case 2 Constant Pressure $P_2 = 1.6 \text{ kN/mm}^2$

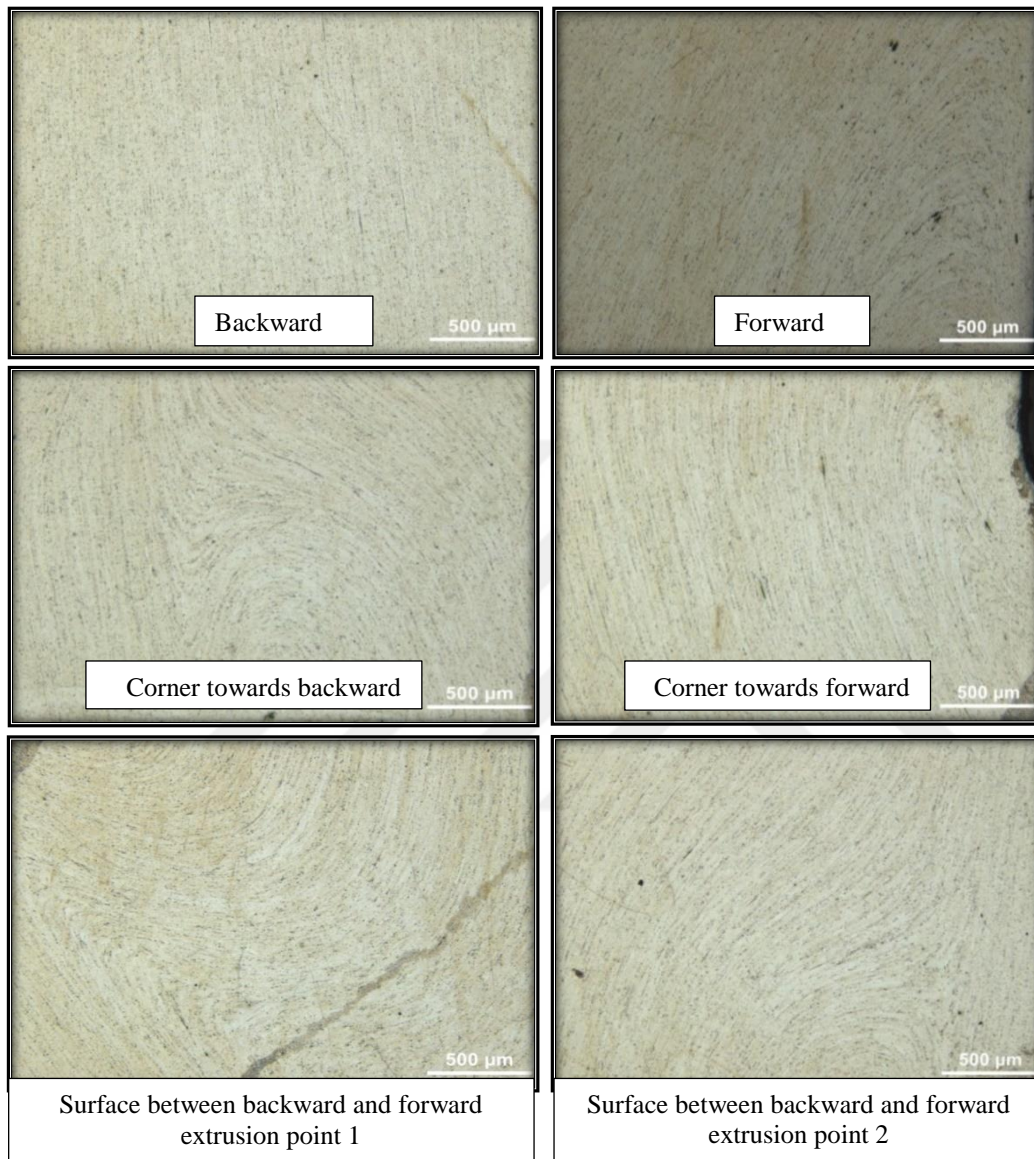


Figure 6.33: Optical scope macrostructure for Case 2 with X50 on all sample regions at $V_1 = 0.25 \text{ mm/s}$

For Case 2 at constant pressure $P_2 = 1.6 \text{ kN/mm}^2$, the figure shows the macrostructure at the forward, backward and corner with the middle regions showing less circulation and more uniform lines and metal movement than that of Case 1 for $P_1 = 1.4 \text{ kN/mm}^2$ because of a decrease in the friction forces and increasing formability of the metal.

3. Case 3 Constant Pressure $P_3 = 1.8 \text{ kN/mm}^2$

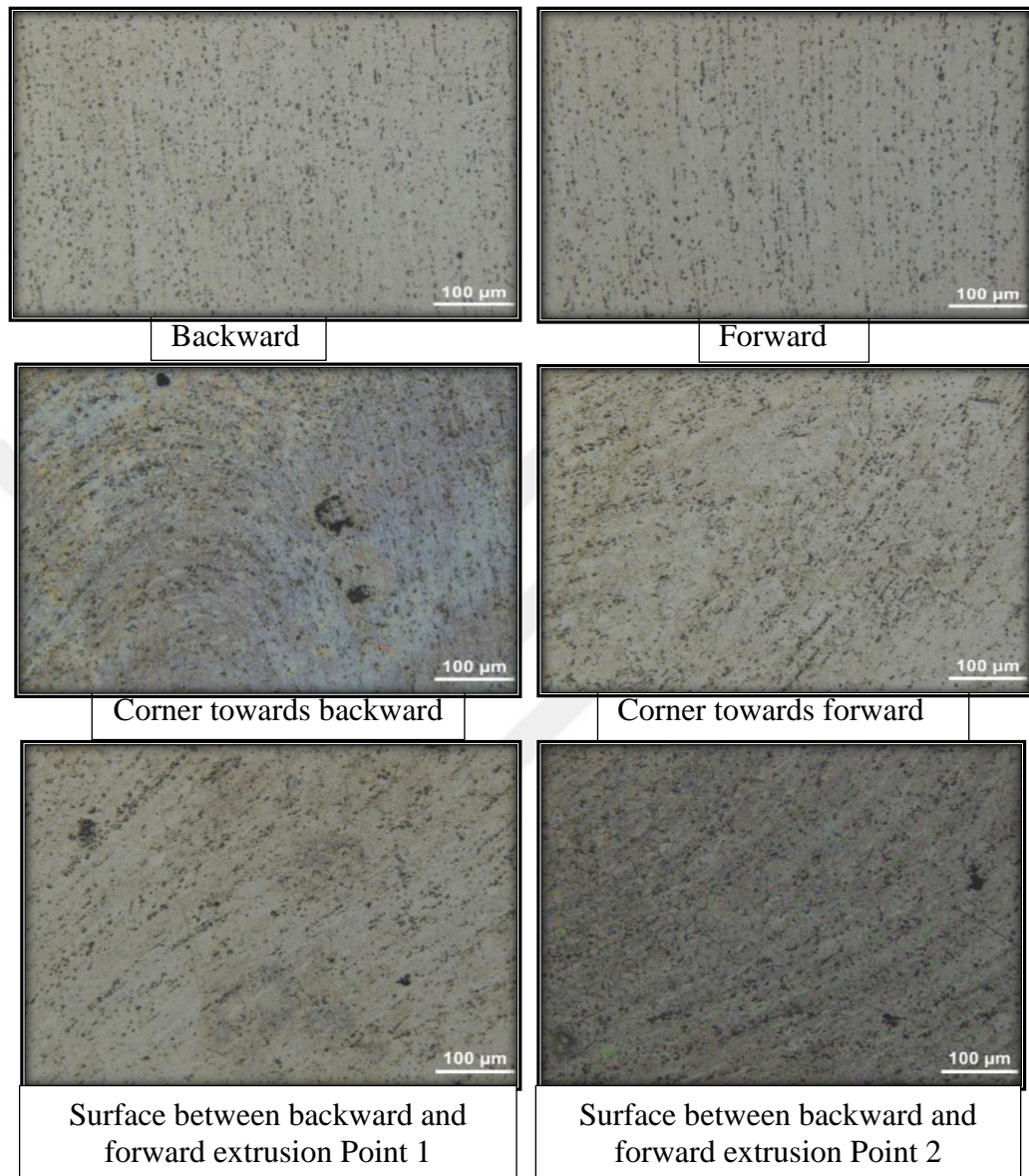


Figure 6.34: Optical scope microstructure for Case 3 with X200 on all sample regions at $V_1 = 0.25 \text{ mm/s}$

The highest pressure $P_3 = 1.8 \text{ kN/mm}^2$ gave the most uniform and homogeneous microstructure lines and deformations through different regions of the product. This shows the best results among other cases of lower pressure. The high pressure ensures a reduction in friction and increases the ability of the metal to slip and deform easily.

6.2.2 Microstructure (Stereo Macro Scope)

Case 1: $P1 = 1.4 \text{ kN/mm}^2$

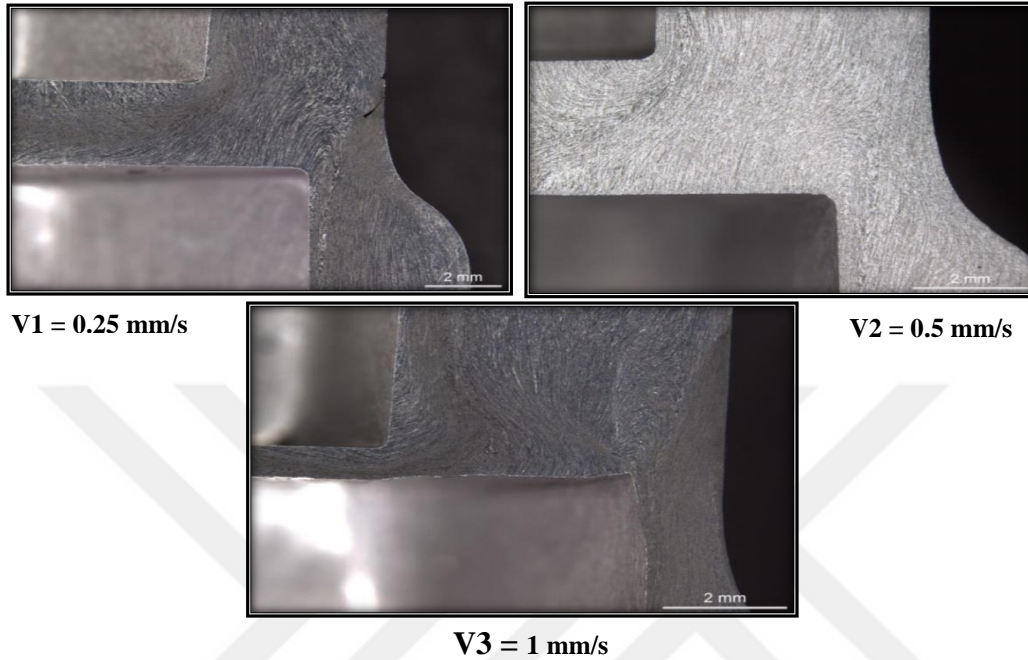


Figure 6.35: Microstructure for backward and forward views at different velocities

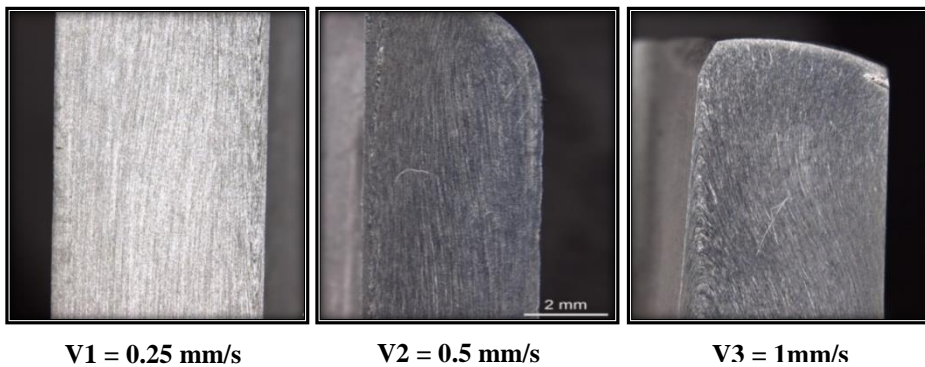


Figure 6.36: Microstructure for backward view points for different velocities

The microstructure test showed a more accurate view of the deformation lines at different velocities for $P1 = 1.4 \text{ kN/mm}^2$. Figure 6.36 shows the lines at the corner between backward and forward extrusions, which is the most random region on the product because of sudden changes in direction and less thick regions that have the effect of opposing punch and metal movements.

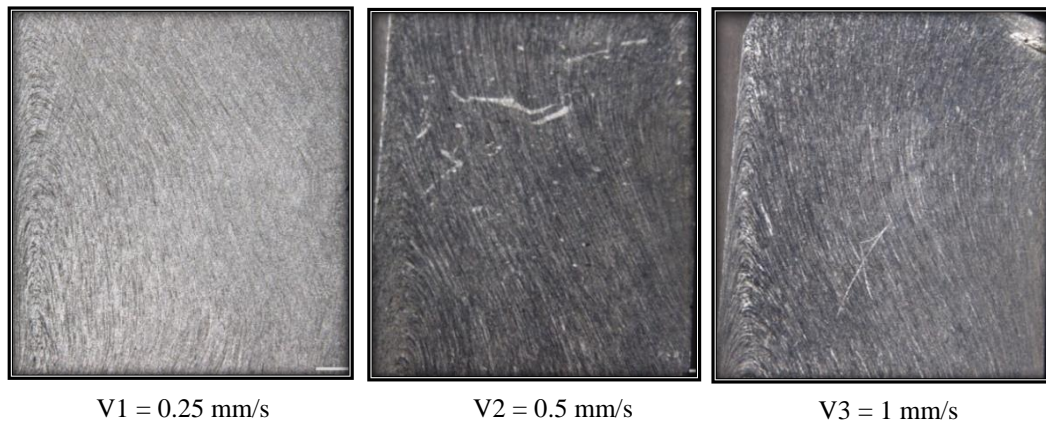


Figure 6.37: Forward view points for different velocities

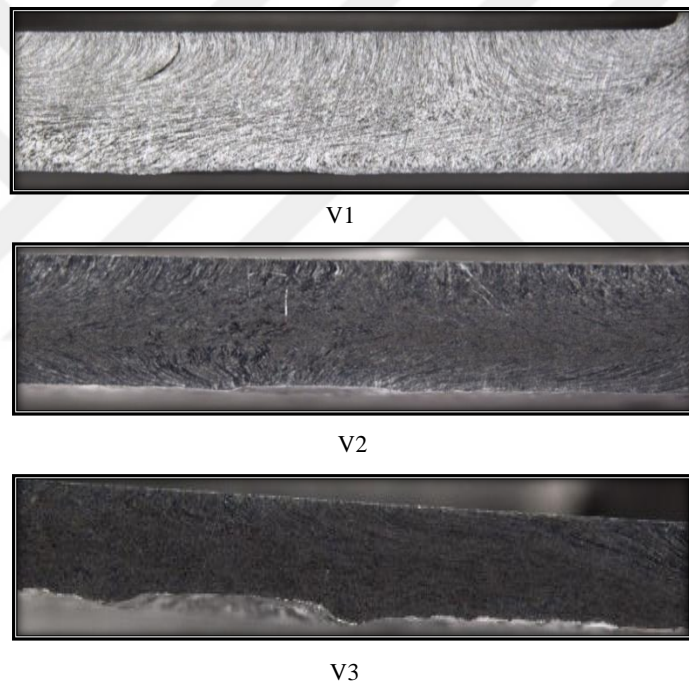


Figure 6.38: Horizontal surfaces between the backward and forward view points for different velocities

Figure 6.37 shows the microstructure in the forward region at different velocities. This shows the best lines and they are homogeneous at the higher velocity of $V1 = 1 \text{ mm/s}$ because of the uniform movement that can avoid turbulence and friction during pressing and deformation. In Figure 6.38, the horizontal middle region shows the highest circulations and non-uniform lines among other product regions.

6.2.3 Residual Stress Test

6.2.3.1 Backward Points Results

The residual stress test was performed using an X-ray machine for two points: (1) the backward region; and (2) the forward region.

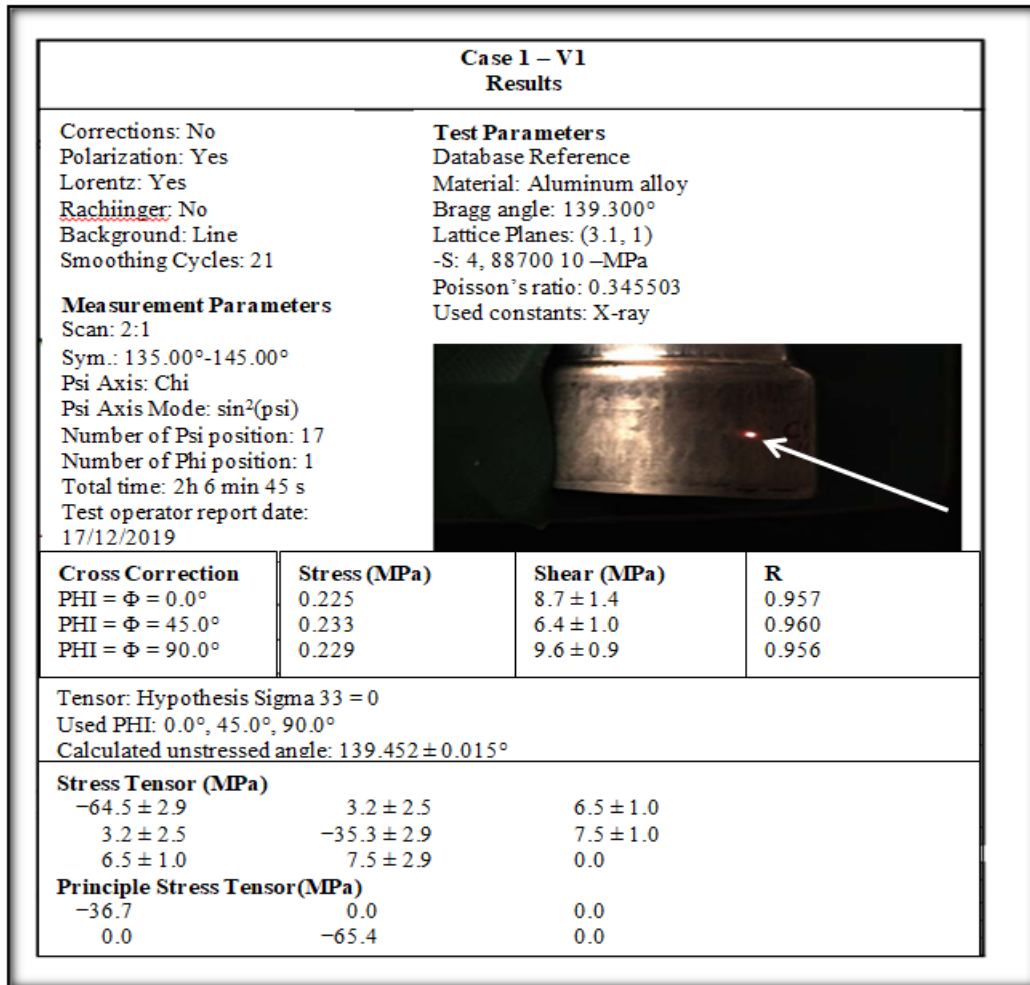


Figure 6.39: Residual stress report for the backward region

An X-ray test was performed to find the residual stresses in the backward region for the three velocities values and three pressures. The test included changing the product angle and position with the X-ray angle, called Bragg's angle, to check for the best result. Figure 6.39 shows the X-ray point in the backward region of the product.

6.2.3.2 Forward Points Results

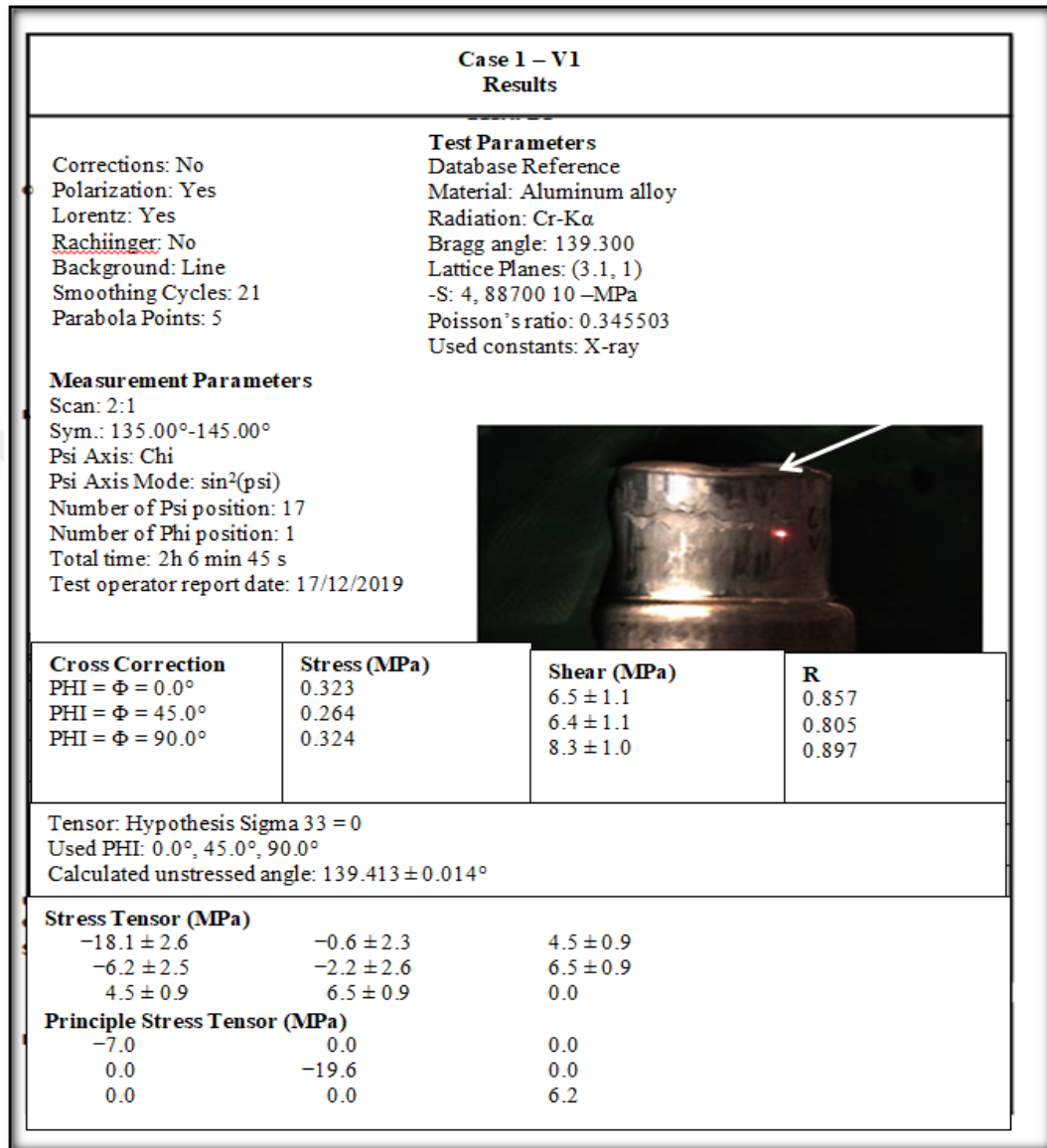


Figure 6.40: Residual stress report for the forward region

The same effect occurs in the forward region when an X-ray test analyzed the stresses by changing different Bragg's X-ray angles. The machine was able to calculate the shear stresses and principles with the residual stresses. The test took more than two hours for each point measurement with many scans by entering some material properties, such as Poisson's ratio and Young's modulus.

6.2.3.3 Stresses at Constant Pressure

Table 6.1: Results of stress for P1 and different velocities in three regions

Constant pressure P1 = 1.4 kN/mm ²			
Velocity (mm/s)	Stresses (MPa) (negative -)		
	Forward	Backward	Middle
V1	500	986	1224
V2	560	973	1278
V3	588	1100	1315

Table 6.2: Results of stress for P2 and different velocities in three regions

Constant pressure P2 = 1.6 kN/mm ²			
Velocity (mm/s)	Stresses (MPa) (negative -)		
	Forward	Backward	Middle
V1	479	860	1171
V2	490	920	1233
V3	491	1150	1235

Table 6.3: Results of stress for P3 and different velocities in three regions

Constant pressure P3 = 1.8 kN/mm ²			
Velocity (mm/s)	Stresses (MPa) (negative -)		
	Forward	Backward	Middle
V1	470	880	1129
V2	550	940	1228
V3	577	990	1240

The results of the stresses show high values especially in the middle regions because of the effect of the opposing two punch directions, which increases friction and turbulent metal flow. The lowest stress value was recorded in the forward region where the metal moved in the same direction as the punch. The stress values with a negative sign are compression stresses. At constant pressure, the stress increases as the velocity increases.

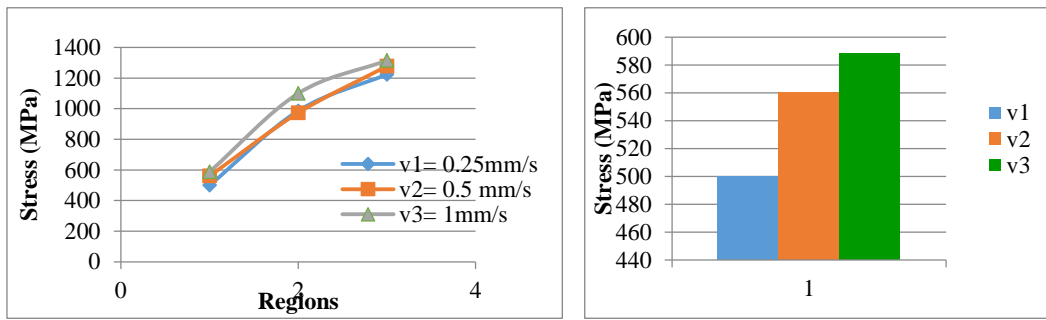


Figure 6.41: Stresses at many regions with constant pressure $P1 = 1.4 \text{ kN/mm}^2$ and different velocities

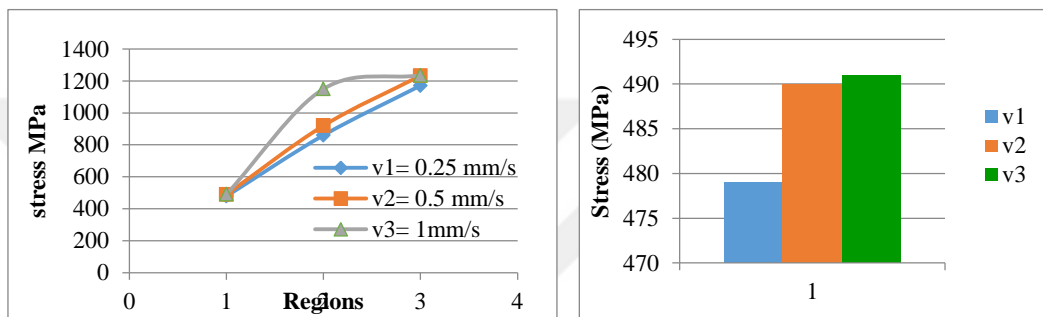


Figure 6.42: Stresses at many regions with constant pressure $P2 = 1.6 \text{ kN/mm}^2$ and different velocities

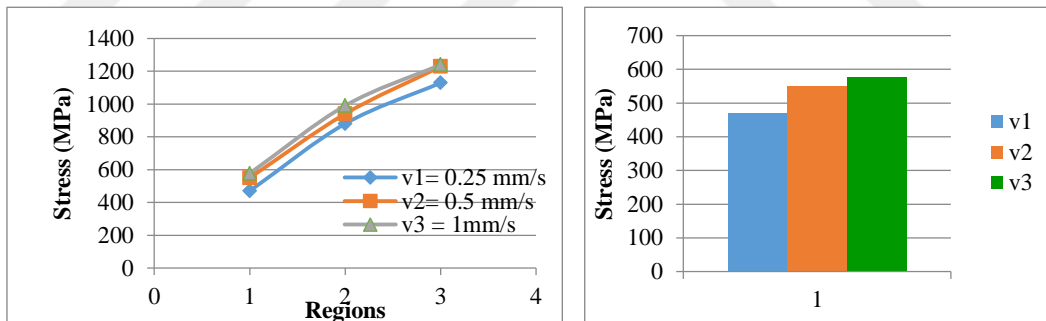


Figure 6.43: Stresses at many regions with constant pressure $P3 = 1.8 \text{ kN/mm}^2$ and different velocities

The stresses were measured with an X-ray machine in the forward, middle and backward regions. Increasing the velocity shows an increase in the residual stresses in each region when the pressure is constant. It can be seen from the graphs and results that the middle region recorded highest stresses between the backward and forward extrusions and the backward region and the minimum values at the forward region.

6.2.3.4 Stresses at Constant Velocity

Table 6.4: Results of stresses for V1 and different pressures in three regions

Constant velocity V1 = 0.25 mm/s			
	Stresses (MPa) (negative -)		
	Forward	Backward	Middle
P1	500	986	1224
P2	479	860	1171
P3	470	880	1129

Table 6.5: Results of stresses for V2 and different pressures in three regions

Constant velocity V2 = 0.5 mm/s			
	Stresses (MPa) (negative -)		
	Forward	Backward	Middle
P1	560	973	1278
P2	490	920	1233
P3	525	900	1150

Table 6.6: Results of stresses for V3 and different pressures in three regions

Constant velocity V3 = 1 mm/s			
	Stresses (MPa) (negative -)		
	Forward	Backward	Middle
P1	588	1100	1315
P2	491	1150	1235
P3	500	990	1240

At constant velocity, increasing the pressure decreases the stresses because high pressures decrease the influence of the friction force and heat generated; therefore; the stresses are reduced.

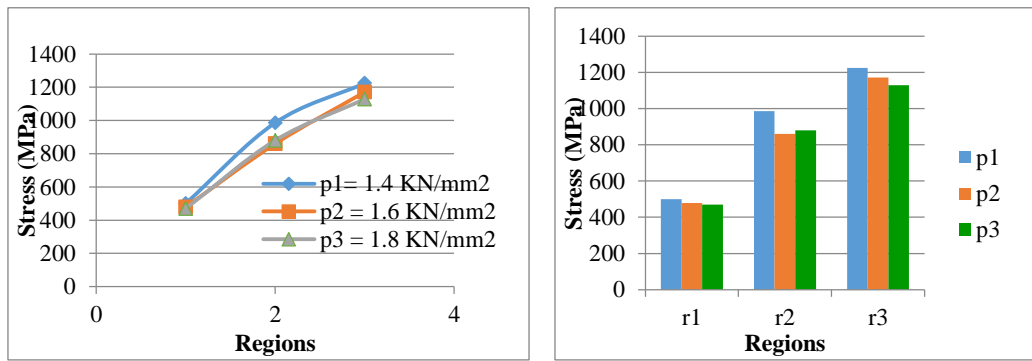


Figure 6.44: Stresses in many regions with constant velocity $V1 = 0.25$ mm/s and different pressures

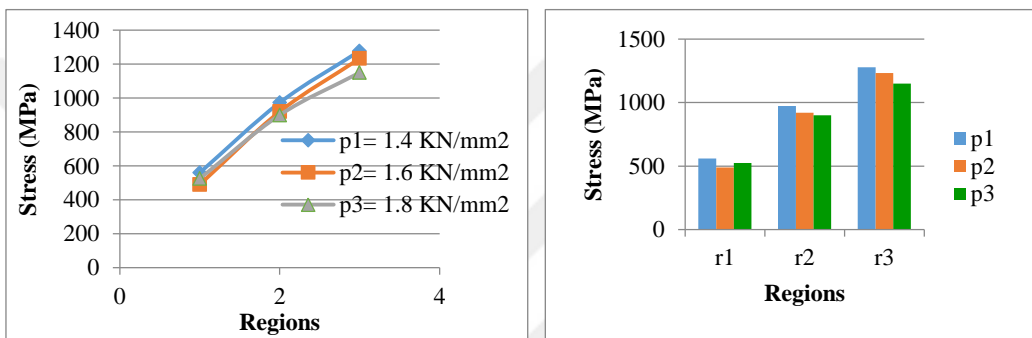


Figure 6.45: Stresses in many regions with constant velocity $V2 = 0.5$ mm/s and different pressures

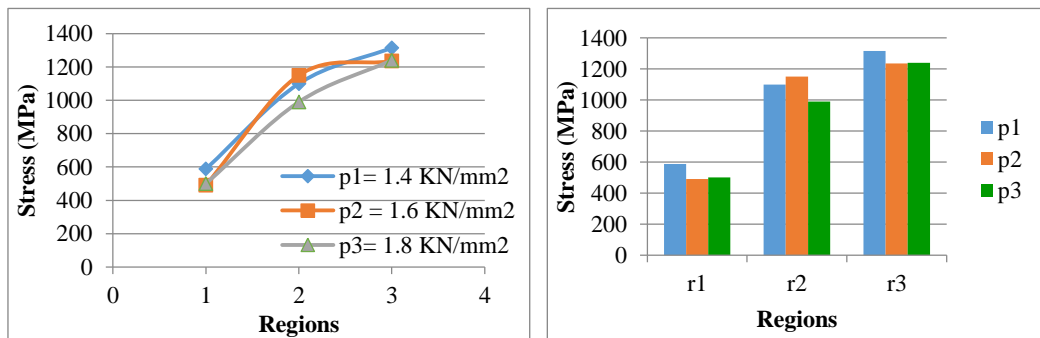


Figure 6.46: Stresses in many regions with constant velocity $V3 = 1$ mm/s and different pressures

The stress value decrease at a constant velocity with pressure increasing and the highest stress was found in the middle region, whereas the lower stress values occurred in the forward region because of the flow direction that was in the same direction of pressing.

6.2.4 Load and Displacement

6.2.4.1 At Constant Pressure

A. from $x = 0$ before punch contact to billet

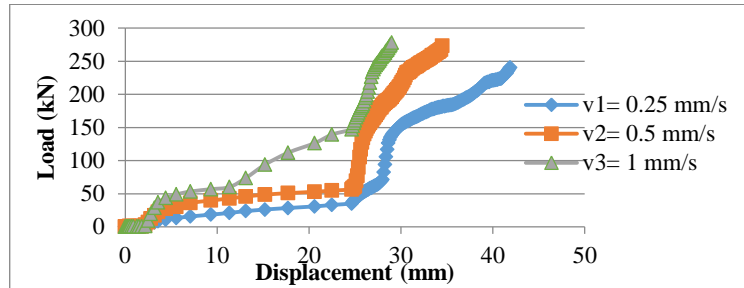


Figure 6.47: loads and displacements for different velocities at $P1 = 1.4 \text{ kN/mm}^2$

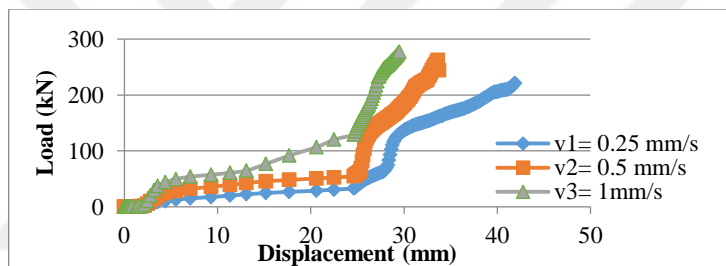


Figure 6.48: loads and displacements for different velocities at $P2 = 1.6 \text{ kN/mm}^2$

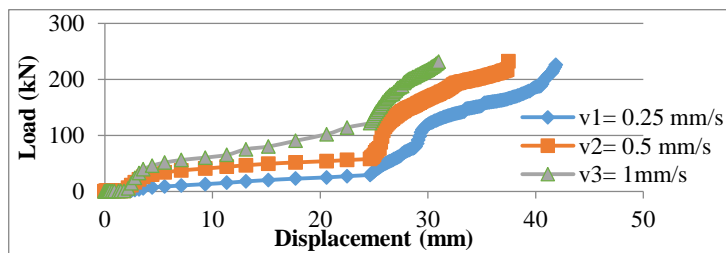


Figure 6.49: loads and displacements for different velocities at $P3 = 1.8 \text{ kN/mm}^2$

Increasing the velocity led to an increase in the load because of the friction force increasing. the minimum process time recorded at the lowest velocity $V1 = 0.25 \text{ mm/s}$ and the highest pressure $P3 = 1.8 \text{ kN/mm}^2$ because of the friction force effects and time decrease which increases uniform deformation.

B. From x at Contact Between Punch with Billet

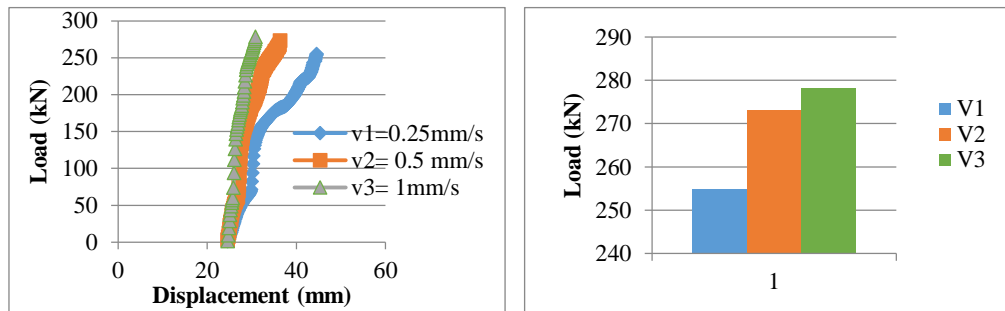


Figure 6.50: Relationship between loads and displacements for velocities at $P1 = 1.4 \text{ kN/mm}^2$

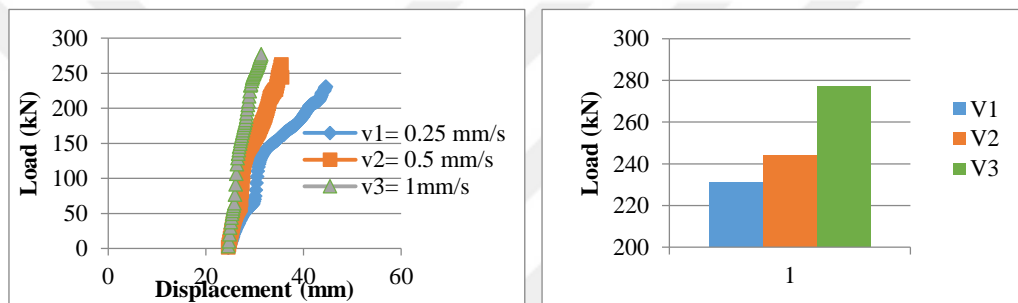


Figure 6.51: Relationship between loads and displacements for velocities at $P2 = 1.6 \text{ kN/mm}^2$

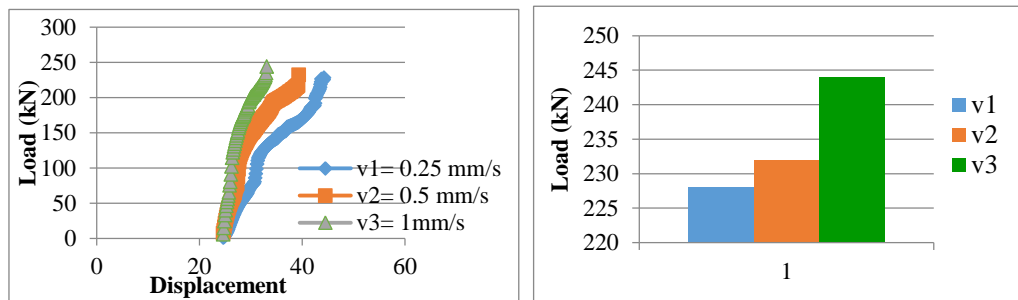


Figure 6.52: Relationship between loads and displacements for velocities at $P3 = 1.8 \text{ kN/mm}^2$

Figures 6.50, 6.51 and 6.52 show the same results as Figures 6.47, 6.48 and 6.49, but the differences are that the last results came at the moment that the two punches of the backward and forward extrusions contact the work piece and the load began to be calculated. The first figures showed the load from the beginning of punch pressing before coming into contact with the work piece

6.2.4.2 At Constant Velocity

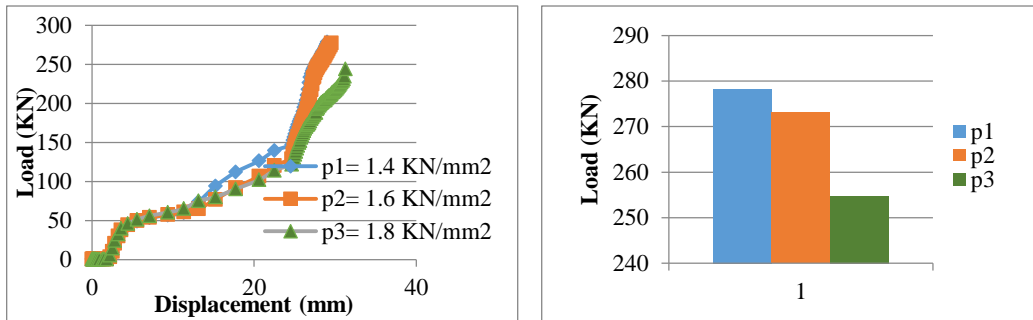


Figure 6.53: Loads for different pressures at $V_1 = 0.25\text{mm/s}$

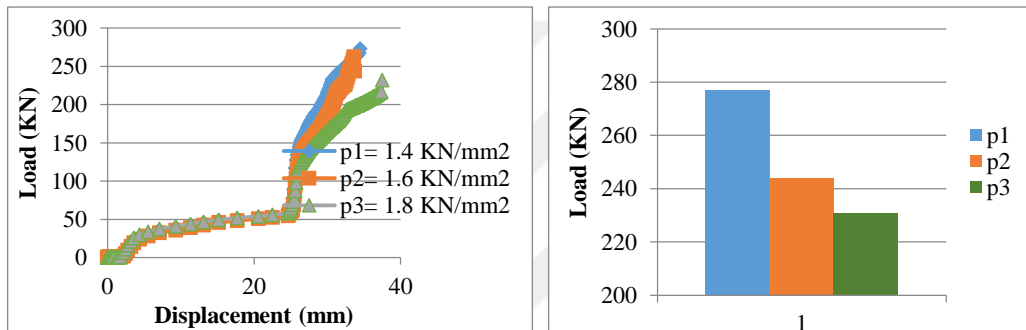


Figure 6.54: Loads for different pressures at $V_2 = 0.5\text{mm/s}$

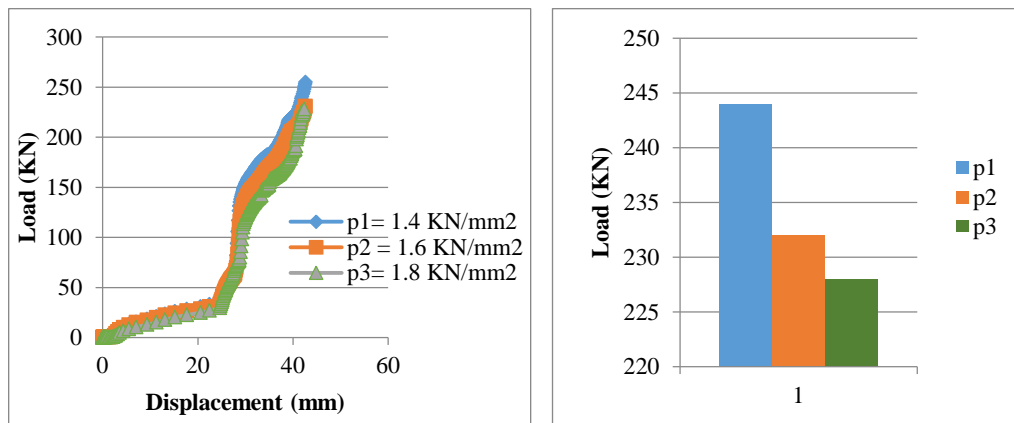


Figure 6.55: Loads for different pressures at $V_3 = 1\text{ mm/s}$

With constant velocity, increasing the pressure decreases the load required to achieve the deformation as the higher pressures can exceed the friction forces and reduce their effects.

6.2.5 Hardness

6.2.5.1 At Constant Pressure

Table 6.7: Hardness values at P1 for three regions with different velocities

Constant pressure P1 = 1.4 kN/mm ²			
	Hardness (HV)		
	Middle	Backward	Forward
V1	105	98	83
V2	95	87	82
V3	92	85	80

Table 6.8: Hardness values at P2 for three regions with different velocities

Constant pressure P2 = 1.6 kN/mm ²			
	Hardness (HV)		
	Middle	Backward	Forward
V1	109	96	84
V2	104	88	80
V3	95	87	77

Table 6.9: Hardness values at P3 for three regions with different velocities

Constant pressure P2 = 1.8 kN/mm ²			
	Hardness (HV)		
	Middle	Backward	Forward
V1	130	100	84
V2	110	94	70
V3	100	90	68

For the hardness values, the results show a decrease with a velocity increase at constant pressure because high velocity increases friction and temperatures, which increases the grain size followed by decreasing metal hardness. The highest hardness value is at middle region where the effect of strain hardening increases due to the opposite directions of the punches.

6.2.5.2 At Constant Velocity

Table 6.10: Hardness values at P3 for three regions with different velocities

Constant velocity V1 = 0.25 mm/s			
	Hardness (HV)		
	Middle	Backward	Forward
P1	105	96	80
P2	109	98	84
P3	130	100	86

Table 6.11: Hardness values at P3 for three regions with different velocities

Constant velocity V2 = 0.5 mm/s			
	Hardness (HV)		
	Middle	Backward	Forward
P1	95	87	80
P2	104	88	82
P3	110	94	89

Table 6.12: Hardness values at P3 for three regions with different velocities

Constant velocity V3 = 1 mm/s			
	Hardness (HV)		
	Middle	Backward	Forward
P1	92	85	80
P2	95	87	77
P3	100	90	80

The tables above show increases of hardness at pressures increasing because high pressure reduces the effect of the friction force. Generated heat decreases; therefore, grain growth reduces and hardness increases at fine grain sizes. The lowest hardness value is at the forward region with the minimum pressure value of $P1 = 1.4 \text{ kN/mm}^2$.

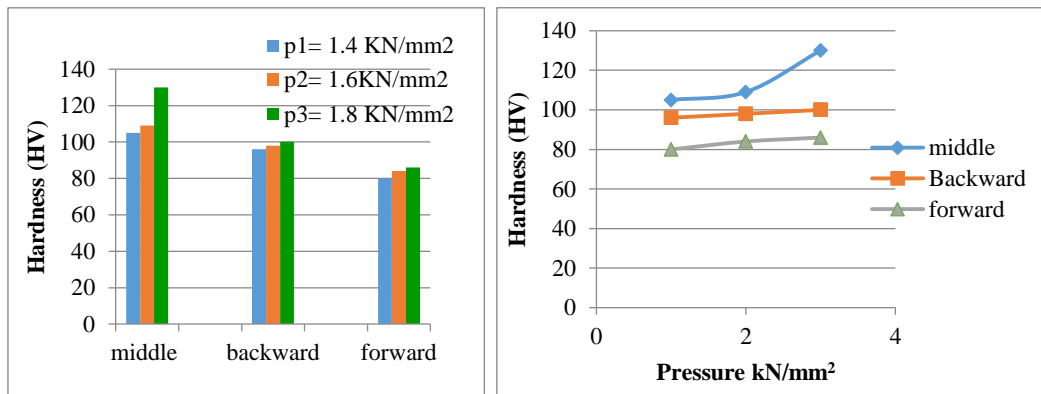


Figure 6.56: Hardness in three regions for constant velocity $V1 = 0.25 \text{ mm/s}$ with different pressures

The hardness test was performed on three regions, namely the forward, backward and middle regions. The maximum hardness value occurred at the middle region because this region was under the high strain hardening of two punches pressing in opposite directions. The minimum hardness value was at forward region because of fewer strain hardening effects due to the punch pressing and metal movement being in the same direction. An increase in the pressure at constant velocity increases the hardness.

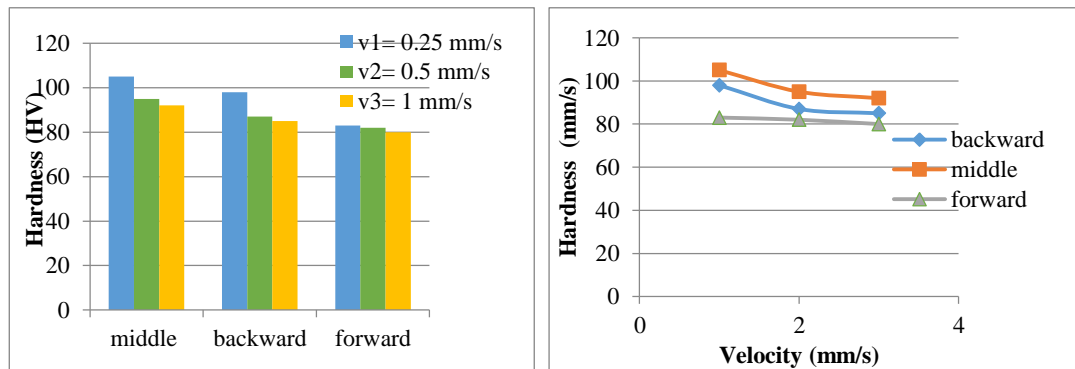


Figure 6.57: Hardness at three regions for constant pressure $P1 = 1.4 \text{ kN/mm}^2$ with different velocities

For constant pressure when the velocity increases, the hardness decreases because an increasing velocity leads to increased heating in the region and a grain size increase followed by a hardness decrease.

6.3 Comparisons Between Simulations and Experiments

6.3.1 Loads and Displacements

Case 1 ($P1 = 1.4 \text{ kN/mm}^2$)

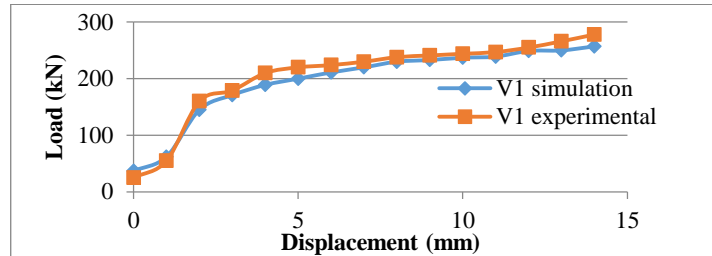


Figure 6.58: Comparison of loads between the simulation and experiment at $V1 = 0.25 \text{ mm/s}$

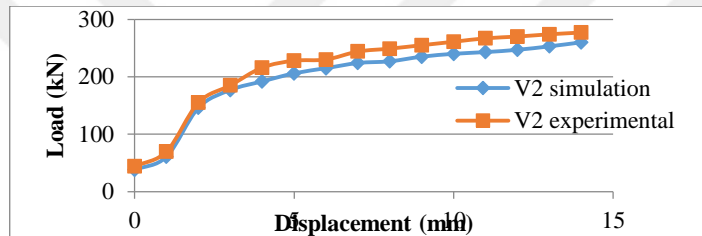


Figure 6.59: Comparison of loads between the simulation and the experiment at $V2 = 0.5 \text{ mm/s}$

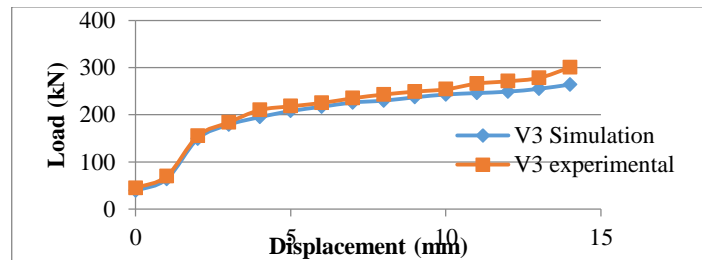


Figure 6.60: Comparison of loads between the simulation and experiment at $V3 = 1 \text{ mm/s}$

The curve of the loads show good agreement between the simulation and the experimental work. The values of the loads for the experimental work are higher than those of the simulation because of the ideal conditions in the simulation and the effects of friction during the experimental work. The best agreement between the simulation and the experimental values for the loads was at $V2 = 0.5 \text{ mm/s}$ to give uniform deformation.

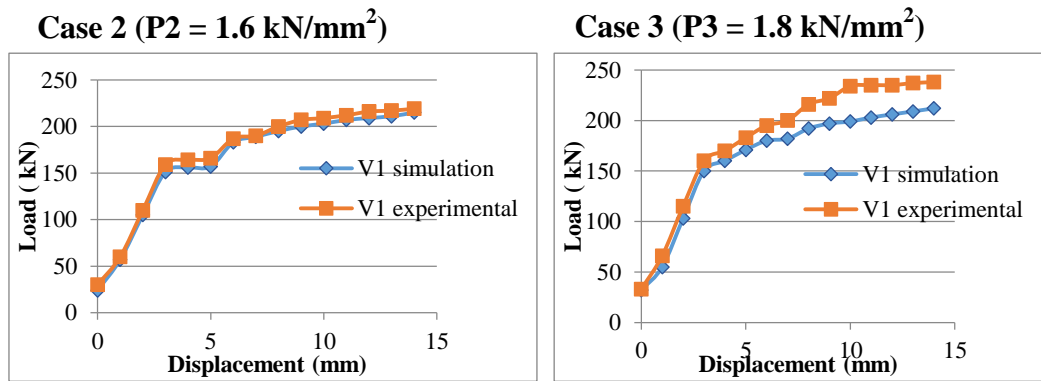


Figure 6.61: Comparison of loads for simulations and experiments at $V1 = 0.25 \text{ mm/s}$

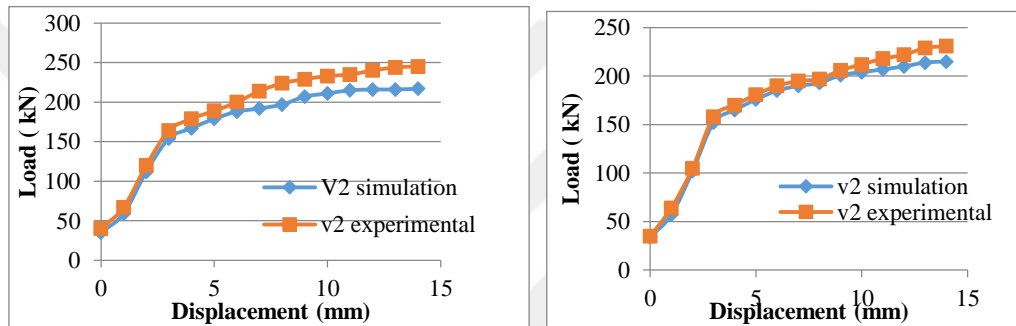


Figure 6.62: Comparison of loads for simulations and experiments at $V2 = 0.5 \text{ mm/s}$

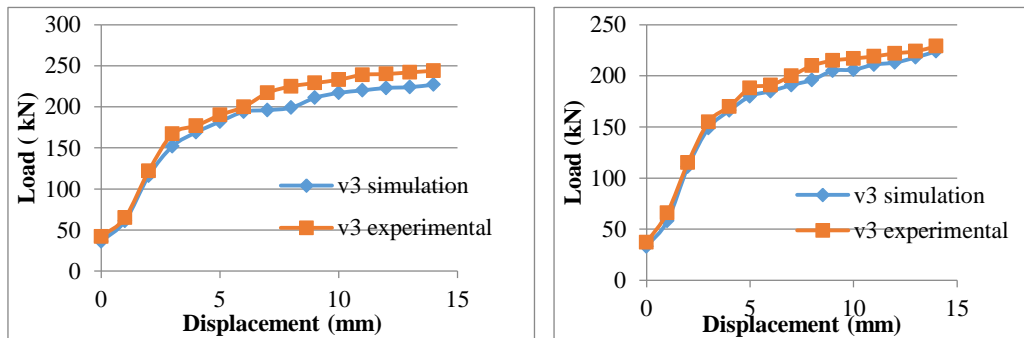


Figure 6.63: Comparison of loads for simulations and experiments at $V3 = 1 \text{ mm/s}$

For Case 2 $P2 = 1.6 \text{ kN/mm}^2$ and Case 3 $P3 = 1.8 \text{ kN/mm}^2$, the agreement between the simulation and the experimental work is better than that of Case 1 $P1 = 1.4 \text{ kN/mm}^2$ because at high pressures, the deformation is more uniform due to the friction force decreasing.

6.3.2 Stress

6.3.2.1 At Constant Pressure

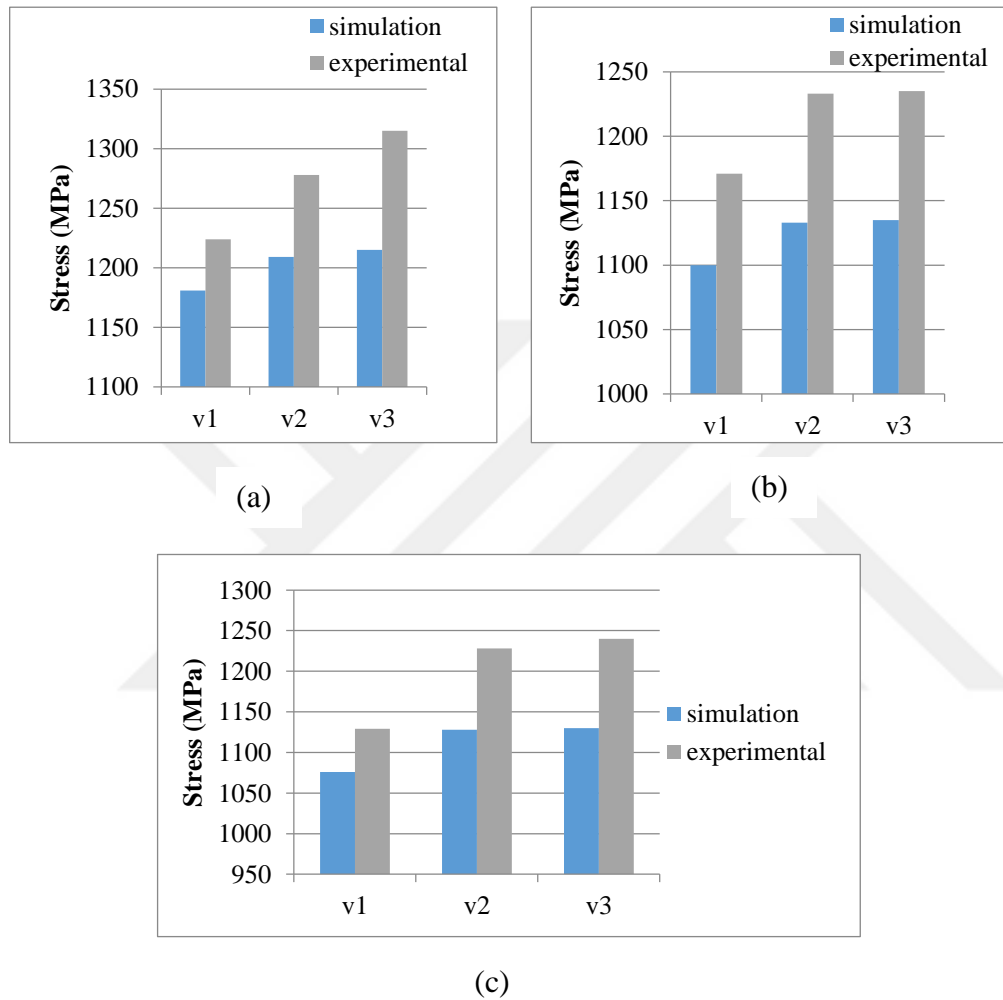


Figure 6.64: Comparison of stresses between simulations and experiments for different velocities at constant pressure: (a) $P1 = 1.4 \text{ kN/mm}^2$, (b) $P2 = 1.6 \text{ kN/mm}^2$ and (c) $P3 = 1.8 \text{ kN/mm}^2$

For stress agreement between the simulations and the experimental work, it can be observed that there are differences between the curves due to the complicated measurements of the X-ray machine for the curved and complex shapes of the product and the ideal boundary conditions that are assigned with numerical analysis.

6.3.2.2 At Constant Velocity

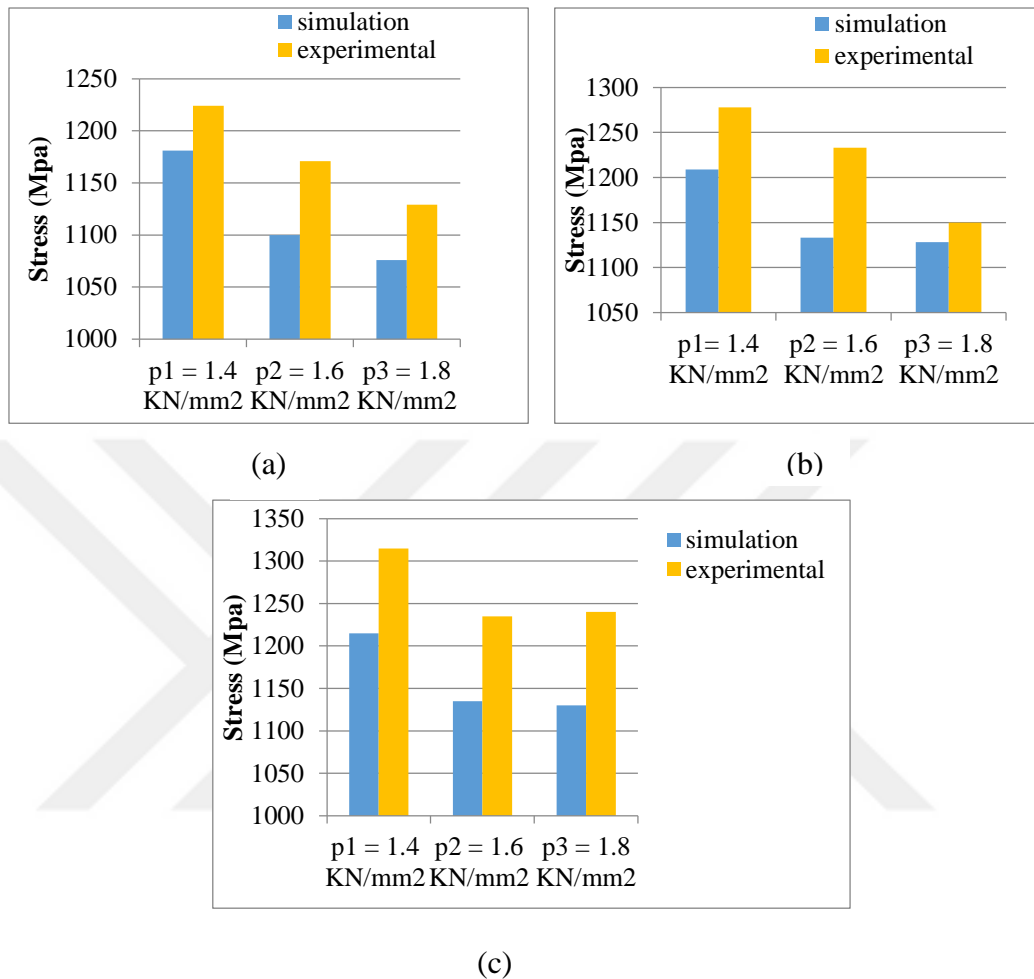


Figure 6.65: Comparison of stresses between simulations and experiments for different pressures at constant velocity: (a) $V_1 = 0.25$ mm/s, (b) $V_2 = 0.5$ mm/s and (c) $V_3 = 1$ mm/s

Stress decreases when pressure increases with constant velocity for both the simulations and the experimental results.

The experimental values were higher than those of the simulation because of the ideal boundary conditions of the numerical analysis and different scans of the X-ray machine which gives various results for the same point and the curved shapes of the product increasing the complexity of the experimental measurements.

6.4 Discussion

The results of the simulations and the experimental work show that increasing the punch velocity from $V1 = 0.25$ mm/s to $V3 = 1$ mm/s increases the residual stresses with the load and power. This leads to many product defects and weaknesses in many parts because of the high residual stresses. However, the lowest velocity leads to non-homogeneous deformation and turbulent metal flow. Therefore, the middle velocity $V2 = 0.5$ mm/s is the optimal choice to ensure the best product results. For the pressure effects, it was observed that the maximum pressure gave the optimal results for the lowest stresses, loads and power. The maximum pressure of $P3 = 1.8$ kN/mm² also made the material flow homogeneously better than the minimum pressure $P1 = 1.4$ kN/mm², which reduced many faults in the parts.

The XRD 3003 X-ray diffraction system was a good and suitable device to measure the residual stresses in different regions on the parts and it showed agreement with simulation stress results. The problem for the experimental stress measurements was the complex and curved shapes of the products, including hollow regions and curved edges. This made measurement with X-rays too difficult, even when making many scans of many regions. The X-ray machine applied rays at different Bragg angles to various positions and angles in the products. Each point took two hours to measure to give an accurate analysis of the stresses.

The values of the experimental residual stress test were greater than those of simulation due to many process conditions taken as ideal and perfect in the simulation, such as friction losses.

The stress distribution during the numerical analysis showed that the lowest stress values were found at the contact area between the upper and lower punches with the work piece surface, while the highest stress values were at the horizontal middle region between the lower backward and upper forward regions due to the effect of opposite punches pressing and the narrow low thickness region.

While under constant pressure, increasing the punch velocity increased the residual stresses on the product because of increasing friction forces. However, at constant

punch velocity, increasing the pressure gave a decrease in the residual stresses because high pressures can exceed friction forces and then reduce temperatures and stresses.

The results showed that the uniform grain size and flow occurred with the maximum velocity $V_3 = 1\text{mm/s}$, which reduced the swirls and made the flow more uniform and laminar.

For the microstructure test, the flow lines in the forward direction and backward direction were uniform in general for all velocity values but they differed from region to region.

Non-uniform flow occurred on all corners and sudden changes toward the backward extrusion, forward extrusion and the center in the surface between the backward and forward extrusion.

In the center on the surface region between the backward and forward extrusion, there were many directions of flow and circulation with swirls because of the low thickness of this region, which did not allow for uniform flow. This region was very near four corners, two of which were related to the forward extrusion direction and the other two corners towards the backward extrusion direction and the sudden changes in direction towards the backward and forward extrusion.

The temperature of the samples were highest on the corners towards the backward extrusion because of the friction due to the opposite directions of the material and punch movements, while the lowest temperatures appeared in the forward direction when the friction was at a minimum. Increasing velocity with constant pressure increased the temperatures because of the increasing friction forces, which in turn increased the heat generated on the contact surfaces, while increasing the pressure with constant velocity led to reducing the work piece temperature due to the friction force effects decreasing under high pressure. The temperature values increased with sharp curves at the beginning of pressing with constant pressure because of the high forces required to change the work piece shape and volume, which increased the heat generated followed by the temperature tending to be

constant since the plastic deformation region required fewer forces to achieve deformation. At constant velocity, increasing the pressure gave more sharp curves increasing the temperature than at constant pressure.

Using lubrication gave a more homogeneous flow with a reduction of the load required, a reduction in temperatures and an increase in product quality since when compared with the process without lubrication, the process did not finish and the product shape was not uniform and had many flakes and cracks. Moreover, the temperature rose, which welded the product and punch while pressing.

Most importantly with regard to lubrication is the type of lubricant as combined extrusion involves high temperatures being generated during the deformation; therefore the lubricant should be suitable for use at high temperatures.

The best lubricant choice for this purpose is MOLYKOTE 557 Dry Film Lubricant 11 oz. in a 16 oz. aerosol. This lubricant is an extreme pressure, dry film lubricant that provides exceptional release and lubricating properties. It contains a wax-like, extreme-pressure lubricant which is supplied as liquid or aerosol; remains as a wax film after solvent evaporation. This type of lubricant is suitable for aluminum alloys and steel.

Many defects appear in some products, such as non-uniform surfaces, flashes, broken samples, flakes, surface cracks, different thicknesses on the sample, incomplete shape of product, high sample thickness and sharp edges. These defects appear for many reasons, including die geometry faults, low punch hardness, high billet hardness, high velocities, non-use of lubrication, high residual stresses, non-uniform plastic deformations, non-centering of the punch and insufficient loads being applied.

These defects can be avoided by following a number of steps: (1) heat treatment to reduce work piece hardness; (2) increasing punch hardness by quenching; (3) changing some die parts from two parts to one piece; (4) avoiding sharp edges in the die geometry and making curved slopes; (5) using suitable types of

lubrication that have good properties at high temperatures; and (6) increasing the loads of press machines.

The QForm numerical analysis software showed a high efficiency with the extrusion and forging processes. There was agreement between the simulations and the experimental results and the predicted results of the simulations, which gave reasonable values of the loads, stresses and temperatures when compared with other studies [10] that used the Upper Bound Method for simulation during combined extrusion. The ABAQUS method [12] gave near results of loads for combined extrusion.

The QForm software gave an indication during analysis for a number of die faults, such as sharp edges and low die wall thicknesses by referring to red points on those regions in the first steps of the simulation. This led to many die design changes before the manufacturing steps. New and more accurate results then appeared after the second simulation. This type of software allowed the use of the half shape of the product for symmetric shapes, which led to a simplification of the analysis and a reduction of complications in the geometry analyses of such products.

The most difficult aspect of hollow polygonal product shapes is the complexity of the closed die in combined backward-forward extrusion and punch centering. This problem makes extraction of a product difficult and it takes time to open all the die parts and remove the product.

The hydraulic press machine was one of the problems that should include special features to achieve this type of process, such as velocity control with moderate loads reaching 450 kN. This leads to the manufacture of additional die support parts to fix the die inside the press machine.



CHAPTER 7

CONCLUSIONS AND RECOMMENDATIONS

7.1 Conclusion

- 1- Metal forming processes for combined backward-forward extrusion process is used to investigate the effect of velocity and pressure intensity on residual stress forms.
- 2- The study demonstrated the ability to produce polygonal hollow shapes by applying a combined forward-backward extrusion process with a suitable die that was made to produce parts with hollow hexagonal sides with backward extrusion and hollow square sides with forward extrusion.
- 3- Combined extrusion had more advantages than separate backward and forward extrusion processes, such as reducing cost and time, improving final product quality, good mechanical properties, uniform residual stresses and more complex shapes.
- 4- Numerical analyses were performed by using the QForm software, which was very efficient with metal forming processes, most notably forging and extrusion.
- 5- The results showed good agreement between the simulations and the experimental work.
- 6- Some defects appeared during the process on samples and dies, including non-uniform surfaces, flashes, sample breaks, flakes, surface cracks, non-uniform thickness in samples, non-completion of product shape, excessive thickness of samples, and sharp edges.

- 7- These defects appear due to a number of reasons which were controlled to avoid the faults of (1) die geometry, (2) low punches hardness, (3) high billet hardness, (4) high velocity, (5) no lubrication use, (6) high residual stress, (7) non-uniform plastic deformation, (8) non-centering of the punch, and (9) insufficient load being applied.
- 8- Aluminum alloy 6061 showed good formability during cold working of the combined extrusion.
- 9- The input parameters of velocity and pressure which depend on three cases of values, namely $V1 = 0.25$ mm/s, $V2 = 0.5$ mm/s and $V3 = 1$ mm/s, and $P1 = 1.4$ kN/mm², $P2 = 1.6$ kN/mm² and $P3 = 1.8$ kN/mm², show suitable comparisons to assign the optimal velocity and pressure that give the uniform and low residual stresses and best product quality. In this case, it is shown that the best pressure is $P3 = 1.8$ kN/mm² and the best velocity is $V2 = 0.5$ mm/s.
- 10- Increasing the pressure to $P3 = 1.8$ kN/mm² led to the best results with regard to the shape of the product, with homogeneous laminar flow and deformation, good surface finish, a reduction in residual stresses, and reduction in the loads required to deform the billet and the time required to do so.
- 11- Increasing the velocity to $V3 = 1$ mm/s led to an increase in the stress, the load required, laminar and homogeneous flow, sample finishing and accuracy as well as reductions in time with temperature. Therefore, the best velocity to use would be $V2 = 0.5$ mm/s as this will reduce the stress and load while keeping the sample quality and homogeneity of flow in a good state.
- 12- The temperature was affected by the velocity value when the pressure was constant. Increasing velocity led to an increase in the temperature values, especially at the die corners because of high friction. The backward region produced higher temperatures than the forward region because of the

opposing directions of the punch and metal during the backward extrusion. This increased the friction forces. Lubrication can be used to reduce or avoid this problem. At constant velocity, increasing the pressure led to a decrease in the temperature.

- 13- The XRD 3003 X-ray diffraction system was shown to be an efficient method to measure residual stresses. The values of the residual stresses via testing were greater than those in the simulation because of the friction losses in the experiments and other optimal conditions that are assigned in the simulation. The higher stress values appeared at the contact areas between punch and the billet.
- 14- For the hardness tests, the results showed that the maximum values of hardness were on the middle regions between the forward and backward regions due to the press effect of two punches (upper and lower punches) that increase the strain hardening effect. The hardness in the backward region was greater than in the forward region due to strain hardening and the movement in opposite directions. The hardness of the sample would increase with the pressure increasing and decrease with the velocity increasing.
- 15- For the optical scope of the macrostructure test, the results showed that the uniform grain size and flow occurred at the maximum velocity of $V_3 = 1\text{mm/s}$, which reduce the swirls and made the flow more uniform and laminar. The flow lines in the forward and backward directions were uniform in general for all velocity values. Most of the circles and non-uniform flows occurred at every corner toward the backward extrusion, forward extrusion and at the center in the surface between the backward and forward extrusions due to the sudden changes in direction of flow and circulation with swirls and the low thickness of this region not allowing uniform flow. This region was very near to four corners, two of which were related to the forward extrusion direction and the other two to the backward extrusion direction.

- 16- The stereo macro and microstructure test showed that sudden changes in sample shape, such as at the corners, would cause more circulation and swirls in the flow; otherwise, the flows would be laminar.

7.2 Recommendations

- 1- This study provided a suitable procedure for combined backward-forward extrusion, so this study can be done for another billet material such as steel.
- 2- Metal forming can be done with hot working instead of cold working.
- 3- New polygonal shapes for two sides of products can be used, including pentagonal and other tetragonal shapes in addition to the square.
- 4- It would be useful to use new types of lubrication and compare the results with previous investigations.
- 5- An attempt may be made to perform the process without lubrication.
- 6- New numerical analyses, such as the upper bound element method, could be employed and compared with the QForm software.
- 7- Another measurement device can be used to find the residual stresses, such as an ultrasonic method.
- 8- Other processes and billet temperatures may be attempted as well as changes in die geometry with different die angles.
- 9- Investigation may be made into other types of extrusion such as backward and radial extrusion to learn about the effects of identical input parameters on stresses.
- 10- Changing boundary conditions according to process conditions and work piece properties may also be another path of investigation that could yield useful data.

REFERENCES

- [1] M. Math and B. Grizelij, "Numerical simulation of combined forward-backward extrusion the body of automatic valve," European Congress On Computational Methods in Applied Sciences and Engineering, Barcelona, pp. 11–14, 2000.
- [2] A. Farhoumand, and R. Ebrahimi, "Analysis of forward-backward radial extrusion process," ELSEVIER, Materials and Design, vol. 30, pp. 2152–2157, 2009.
- [3] S.A. Alkhadam, and F.A. Alshammaa, "Upper bound analysis for round and hexagonal geometric in backward forward extrusion," University of Baghdad, College of Engineering, Mec. Dept., 2015.
- [4] K.C. Nayak and Susanta Kumar Sahoo, "Three dimensional analysis of combined extrusion –forging process," National Institute of Technology Rourkela 769008, India, 2013.
- [5] P.K. Saha, "Aluminum extrusion technology," ASM international, The Materials Information Society, Materials Park, 2000.
- [6] K., Siegert and M. Kammerer, "Impact extrusion processes," Talat Lecture 3502 EAA–European Aluminum Association, 1994.
- [7] K. Kuzman, E. Pfeifer, N. Bay and J. Hunding, "Control of material flow in a combined backward can forward rod extrusion," Journal of Material Processing Technology vol. 60, pp. 141–147, 1996.
- [8] W. Shi –Chun and T. Cai–rong, "An upper bound solution for the force of combined backward-forward extrusion," Northwestern Poly Technical University, English edition, vol. 3, no. 6, China 1982.
- [9] J.C. Choi, J.H. Park and B.M. Kim, "Finite element analysis of the combined extrusion of semi-solid material and its experimental verification," Journal of Materials Processing Technology, vol. 105, pp. 49–54, 2000.
- [10] B.C. Hwang, H.I. Lee, and W.B. Bae, "UBET analysis of the non-axisymmetric combined extrusion process," Journal of Material Processing Technology, vol. 139, pp. 547–552, 2003.

- [11] P. Petrov, V. Perfilvo, and M. Petro, "Development and research on near net shape forging technology of round part with flange made of aluminum alloy A95456," Moscow State Technical University, Russia. Metal Forming, 2004.
- [12] M. Milutinovic, D. Cupkovic, D. Vilotic, and T. Pepelnjak, "Stress-Strain state of combined backward-radial extrusion process of can-flanged part," Journal for Technology of Plasticity, vol. 31 no. 1–2, 2006.
- [13] H. Haghghat, M. M. Mahdavi, "Upper bound analysis of bimetallic rod extrusion process through rotating conical dies," Journal of Theoretical and Applied Mechanics, vol. 51, no. 3, pp. 627–637 Warsaw, 2013.
- [14] A. Milenin, P. Kustra, D. Byrska–Wójcik, and Maciej Pietrzyk, "Numerical prediction of fracture during manufacturing of thick wall tubes from low ductility steels in flow forming processes," Informatyka Technologii Materialow, vol. 15, no. 4, 2015.
- [15] T. Milik, B. Kowalik, and B. Kulinski, "Evaluation of the possibility of performing cold backward extrusion of axisymmetric thin walled aluminum die stampings with square section," Archives of Metallurgy and Materials, vol. 60, 2015.
- [16] R.K. Sahu, R. Das, B. Dash, and B.C. Routara, "Finite element analysis and experimental study on forward, backward and forward-backward multi-hole extrusion process," Materials Today Proceedings, vol. 5, pp. 5229–5234, 2018.
- [17] P. Abhari, and I. Aliiev, "Finite element simulation of flashless radial extrusion process," IOSR Journal of Mechanical and Civil Engineering (IOSR-JMCE) vol. 14, no. 4, pp. 79–83, 2017.
- [18] B. Moroz, S. Stebunov, and N. Biba, "Results of investigation forward and backward extrusion with FEM program QForm," Eighth International Aluminum Extrusion Technology Seminar, Orlando, Florida, vol. 5, pp. 38–41, 2004.
- [19] K.C. Nayak, and S. K. Sahoo, "Experimental and finite element analysis of closed die combined extrusion – forging process development of socket adapter," Materials today Proceedings, vol. 18, pp. 3482–3491, 2019.

- [20] E.H. Lee, and R. L. Mallett, "Stress and deformation analysis of the metal extrusion process," North Holland Publishing Company, pp. 339–353, 1977.
- [21] R.M. McMeeking, and E. H. Lee, "The generation of residual stresses in metal forming," Rensselaer Polytechnic institute, Troy, NY 12181, Urbana, IL 61801, 1982.
- [22] D.J. Lee, D. J. Kim, and B. M. Kim, "New processes to prevent a flow defect in the combined forward-backward cold extrusion of a piston-pin," *Journal of Materials Processing Technology*, vol. 139, pp. 422–427, 2003.
- [23] X. Ma, M. B. De Rooij, and D. J. Schipper, "Modeling of contact and friction in aluminum extrusion," *ELSEVIER Tribology International*, vol. 43, pp. 1138–1144, 2010.
- [24] N.S. Rossini, M. Dassisti, K.Y. Benyounis, and A. G. Olabi, "Methods of measuring residual stresses in components," *ELSEVIER, Materials and Design*, vol. 35, pp. 572–588, 2012.
- [25] P. Abhari, "The study of folding defects during the radial-forward extrusion in the enclosed dies," *International Journal of Science and Research IJSR*, 2015.
- [26] D.J. Yoon, S. J. Lim, H.G. Jeong, E.Z. Kim, and C.D. Cho, "Forming characteristics of AZ31 B magnesium alloy in bidirectional extrusion process," *ELSEVIER Journal of Materials Processing Technology*, vol. 201, no. 1–3, pp. 179–182, 2008.
- [27] J.H. Muhamed, M. J. Jweeg, and A.H. Saleh, "The effect of area reduction of forward die on the combined forward –backward extrusion process," *Nahrain University, College of Engineering Journal (NUCEJ)* vol. 12, pp. 108–121, 2009.
- [28] R.A. Hussien, "Effect of die shape on the temperature and stresses distribution in the compound forward-backward extrusion process," *The Iraqi Journal for Mechanical and Material Engineering*, vol. 11, no. 1, 2011.

- [29] H. Alihossieni, M.A. Zaeem, K. Dehghani, and H.A. Shivaee, "Producing ultrafine-grained aluminum rods by cyclic forward-backward extrusion study the microstructures and mechanical properties," *ELSEVIER, Materials Letters*, vol. 74, pp. 147–150, 2012.
- [30] H. Alihossieni, M. A. Zaeem, and K. Dehghani, "A cyclic forward-backward extrusion process as a novel severe plastic deformation for production of ultrafine grains materials," *ELSEVIER, Materials Letters*, vol. 68, pp. 204–208, 2012.
- [31] R. Matsumoto, K. Hayashi, and H. Utsunomiya, "Experimental and numerical analysis of friction in high aspect ratio combined forward-backward extrusion with retreat and advance pulse ram motion on a servo press," *ELSEVIER, Journal of Materials Processing Technology*, vol. 214, pp. 936–944, 2014.
- [32] H. Jafarzadeh, S. Barzegar and A. Bsbaei, "Analysis of deformation behavior backward-radial-forward extrusion process," *Metallurgy Materials Engineering, The Indian Institute of Metals*, vol. 68, no. 2, pp. 191–199, 2015.
- [33] J. Piwnik, K. Mogielnicki, M. Gabrylewski and P. Baranowski, "The friction in rod forward and backward micro extrusion," *Archives of Foundry Engineering*, vol. 10, no. 1, pp. 447–450, 2010.
- [34] P. Koprowski, M. Bieda, S. Boczkal, A. Jarzebska, P. Ostachowski, J. Kawałko, and K. Sztwiertnia, "AA6013 aluminum alloy deformed by forward-backward rotating die (KoBo) Microstructure and mechanical properties control by changing the die oscillation frequency," *Journal of Materials Processing Tech*, vol. 253, pp. 34–42, 2018.
- [35] C. Hu, Q. Yin, and Z. Zhao, "A novel method for determining friction in cold forging of complex parts using a steady combined forward and backward extrusion test," *Journal of materials processing technology*, vol. 249, pp. 57–66, 2017.
- [36] C.Y. Sun, Y. Xiang, M. W. Fu, Z. H.Sun, M.Q. Wang and J. Yang, "The combined lateral and axial extrusion process of a branched component with two asymmetrically radial features," *Materials and Design*, vol. 111, pp. 492–503, 2016.

- [37] C.C. Chang, C.H. Hsu, and J.C. Lai, “Estimation of friction factor at work piece – die interface in combined forward and backward hollow extrusion of brass at micro scale,” *Materials Research Innovations*, vol. 18, 2016.
- [38] S. S. Jamali, G. Faraji, and K. Abrinia, “Evaluation of mechanical and metallurgical properties of AZ91 seamless tubes produced by radial – forward extrusion method,” *Materials Science and Engineering A*, vol. 666, pp. 176–183, 2016.
- [39] M. H. Paydar, M. Reihanian, E. Bagherpour, M. Sharifzadeh, M. Zarinejad and T. A. Dean, “Consolidation of AL particles through forward extrusion – equal channel angular pressing (FE–ECAP),” *Science Direct, Materials Letters*, vol. 62, no. 17–18, pp. 3266–3268, 2008.
- [40] A K. Rout, R. Das and B.C. Routara, “FEA analysis during extrusion of polygonal sections from round billet through linearly converging dies SERR technique,” *International Journal of Current Engineering and Technology*, 2014.
- [41] M. Plancak, D. Vilotić, A. Ivanišević, D. Movrin, and M. Kršulja, “Backward cold extrusion of aluminum and steel billets by non-circular punch,” *Transfer Inovacii*, vol. 22, no. 1, p. 179, 2012.
- [42] AZO Materials, “Aluminum and aluminum alloys extrusion,” <https://www.azom.com/article.aspx?ArticleID=1554>, 2002.
- [43] Jainex Steel and Metal, “Steel bars,” <https://www.stainlesssteelcoils.in/inconel-718.html>, 2018.
- [44] Tianjin Tiangang Weiye Steel Tube Co., Ltd, “Brass square bar,” <https://tjtgwy.en.made-in-china.com/product/DqoQOHKbwypZ/China-Brass-Square-Bar-Brass-Square-Rod.html>, 2018.
- [45] M. Bauser, G. Sauser, and K. Siegert, “Fundamental of extrusion,” ASM International, The Materials Information Society, Second edition. Materials Park, Ohio 44073–0002, 2006.
- [46] M. P. Groover, “Fundamentals of modern manufacturing materials, processes and systems,” Prentice Hall, Inc., John Wiley and Sons, Inc., Upper Saddle River, 07458, New Jersey, United States of America, 2020.

- [47] Polyphil, “Rubber and plastic products,” <https://www.rubberandplastic.co.uk/>, 2020.
- [48] Raj Hirvate, “Top 7 reasons to use aluminum extrusion for your next manufacturing project,” <https://techlogitic.net/top-7-reasons-to-use-aluminum-extrusion-for-your-next-manufacturing-project/>, 2020.
- [49] Cometao, “Various types of bolting tools used in industries for better quality and safety,” <https://www.cometao.net/archives/1657/various-types-of-bolting-tools-used-in-industries-for-better-quality-and-safety.htm>, 2015.
- [50] M. Bhupatiraju, and R. Greczanik, “Cold extrusion,” American axle and Manufacturing ASM Hand book, vol. 14A, Metal Forming, pp. 405–418, 2013.
- [51] The library of Manufacturing, “Metal extrusion,” <https://thelibraryofmanufacturing.com/extrusion.html>, 2020.
- [52] L. Wang, J. Zhou, J. Duszczyk and L. Katgerman, “Friction in aluminum extrusion – Part 1: a review of friction testing techniques for aluminum extrusion,” Tribology International, vol. 56, pp. 89–98, 2012.
- [53] H. F. Giles Jr, E. M. Mount III, and J. R. Wagner, “Extrusion: the definitive processing guide and hand book,” William Andrew Publishing Library of Congress Cataloging in Publishing Data, 2005.
- [54] M. Zahner, and M. Merklein, “Analysis of combined extrusion micro coining process to manufacture micro structured tappets,” Procedia Manufacturing, vol. 15, pp. 272–279, Japan, 2018.
- [55] V. Segal, “Review: modes and processes of severe plastic deformation (SPD),” Materials, vol. 11, no. 7, pp. 1175. USA, 2018.
- [56] V.K. Jain, U.S. Dixit, C.P. Paul and A. Kumar, “Micro manufacturing: A review part II,” Proceedings of the Institution of Mechanical Engineers, Part B: Journal of Engineering Manufacture, vol. 228, no. 9, 2014.
- [57] S. Potnuru¹, T. Tudu¹, S.K. Sahoo, S.K. Sahoo, “Combined forward-backward extrusion of socket adapter: An Experimental and Numerical Analysis,” srikar potnuru, 2015.

- [58] T. Koizumi and M. Kuroda, "Grain size effects in aluminum processed by severe plastic deformation," *Materials Science and Engineering: A*, vol. 710, pp. 300–308. 2018.
- [59] H.H. Lin, K. Kawakami, and H. Kudo, "Metal flow control in cold simultaneous forward-backward extrusion," *Annals of the CIRP*, vol. 37, no. 1, 1988.
- [60] TWI 75th anniversary, "Fatigue testing – Part 2," <https://www.twi-global.com/technical-knowledge/job-knowledge/fatigue-testing-part-2-079>, 2021.
- [61] A. Fatemi, "Residual stresses and their effects on fatigue resistance," Chapter 8 – Residual Stresses and Their Effects. Toledo, 2004.
- [62] P. Hartley, I. Pillinger and C. Sturgess, "Numerical modeling of material deformation processes," Springer-Verlag, London, 2012.
- [63] C.C. Roberts, Jr, "The consequences of bolt failures," <http://www.croberts.com/bolt.htm>, 2020.
- [64] W. Cheng, and L. Finnie, "Residual stress measurement and the slitting method," mechanical engineering series, Springer, Berkeley Engineering and Research, Inc, USA, 2007.
- [65] E. Piispanen, "X-ray measurement reporting automation," Bachelor's thesis, School of Technology Degree Programme in Software Engineering, jamk.fi, 2019.
- [66] P.J. Withers and H. K. D. H. Bhadeshia, "Residual stress Part 1 measurement techniques," *Materials Science and Technology*, vol. 17, no. 4, pp. 355–365, 2001.
- [67] E. Kula, V. Welss, "Residual stress and stress relaxation," Sagamore Army, Materials Research, conference proceedings, Springer Science Business Media, LLC New York, 2013.
- [68] O. Andergolu, "Residual stress measurement using X-ray diffraction," Office of Graduate Studies of Texas A and M University, 2005.


- [69] J. Guo, H. Fu, B. Pan and R. Kang, “Recent progress of residual stress measurement methods: a review,” *Chinese Journal of Aeronautics*, 2019.
- [70] D.J. Gardiner, “Practical Raman Spectroscopy,” Springer-Verlag, 1989.
- [71] P.R.G.D.J. Graves, and D. Gardiner, “Practical Raman Spectroscopy,” Springer-Verlag, 1989.
- [72] P.J. Withers, and P. J. Webster, “Neutron and synchrotron X-ray strain scanning,” *Strain* Vol. 37, no. 1, pp. 19–33, 2001.
- [73] A. Ajovalasit, M. Scafidi, B. Zuccarello, M. Beghini, L. Bertini, C. Santus, “The hole-drilling strain gauge method for the measurement of uniform or non-uniform residual stresses,” Italy, 2010.
- [74] VISHAY Precision Group, “Measurement of residual stresses by the hole-Drilling Strain Gage Method,” *Micro measurements*, Teck 503 N, Document Number: 11053, 2010.
- [75] M.B. Prime, “Residual stress measurement by successive extension of a slot: The crack compliance method,” vol. 52, no. 2, pp. 75–96, 1999.
- [76] M.B. Prime, “Experimental procedure for crack compliance (Slitting) measurements of residual stresses,” *Los Alamos National Laborer Report (LA-UR-03-8629)*, 2003.
- [77] Quantor Form Ltd, “The program of simulation of metal forming,” *QForm 2D/3D Version V8 part 4*, www.qform3d.com, 2015.
- [78] P.S. Prevey, “X-ray diffraction residual stress technique,” *ASM International, ASM Handbook*. vol. 10, pp. 380–392, 1986.
- [79] M.E. Fitzpatrick, A. T. Fry, P. Holdway, F. A. Kandil, J. Shackleton, and L. Suominen, “Determination of residual stresses by X-ray diffraction,” *National Physical Laboratory Teddington, Middlesex, United Kingdom*, 2005.
- [80] ASTM, “Standard test method for determining the X-ray elastic constants for use in the measurement of X-ray diffraction techniques,” E1426–14, 2019.

- [81] H. Czichos, and T. Saito, "Springer handbook of materials measurement Methods," Ed. Leslie Smith. vol. 978, L. Smith Ed. Berlin, Springer, 2006.
- [82] G. Li, W. Wu¹, P. Chigurupati, J. Fluhrer, and S. Andreoli, "Recent advancements of extrusion simulation in DEFORM-3D," Latest advances on extrusion technology and simulation in Europe, Bologna, Italy, 2007.
- [83] R.F. Muraca, and J. S. Whittick, "Materials data hand book aluminum alloy 6061," 2nd edition, Western Applied Research and Development, Inc., 1972.
- [84] ASM International Hand Book Committee, "Properties and selection nonferrous alloys and special-purpose materials," The materials Information Company, vol. 2 of Metals Hand Book, pp. 1143-1144, 1992.
- [85] C. Højerslev, "Tool steel," Risø National Laboratory, Roskilde, Forskningscenter Risoe. Risoe-R, no. 1244, Denmark, 2001.
- [86] J.D. Verhoeven, "Steel Metallurgy for the Non Metallurgist," ASM International, pp. 001, 2007.
- [87] M.O. Mutlu, C. G. Guleryuz and Z. Parlar, "Numerical investigation of the effect of friction conditions to increase die life," 13th International Conference on Tribology, ROTRIB 16, IOP Publishing Materials Science and Engineering, vol. 174, no. 1, pp. 012046, 2017.
- [88] B. Grizelj, M. Placak, and B. Barisic, "Numerical simulation of combined forward-backer extrusion," Extrusion Workshop, Latest advances on extrusion technology and Simulation in Europe, Bologna, Italy, vol. 367, pp. 193-200, 2008.
- [89] N. Biba, A. Vlasov, and S. Stebounov, "The simulation of the extrusion process using QForm 3D," Extrusion Workshop, Latest Advances on Extrusion Technology and Simulation in Europe, Bologna, Italy, 2007.
- [90] P. den Dikken¹, and D. Swinkels, "Integrating FEM simulation in the extrusion die design process," Extrusion Workshop, Latest advances on extrusion technology and Simulation in Europe, Bologna, Italy, 2007.
- [91] L. Fluice, F. Gagliardi, and F. Micari, "Development of an extrusion equipment to measure force and pressure in hollow components manufacturing," Italy, 2007.

- [92] V. Jayaseelan, and K. Kalaichelvan, "Influence of friction factor on extrusion process," *Advanced Materials Research*, Trans Tech Publication Ltd, vol. 622, pp. 457–460, 2013.
- [93] M. Samuel, and G. Anthony, "Effects of vegetable based oils lubricants in the extrusion of aluminum," *International Journal of Scientific and Technology Research*, vol. 5, no. 08, 2016.
- [94] R. Kuppuswamy, "Metallographic etching of aluminium and its alloys for restoration of obliterated marks in forensic science practice and investigations," *T. Kvacakj. Aluminium Alloys, Theory and Applications*, pp. 331–352, 2011.
- [95] ASM hand book "etching of aluminum and its alloy," vol. 2A, *Aluminum Science and Technology*, 2018.
- [96] W.R. Graff, and D. C. Sargent, "A new grain-boundary etchant for aluminum alloys," *Metallography*, vol. 14, no. 1, pp. 69–72, 1981.
- [97] N.K. Walter, J. D. C. Atkins and G. S. Douglas, "Process for etching aluminum alloy surfaces," U.S. Patent no. 2, 795, 490, 1957.
- [98] A. Kumar, U. Welzel, M. Wohlschlägel, W. Baumann, and E. J. Mittemeijer, "An X-ray diffraction method to determine stress at constant penetration/information depth," *Materials Science Forum*, vol. 524, pp. 13–18 Trans Tech Publications Ltd, 2006.
- [99] I.C. Noyan, and J.B. Cohen, "Residual stress measurement by diffraction and interpretation," Springer-Verlag, New York Inc., 2013.
- [100] J.R. Davis, "Aluminum and aluminum alloys," ASM International, 1993.

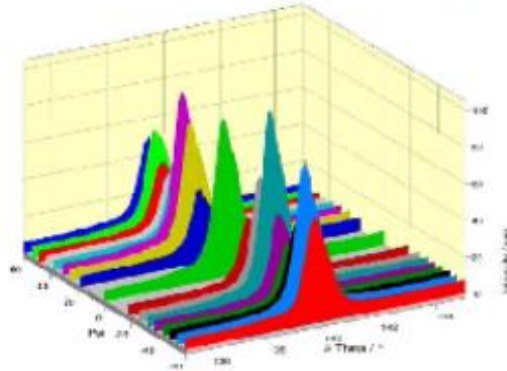
APPENDICES

A. Stresses Reports

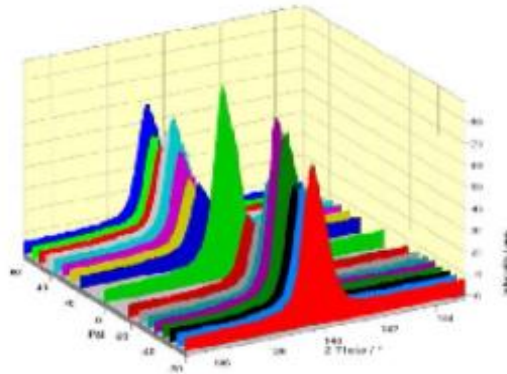
Case 1- V1 (6) Results																					
<p>Corrections: No Polarization: Yes Lorentz: Yes Rachiinger : No Background: Line Smoothing Cycles: 21 Parabola Points: 5</p> <p>Measurement Parameters Scan: 2:1 Sym.: 135.00°-145.00° Psi Axis: Chi Psi Axis mode: sin²(psi) Number of Psi position: 17 Number of Phi position: 1 Total time: 2h 6 min 45 s Test operator report date: 17/12/2019</p>	<p>Test Parameters Database Reference Material: Aluminum alloy Radiation: Cr-Kα Bragg angle: 139.300° Lattice Planes: (3.1, 1) -S: 4, 88700 10 -MPa Poisson's ratio: 0.345503 Used constants: X-ray</p>																				
<p>Cross Correction PHI = Φ = 0.0 PHI = Φ = 45.0 PHI = Φ = 90.0</p>	<p>Stress (MPa) 0.225 0.233 0.229</p>	<p>Shear (MPa) 8.7 \pm 1.4 6.4 \pm 1.0 9.6 \pm 0.9</p>	<p>R 0.957 0.960 0.956</p>																		
<p>Tensor: Hypothesis Sigma 33 = 0 Used PHI: 0.0°, 45.0°, 90.0° Calculated unstressed angle: 13 9, 452° \pm 0.015</p>																					
<p>Stress Tensor (MPa)</p> <table style="width: 100%; border-collapse: collapse;"> <tr> <td style="width: 33%;">-64.5 \pm 2.9</td> <td style="width: 33%;">3.2 \pm 2.5</td> <td style="width: 33%;">6.5 \pm 1.0</td> </tr> <tr> <td>3.2 \pm 2.5</td> <td>-35.3 \pm 2.9</td> <td>7.5 \pm 1.0</td> </tr> <tr> <td>6.5 \pm 1.0</td> <td>7.5 \pm 2.9</td> <td>0.0</td> </tr> </table> <p>Principle Stress Tensor(MPa)</p> <table style="width: 100%; border-collapse: collapse;"> <tr> <td style="width: 33%;">-36.7</td> <td style="width: 33%;">0.0</td> <td style="width: 33%;">0.0</td> </tr> <tr> <td>0.0</td> <td>-65.4</td> <td>0.0</td> </tr> <tr> <td>0.0</td> <td>0.0</td> <td>2.3</td> </tr> </table>				-64.5 \pm 2.9	3.2 \pm 2.5	6.5 \pm 1.0	3.2 \pm 2.5	-35.3 \pm 2.9	7.5 \pm 1.0	6.5 \pm 1.0	7.5 \pm 2.9	0.0	-36.7	0.0	0.0	0.0	-65.4	0.0	0.0	0.0	2.3
-64.5 \pm 2.9	3.2 \pm 2.5	6.5 \pm 1.0																			
3.2 \pm 2.5	-35.3 \pm 2.9	7.5 \pm 1.0																			
6.5 \pm 1.0	7.5 \pm 2.9	0.0																			
-36.7	0.0	0.0																			
0.0	-65.4	0.0																			
0.0	0.0	2.3																			
<p>Stress Tensor (MPa)</p> <table style="width: 100%; border-collapse: collapse;"> <tr> <td style="width: 33%;">-64.5 \pm 2.9</td> <td style="width: 33%;">3.2 \pm 2.5</td> <td style="width: 33%;">6.5 \pm 1.0</td> </tr> <tr> <td>3.2 \pm 2.5</td> <td>-35.3 \pm 2.9</td> <td>7.5 \pm 1.0</td> </tr> <tr> <td>6.5 \pm 1.0</td> <td>7.5 \pm 2.9</td> <td>0.0</td> </tr> </table> <p>Principle Stress Tensor(MPa)</p> <table style="width: 100%; border-collapse: collapse;"> <tr> <td style="width: 33%;">-36.7</td> <td style="width: 33%;">0.0</td> <td style="width: 33%;">0.0</td> </tr> <tr> <td>0.0</td> <td>-65.4</td> <td>0.0</td> </tr> <tr> <td>0.0</td> <td>0.0</td> <td>2.3</td> </tr> </table>				-64.5 \pm 2.9	3.2 \pm 2.5	6.5 \pm 1.0	3.2 \pm 2.5	-35.3 \pm 2.9	7.5 \pm 1.0	6.5 \pm 1.0	7.5 \pm 2.9	0.0	-36.7	0.0	0.0	0.0	-65.4	0.0	0.0	0.0	2.3
-64.5 \pm 2.9	3.2 \pm 2.5	6.5 \pm 1.0																			
3.2 \pm 2.5	-35.3 \pm 2.9	7.5 \pm 1.0																			
6.5 \pm 1.0	7.5 \pm 2.9	0.0																			
-36.7	0.0	0.0																			
0.0	-65.4	0.0																			
0.0	0.0	2.3																			

**CASE-1_V1(6)
RESULTS**

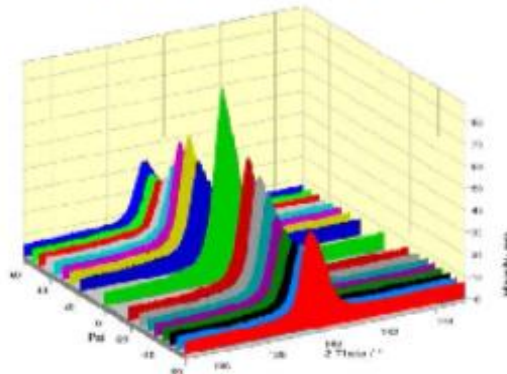
PHI=0.0° GRAPH (AXIAL)



PHI=45.0° GRAPH

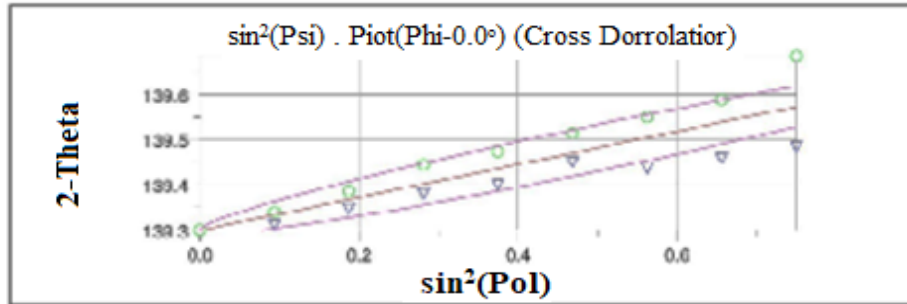


PHI=90.0° GRAPH (TANGENTIAL)

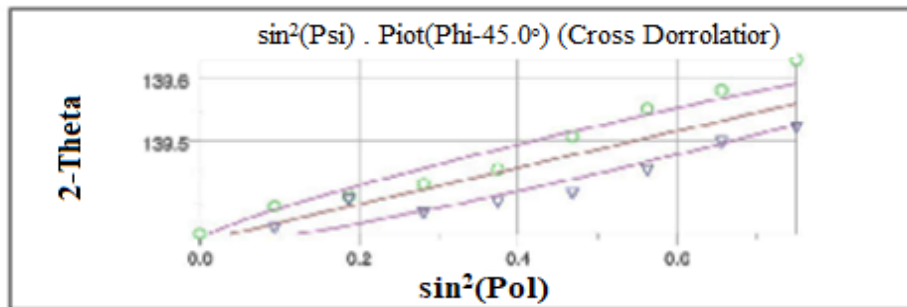


**CASE-1_V1(6)
RESULTS**

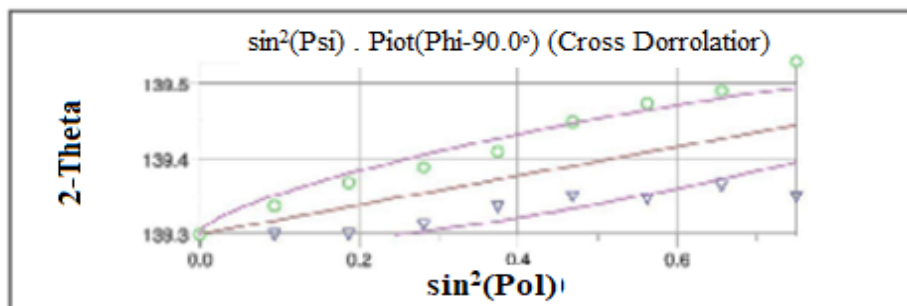
PHI=0.0° GRAPH (AXIAL)



PHI=45.0° GRAPH

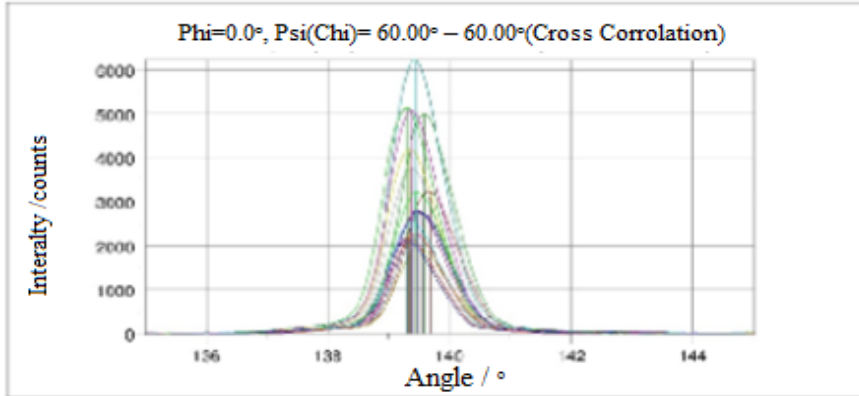


PHI=90.0° GRAPH (TANGENTIAL)

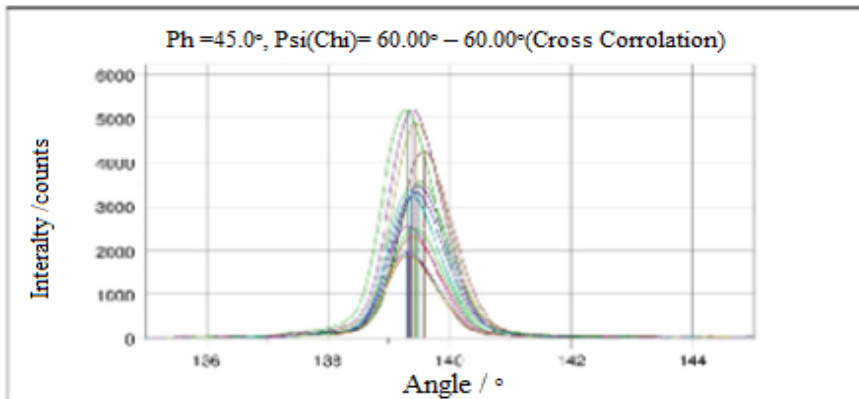


**CASE-1_V1(6)
RESULTS**

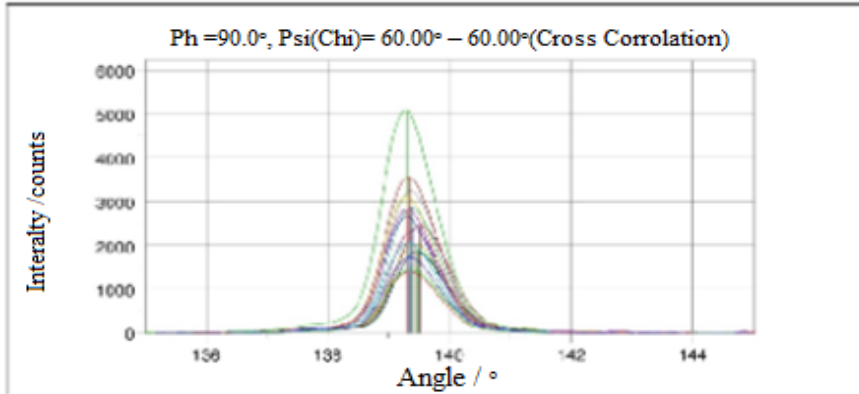
PHI=0.0° GRAPH (AXIAL)



PHI=45.0° GRAPH



PHI=90.0° GRAPH (TANGENTIAL)



B. Aluminum Alloy 6061 Chemical Composition



SEYDİŞEHİR ALÜMİNYUM METAL
PAZARLAMA SANAYİ ve TİC. LTD. ŞTİ.
info@seydisehiraluminyum.com.tr
bilgi@seydisehiraluminyum.com.tr

MUAYENE RAPORU / INSPECTION CERTIFICATE / ABNAHMEPRÜFZEUGNIS

MUAYENE RAPORU INSPECTION CERTIFICATE ABNAHMEPRÜFZEUGNIS	EN 10 204 - 3.1B (DIN 50049)	TARİH: 29.06.2018 DATE: DATUM:	No: 20180629 No: Nr:
MÜŞTERİ: COSTUMER: KUNDE:		FATURA No: INVOICE No RECHNUNG Nr	004967
MÜŞTERİ SİPARİŞ No: CUST. ORDER No AUFTRAGS Nr.		PROFIL No: SECTION No PROFIL Nr.	Ø 20 Ø 30 Ø 40
MÜŞTERİ PROFİL No: CUST. SECTION No: PROFIL Nr. KUNDE:	Ø 20 Ø 30 Ø 40	MIKTAR: WEIGHT: GEWICHT:	314 kg 302 kg 378 kg
		ALAŞIM: ALLOY: LEGIERUNG	EN AW 6061 T6

KİMYASAL ANALİZ / CHEMICAL COMPOSITION / CHEMISCHE ZUSAMMENSETZUNG

ŞARJ / CHARGE	% Si	% Fe	% Cu	% Mn	% Mg	% Cr	% Zn	% Ti	% Pb	% Sn
18-186	0,78	0,47	0,26	0,08	0,95	0,14	0,16	0,01		
SİNİR:	0,40	0,70	0,15	0,15	0,80	0,04	0,25	0,15		
LIMIT:	0,80		0,40		0,20	0,35				
NORM:										

MUKAVEMET DEĞERLERİ / MECHANICAL PROPERTIES / MECHANISCHE EIGENSCHAFTEN

NUMUNE No: SAMPLE No: PROBE Nr.	Rp 0.2 N / mm ²	Rm N / mm ²	A5 %	Ø2,5 / 62,5 HB	Webster
Numune 1				102	
Numune 2				95	
Numune 3				105	
SİNİR: LIMIT: NORM:					

SEYDİŞEHİR ALÜMİNYUM METAL
PAZARLAMA SAN. ve TİC. LTD. ŞTİ.
Ankara Caddesi No: 82 Orta / ANKARA
Tel: (0312) 385 34 26-385 34 44-354 04 16
Fax: (0312) 385 34 22 Tic. Sic. No: 179198
OSTİM VERGİ DAİRESİ: 754 046 0907

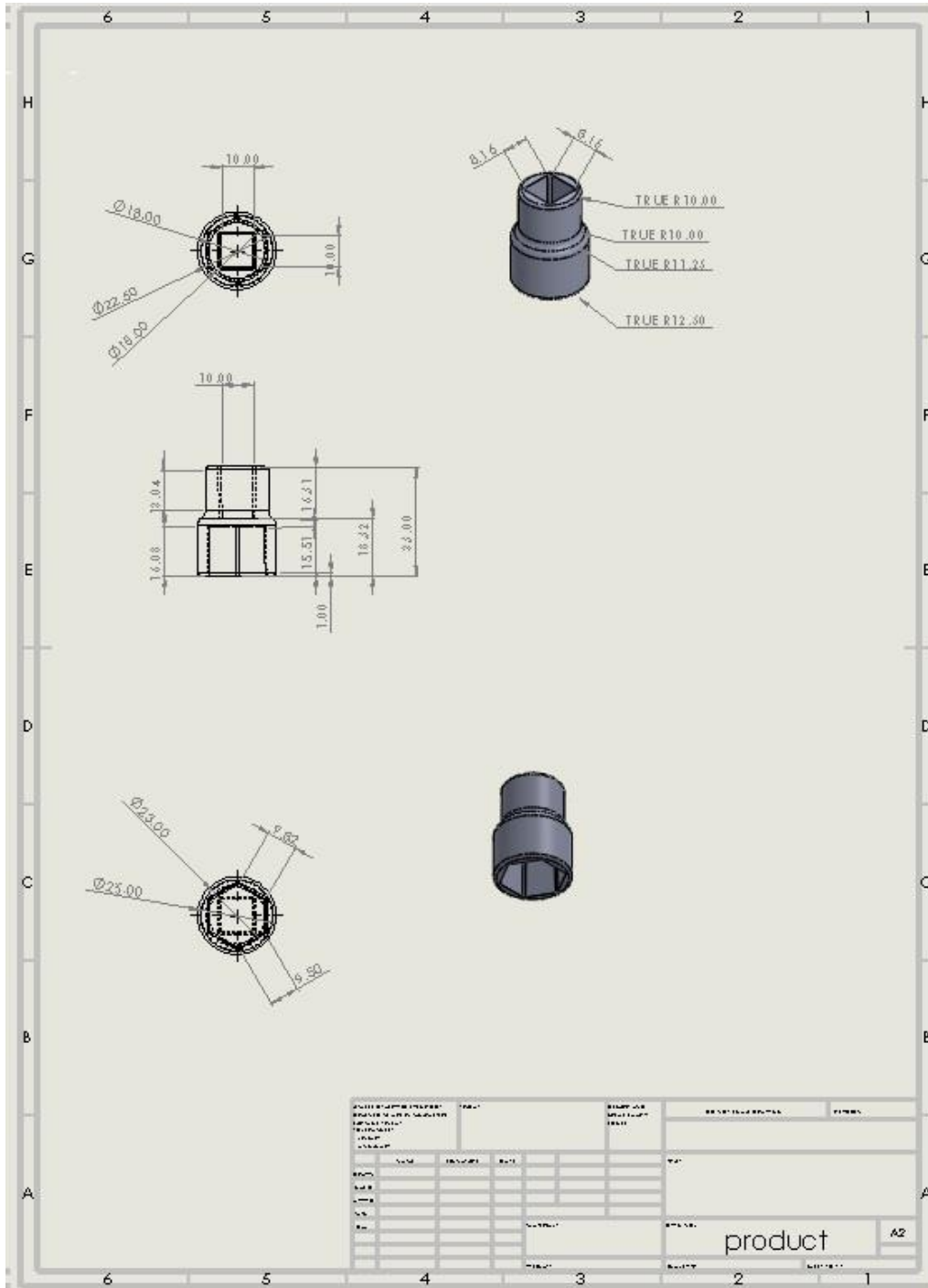
Yukarıdaki malzemenin muayene edildiğini ve siparişteki şartlara uygunluğunu bildiririz.
We hereby certify, that material described above has been tested and complies with the terms of the confirmation of order.
Es wird bestätigt, dass die Lieferung geprüft wurde und den Vereinbarungen bei der Auftragsbestätigung entspricht.

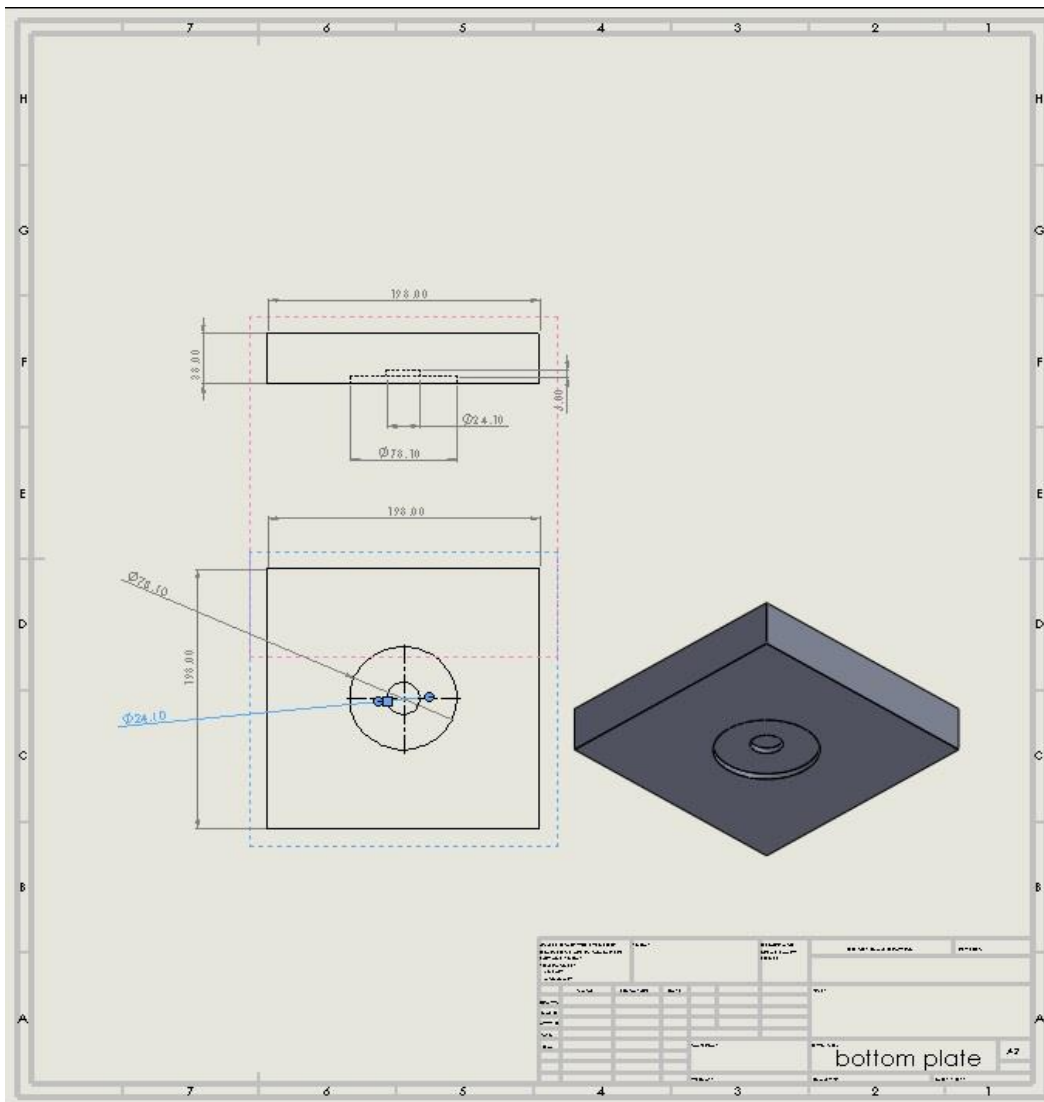
Aluminum Certificate

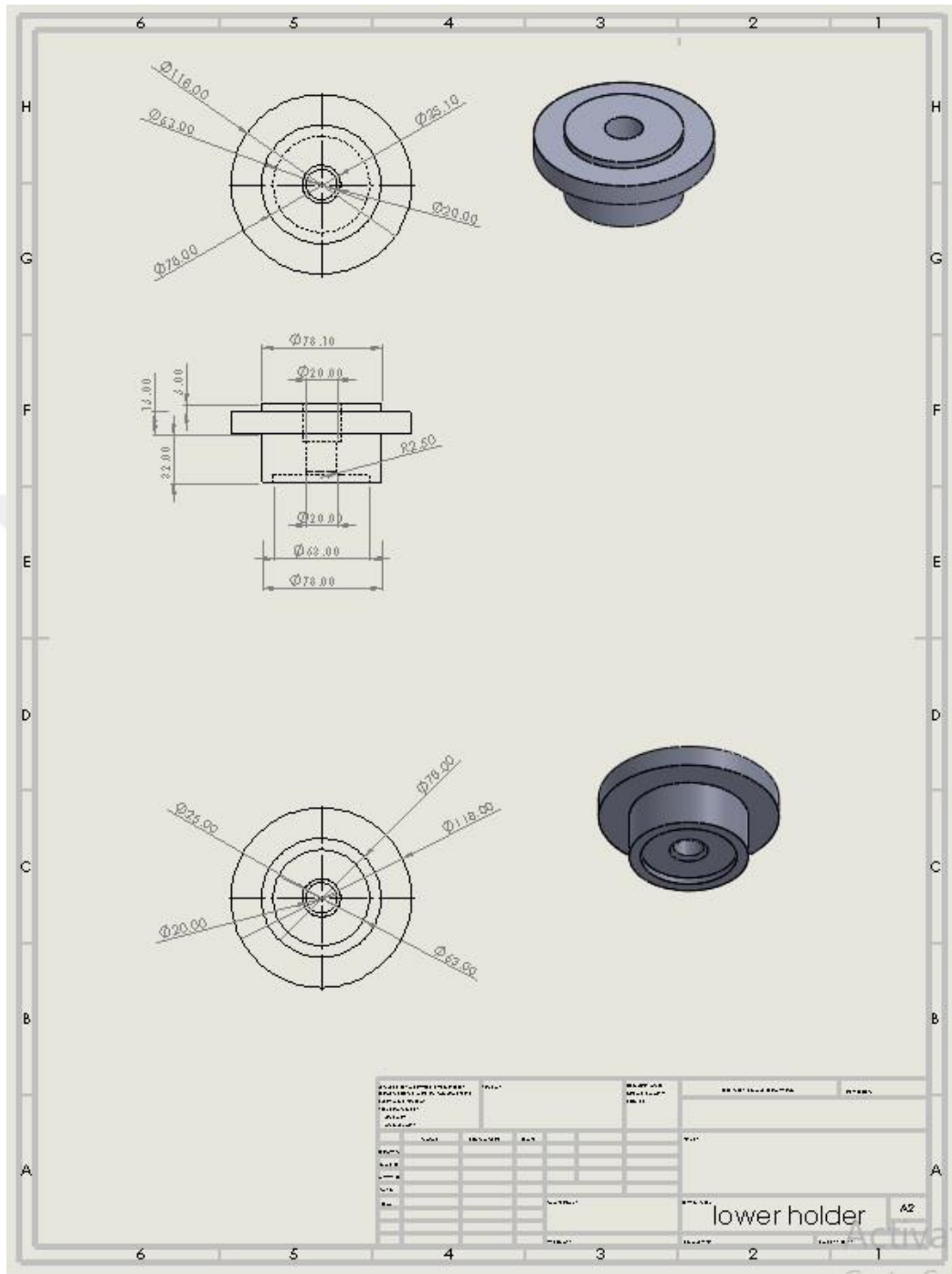
Ahi Evran Caddesi No: 82 (06370) Ostim/ANKARA Tel: 0.312, 385 34 26 - 354 04 16 - 385 34 22 | Faks: 0.312.385 34 8

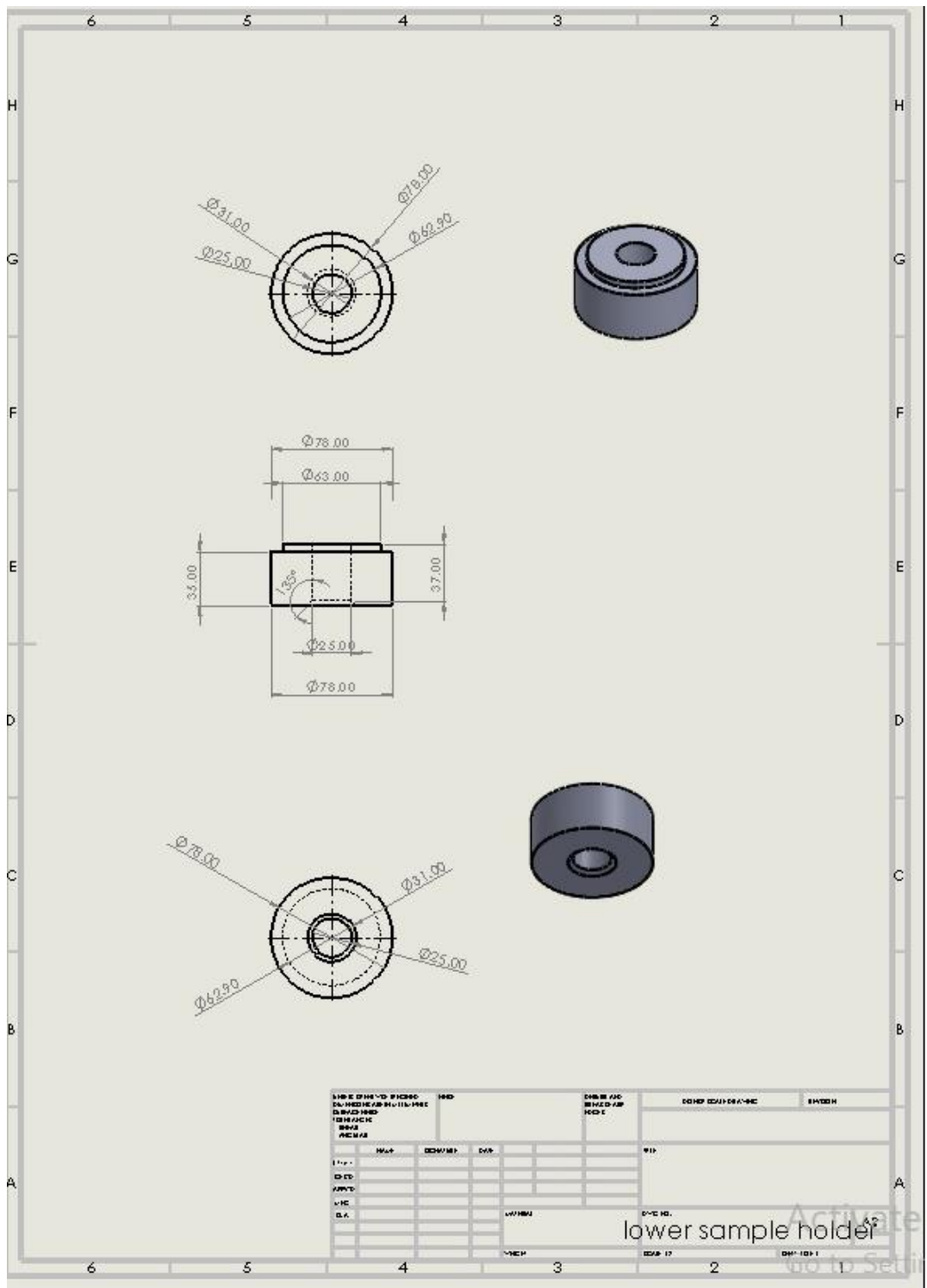
www.seydisehiraluminyum.com.tr

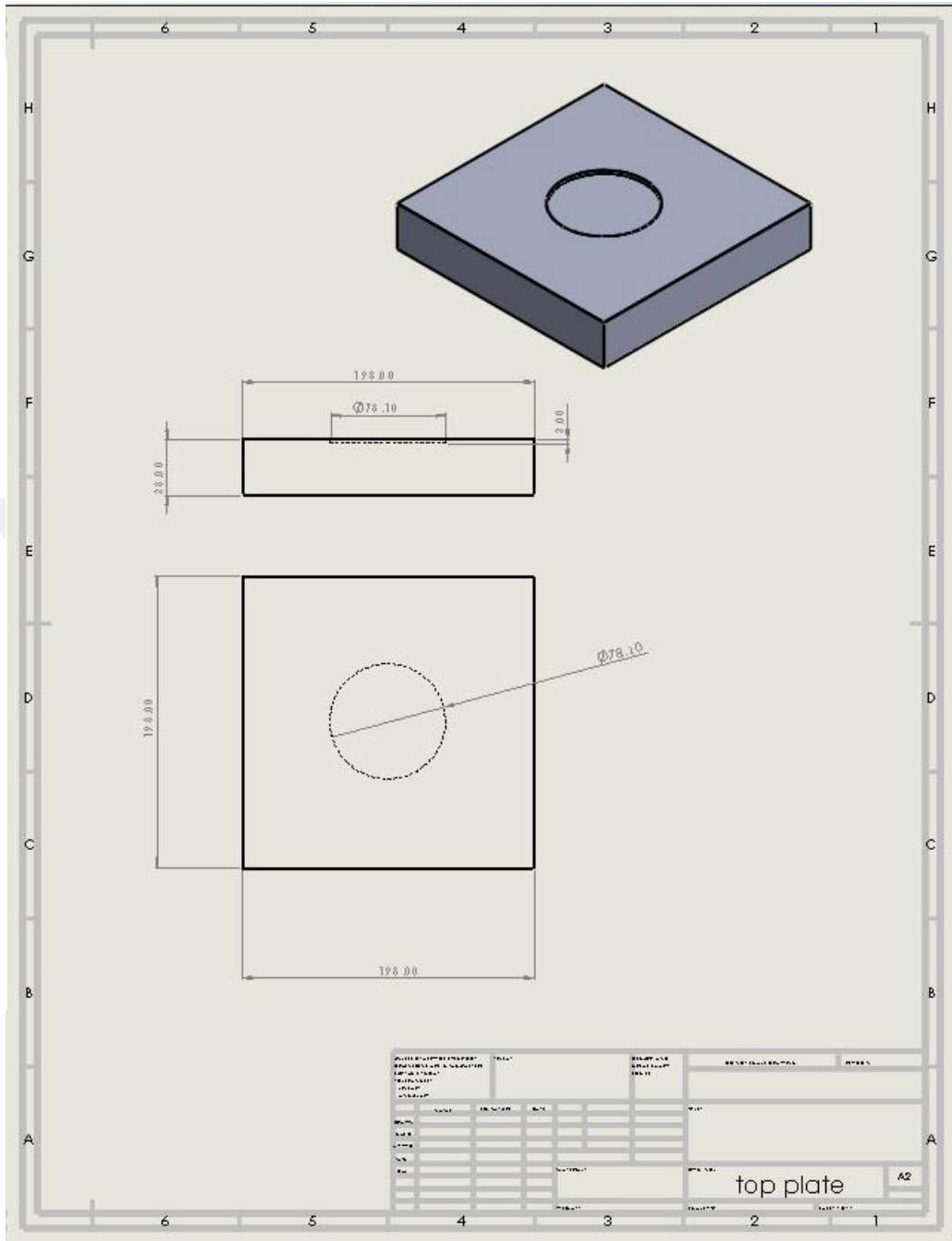
C. Engineering Drawings

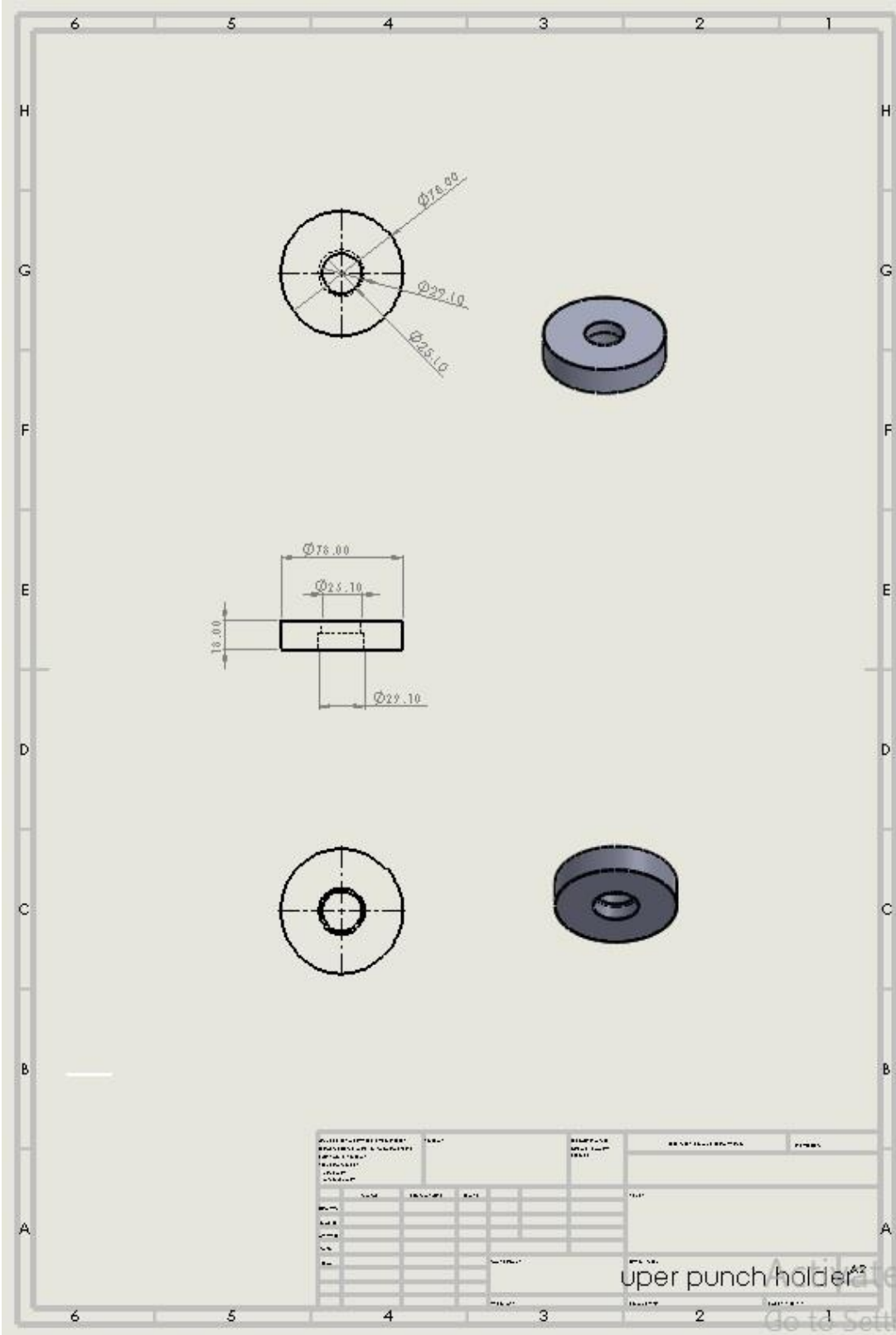












PUBLICATIONS

1. Ban AL-AMER, Çetin KARATAŞ, Faruk MERT, Haitham AL-JAWAD (Combined Forward-Backward Extrusion Process For Aluminum Alloys), 1st International Symposium on Light Alloys and Composite Materials (ISLAC 18), p. 176, Karabük, Turkey, March (2018).
2. Ban AL-AMER, Çetin KARATAŞ, Faruk MERT, Haitham AL-JAWAD (Studying the Effect of Temperature During Hot Forming for Combined Backward Forward Extrusion Process for Copper Alloys), 3rd International Conference of Material Science and Technology in Cappadocia (IMSTEC 18), pp. 456-460). Nevşehir, Turkey, September (2018).
3. Ban AL-AMER, Çetin KARATAŞ, Faruk MERT, Haitham AL-JAWAD (Effect of Lubrication and Friction Coefficients on Temperature Distribution for Combined Backward Forward Extrusion Process For Alloy Steel). 6th International Symposium on Innovative Technologies in Engineering and Science (ISITES 18), pp. 352-357, Alanya, Antalya, Turkey, November (2018).
4. Ban AL-AMER, Haitham AL-JAWAD, Faruk MERT, Çetin KARATAŞ (Investigation of the Effect of Lubrication and Friction Factors on Loads in Forward Extrusion Processes For Aluminum Alloy 7075 by QForm), 2nd International Congress on Engineering and Architecture (ENAR), pp. 1117-1122, Marmaris, Turkey, April (2019).
5. Ban AL-AMER, Haitham AL-JAWAD, Faruk MERT, Çetin KARATAŞ (Numerical Analysis to Investigate the Effect of Velocity on Stress For Backward Extrusion Process of Aluminum Alloy 6082), 2nd International Congress on Engineering and Architecture (ENAR), pp. 1613-1618, Marmaris, Turkey, April (2019).
6. Ban AL-AMER, Haitham AL-JAWAD, Faruk MERT, Çetin KARATAŞ (*Effects of Zinc Content and Velocity on Load During Backward Extrusion Processes in Aluminum Alloys*) The International Conference on Materials Science, Mechanical and Automotive Engineering and Technology (IMSMATEC 19), pp. 433-437, Cappadocia, Turkey, June (2019).
7. Ban AL-AMER, Haitham AL-JAWAD, Faruk MERT, Çetin KARATAŞ (Simulation of Forward Extrusion Process for Aluminum Alloys To Investigate the Influence of Lubrication on Stress Generated), International Symposium on Automotive Science and Technology (ISASTECH), pp. 175-180, Ankara, Turkey, September (2019).

8. Ban AL-AMER, Haitham AL-JAWAD, Faruk MERT, Çetin KARATAŞ (QForm Simulation of Temperature Influence on Load During Combined Backward Forward Extrusion Process of Cu OFE), 4th International Conference on Material Science and Technology (IMSTEC), pp. 476-480, Kızılcahamam, Ankara, Turkey, October (2019).8.

